UNIVERSITÀ DI PADOVA  FACOLTÀ DI INGEGNERIA

Dipartimento di Ingegneria dell'Informazione

Scuola di Dottorato di Ricerca in Ingegneria dell'Informazione
Indirizzo: Bioingegneria

CICLO XXII

DYNAMICS OF PANCREATIC BETA CELLS: Evidence for Beta Cell Turnover and Attempted Regeneration in Diabetes from Sources of Beta Cells other than Beta Cell Replication in Rats, Monkeys, and Humans

Direttore della Scuola: Ch.mo Prof. Matteo Bertocco

Supervisore: Ch.mo Prof.ssa Chiara Dalla Man

Dottoranda: Ing. Erica Manesso

Gennaio 2010

Dynamics of Pancratic Beta Cells: Evidence for Beta Cell Turnover and Attempted Regeneration in Diabetes from Sources of Beta Cells other than Beta Cell Replication in Rats, Monkeys, and Humans

Erica Manesso

2010

To My Family

Abstract (Italian version)

L'interesse verso una potenziale rigenerazione della massa beta cellulare *è* in aumento poich*é* un difetto della stessa caratterizza sia il diabete di tipo 1 che quello di tipo 2. In questo contesto un'analisi quantitativa del *turnover* beta cellulare diviene essenziale per comprendere la varietà dei meccanismi che lo regolano. Per esempio, la massa beta cellulare si adatta all'obesità? Si preserva con l'età? Come si espande nell'infanzia?

In collaborazione con il Larry Hillblom Islet Research at David Geffen School of Medicine, University of California Los Angeles, *è* stato sviluppato un modello dinamico per la stima del *turnover* beta cellulare. Assumendo un comportamento omogeneo delle beta cellule in termini di *turnover*, il modello riesce a descrivere la massa beta cellulare come il bilancio tra la formazione e la morte di beta cellule. Le beta cellule si formano o dalla duplicazione di beta cellule esistenti o da altre sorgenti (abbreviate con OSB, dall'inglese *Other Sources of Beta cells*) e muoiono principalmente per apoptosi. Dal momento che tutti i parametri del modello possono essere determinati ad eccezione di OSB, dal modello si determina questa quantità incognita. Le componenti del *turnover* beta cellulare, ovvero la formazione di nuove beta cellule (duplicazione di beta cellule esistenti sommata a OSB) e l'apoptosi, sono state impiegate nello sviluppo di un modello di popolazione per la stima dell'età e dell'aspettativa di vita medie di una beta cellula. Il modello risultante *è* una variazione della classica equazione di McKendrick-von Foerster e descrive le beta cellule come una popolazione di cellule che differiscono l'una dall'altra per la loro età.

Gli innovativi risultati che emergono dall'applicazione dei modelli a specie differenti, ovvero ratti, scimmie e individui sono: 1) c'*è* *turnover* beta cellulare nei ratti, nelle scimmie e negli individui non diabetici in età adulta; 2) la formazione ed il mantenimento della massa beta cellulare dipendono maggiormente da OSB; 3) la formazione di nuove beta cellule da parte di OSB aumenta in modo sostanziale a fronte di un incremento di apoptosi nei ratti di tipo HIP, modello animale del diabete di tipo 2, rallentando in

questo modo il declino della massa beta cellulare. In contrasto, il *turnover* beta cellulare *è* ridotto nelle scimmie di tipo STZ (ovvero scimmie trattate con *streptozotocin*), modello animale del diabete di tipo 1, rispetto alle scimmie non diabetiche di controllo. Inoltre la formazione di nuove beta cellule nelle scimmie di tipo STZ *è* dovuta in gran parte a OSB. 4) La duplicazione di beta cellule esistenti *è* il meccanismo primario che regola l'espansione della massa beta cellulare nell'infanzia, mentre in età adulta OSB *è* responsabile del mantenimento della massa beta cellulare a fronte di un incremento dell'apoptosi; 5) la massa ed il *turnover* beta cellulari aumentano in risposta all'obesità negli individui; 6) le stime ottenute per l'età media di una beta cellula (1-2 mesi nei ratti, 2-5 mesi nelle scimmie e 6 mesi-2 anni negli individui) e per la sua aspettativa di vita media (1-3 mesi nei ratti, 2-5 mesi nelle scimmie e 6 mesi-2 anni negli individui) sono potenzialmente compatibili con la rigenerazione endogena della massa beta cellulare nel diabete, qualora fosse possibile alterare il *turnover* beta cellulare in modo terapeutico.

I modelli presentati forniscono per la prima volta informazioni sulla presenza di sorgenti di beta cellule diverse dalla duplicazione di beta cellule e stime dell'età e dell'aspettativa di vita medie di una beta cellula nei ratti, nelle scimmie e negli individui. I risultati ottenuti hanno un impatto dal punto di vista clinico considerando che: a) l'origine delle beta cellule *è* causa di accesi dibattiti: alcuni ricercatori suggeriscono come origine principale la duplicazione delle beta cellule esistenti, altri la formazione di nuove beta cellule da svariate sorgenti diverse dalla duplicazione beta cellulare; b) il ripristino del controllo glicemico sia nel diabete di tipo 1 sia in quello di tipo 2 attraverso una rigenerazione interna potrebbe essere una potenziale strategia alternativa al trapianto di pancreas, dati il numero insufficiente di pancreas disponibili per il trapianto e i rischi di una prolungata terapia immunosoppressiva; c) l'unico approccio sperimentale che consente di identificare le sorgenti di nuove beta cellule diverse dalla duplicazione beta cellulare *è* la *cell-lineage tracing*, non disponibile negli studi clinici. In aggiunta i risultati incoraggiano: a) studi futuri sul *turnover* beta cellulare nei pazienti diabetici; b) lo sviluppo di esperimenti *ad hoc* atti ad identificare OSB; c) la messa a punto di esperimenti e modelli matematici in grado di stabilire le modalità ed i tempi richiesti per la rigenerazione endogena della massa beta cellulare.

Abstract (English version)

Since the fundamental defect in both type 1 (T1DM) and type 2 diabetes (T2DM) is beta cell failure, there is increasing interest in the capacity, if any, for beta cell regeneration. In this context quantitative analysis of beta cell turnover becomes essential to permit investigation of the mechanisms that regulate it. For example, how does beta cell mass adapt to obesity? How is beta cell mass preserved during aging? How does beta cell mass expand during childhood?

In collaboration with the Larry Hillblom Islet Research at David Geffen School of Medicine, University of California Los Angeles, we developed a dynamic model to estimate beta cell turnover. Assuming homogeneity of beta cells, the model describes beta cell mass as the balance between beta cell formation and loss. Beta cells are added either by replication of existing beta cells or by other sources of beta cells (OSB), and they are mainly lost through beta cell apoptosis. Since all the model parameters can be quantified with the exception of OSB, it was possible to solve for this unknown. The resulting components of beta cell turnover, i.e. new beta cell formation (replication of existing beta cells plus other sources of beta cells rather than beta cell replication) and beta cell death (apoptosis), were used to develop a population model to assess the mean age of a beta cell as well as the mean beta cell lifetime. The resulting model is a variation of the classical McKendrick-von Foerster equation and describes beta cells as a variegate population of cells that differ each other by their own age.

The novel insights that emerge by applying the model to different species, i.e. rats, monkeys, and humans are: 1) there is ongoing beta cell turnover in non diabetic rats, monkeys, and humans through adult life; 2) formation and maintenance of the population of adult beta cells largely depend on OSB in non diabetic rats, monkeys, and humans; 3) the formation of new beta cells from other sources of beta cells increases substantially in the face of the increased beta cell apoptosis in the HIP rat model of type 2 diabetes, delaying the decline in beta cell mass. In contrast, beta cell turnover is low in the

streptozotocin (STZ) monkey model of T1DM, compared to non diabetic controls. The extent that beta cells are formed in the STZ monkey is again primarily from *OSB*. 4) Beta cell replication is the primary mechanism subserving the postnatal expansion of beta cell mass in childhood, while in adulthood *OSB* is the principal mechanism for maintaining beta cell mass in face of an increased beta cell apoptosis; 5) beta cell mass and beta cell turnover increase in response to obesity in humans; 6) the estimated mean age of a beta cell (1-2 months in rats, 2-5 months in monkeys, and 6 months-2 years in humans) and the mean beta cell lifetime (1-3 months in rats, 2-5 months in monkeys, and 6 months-2 years in humans) potentially permit endogenous regeneration of beta cell mass in diabetes if beta cell turnover could be altered therapeutically.

The presented models provide, for the first time, information about sources of beta cells other than those derived from beta cell replication and estimates of the mean age of a beta cell and the mean beta cell lifetime in rats, monkeys, and humans. The results have an impact from a clinical point of view considering that: a) the origin of beta cells is actively debated, i.e. some propose duplication of existing beta cells, and others suggest formation of new beta cells from a variety of sources; b) restoration of glycemic control in type 1 and type 2 diabetes through endogenous regeneration could be a potential alternative strategy to pancreas transplantation given the insufficient number of pancreases available for transplantation and the risks of prolonged immunosuppression; c) the unique experimental approach to identify other sources of beta cells is the cell-lineage tracing that is not available in humans. Furthermore, the results encourage: a) future studies on beta cell turnover in patients with diabetes; b) the development of *ad hoc* experiments that identify the possible other sources of beta cells rather than beta cell replication; c) to plan both experiments and mathematical models to establish the forms and the time required for endogenous regeneration of beta cell mass.

Introduction

Pancreatic beta cells play an essential role in determining the amount of insulin that is secreted to maintain blood glucose levels within a narrow range [64]. Both type 1 (T1DM) and type 2 (T2DM) diabetes are characterized by a deficit in beta cell mass and increasing beta cell apoptosis [2, 13]. As a consequence of the progressive beta cell loss and dysfunction underlying both T1DM and T2DM, insulin daily demand eventually exceeds insulin secretion leading to diabetes [64]. Since the fundamental defect in both T1DM and T2DM is beta cell failure, there is increasing interest in the capacity, if any, for beta cell regeneration [15]. In this contest quantitative analysis of beta cell turnover becomes essential to understand the variety of mechanisms that regulate it, including aging effects on beta cell mass, beta cell expansion during childhood, and the ability of beta cell mass to adapt to obesity.

Beta cell mass depends on the balance between beta cell formation and loss. Beta cells are added either by replication of existing beta cells or by other sources of beta cells (OSB), and they are mainly lost through beta cell apoptosis. Prior attempts to evaluate beta cell mass balance in rodents have been reported [30, 97]. Despite the simple balance equation, these approaches present two main limitations. First, the rate of beta cell replication was estimated by bromodeoxyuridine (BrdU) incorporation into beta cells, but this cannot be employed in humans due to its toxic and mutagenic characteristics; moreover BrdU use cannot distinguish cell replication from DNA repair [15]. Second, these studies did not include the measurement of beta cell apoptosis preventing the quantification of the contribution of beta cell formation arising from beta cell replication *versus* other sources of beta cells, that is, these studies only provided a measurement of a *net balance* that included both apoptosis and OSB (called net neogenesis in [30, 97]).

These limitations are overcome by techniques adopted by the Larry Hillblom Islet Research Center (LHIRC) at University of California Los Angeles, the worldwide leading research group in the study of pancreas. The center provides unique measurements of beta cell mass, replication, and apoptosis in different species, i.e. rats, monkeys, and humans. In collaboration with the LHIRC, this PhD thesis seeks to develop models to estimate beta cell

turnover, the mean age of a beta cell, and the mean beta cell lifetime from the available measurements to address the following questions:

1. Is there ongoing beta cell turnover in non diabetic adult rats, monkeys, and humans?
2. What proportion of beta cells are derived from replication of existing beta cells versus derived from other sources of beta cells (OSB) in non diabetic rats, monkeys, and humans?
3. Is beta cell loss in the HIP rat model of T2DM and in the streptozotocin monkey model of T1DM countered by attempted beta cell regeneration, and if so to what extent do $OSBs$ contribute?
4. Which is the extent, timing, and predominant source of beta cell formation in young humans?
5. Does beta cell mass increase in response to obesity in adult humans and if so, by what mechanism?
6. What is the turnover relation to the defect? In other words, how long would it take if apoptosis was decreased to normal to restore beta cell mass?

Chapter 1 illustrates the pancreatic morphology and pathology to provide a comprehensive up-to-date review of the beta cell in health and disease. In *Chapter 2* LHIRC techniques to analyze pancreas morphology are described and the studies designed at the LHIRC to gain insights into beta cell turnover in rats, monkeys, and humans are shown. To develop models to quantify beta cell mass turnover from pancreas tissue, beta cell replication and apoptosis must be expressed as rates (mass/time). Unfortunately, the available techniques offer measurements of frequency of beta cell replication (fractional replicated beta cells) and apoptosis (fractional apoptotic beta cells). This obstacle was addressed in rat islets by the combination of time-lapse video microscopy and immunostaining techniques (*Chapter 3*). The first approach provides a measure of the event rates of beta cell replication and apoptosis (fractional replicated (apoptotic) beta cells/time), the second a measure of the corresponding frequencies. Conversion factors from the frequency to event rate are determined as the slope of the line estimated by linear regression analysis. These resulting conversion factors are used to develop dynamic models to quantify beta cell turnover based on the mass balance principle (*Chapter 4*). Then, to assess the mean age of a beta cell and the mean beta cell lifetime, a variation of the classical McKendrick-von Foerster equation is applied considering total beta cell number as a variegated population of cells that differ each other by their own age (*Chapter 4*). The development and implementation of the solutions required to address

these questions by a model-based approach in each dataset is described in *Chapter 5*. Finally, the results of the rat, monkey, and human studies shown in *Chapter 6* are discussed in *Chapter 7*.

Chapter 1

Pancreatic Beta Cells

Pancreatic beta cells play an essential role in determining the amount of insulin that is secreted to maintain blood glucose levels within a narrow range [64]. In adult humans there are 2000-3000 beta cells per islet of Langerhans [90], with approximately 1 million islets scattered throughout the pancreas. Collectively, the beta cells in the pancreas of an individual are sometimes referred as the beta cell mass [15]. Beta cell mass results from the balance between beta cell formation and loss. Beta cells are added either by replication of existing beta cells or from other sources of beta cells, and they are mainly lost through beta cell apoptosis. Both type 1 (T1DM) and type 2 (T2DM) diabetes are characterized by a deficit in beta cell mass and increasing beta cell apoptosis [2, 13]. As a consequence of the progressive beta cell loss and dysfunction underlying both T1DM and T2DM, insulin daily demand eventually exceeds insulin secretion leading to diabetes [64].

1.1 Pancreatic Islet Morphology

The islet of Langerhans or pancreatic islets are three-dimensional regions of the pancreas that contain several different cell types, including endocrine cells, endothelial cells, nerves, and fibroblasts. The islets constitute approximately 1-2% of the pancreas. Focusing on the endocrine cell composition, there are five different types of cells: insulin-producing beta cells, glucagon-producing alpha cells, ghrelin-producing epsilon cells, and somatostatin-producing delta cells [10]. As shown in Figure 1.1, the architecture of pancreatic islets differs among species [9, 16, 42]. In particular, while rodent islets are characterized by a predominant proportion of insulin-producing beta cells in the core of the cluster with few non-beta cells around the islet periphery, non-human primate as well as human islets display alpha and beta cells in close relationship each other throughout the cluster [16, 42]. There are few data about differences in islet function between rodents and

humans, but a recent report [16] suggests that differences in islet architecture are associated with differences in islet function.

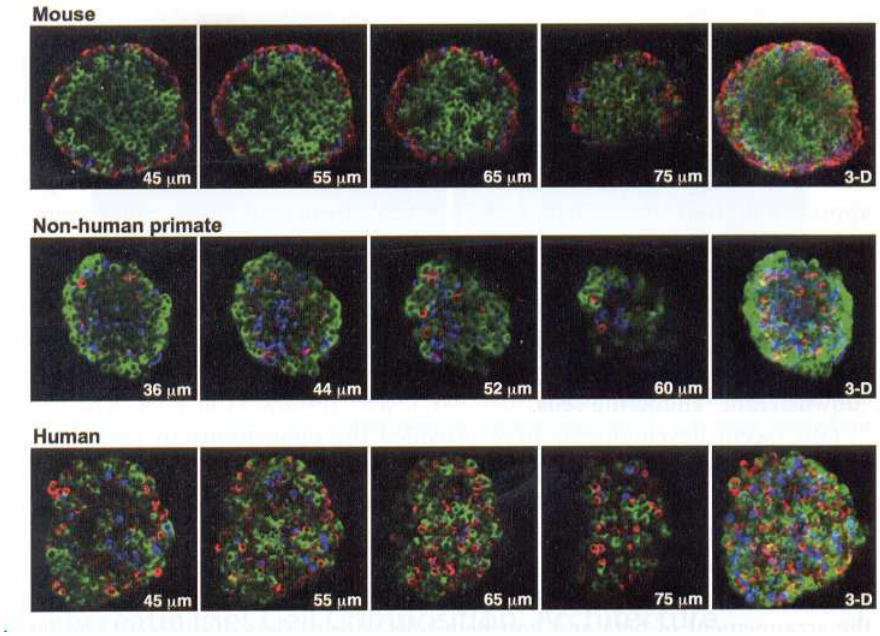

Figure 1.1: Pancreatic islets in mice, non-human primates, and humans. Series of optical sections through an entire isolated mouse (top panel), non-human primate, i.e. rhesus macaques (middle panel), and human islet (lower panel) acquired at 1μm intervals in axial (z) dimension. The stack of optical sections was 3-D reconstructed and the islet projection is shown on the right panels. Beta cells are in green, alpha cells in red, and delta cells in blue. In contrast to mouse, beta cells are intermingled with alpha and delta cells in non-human primate and human islets. Reproduced from [10].

1.2 Beta Cell Formation

Beta cell formation is complex and contributed by several mechanisms, including replication of existing beta cells and other sources of beta cells other than beta cell replication. These are considered individually below.

Replication

Beta cells expand in number after birth in both rodents and humans at least in part through the mechanism of duplication of existing beta cells, i.e. beta cell replication [25, 48, 63, 94]. The frequency of beta cell replication declines in adult through epigenetic modification of aging beta cells [12, 48,

60, 63, 98]. Like other somatic cells, beta cells regulate proliferation by entering and progressing through the growth, DNA synthesis S and mitosis M phases of the cell cycle (Figure 1.2); growth arrest occurs by exiting the cell cycle [15]. Several peptide growth factors (e.g. insulin-like growth factor-1, IGF-1) and nutrients, including glucose, have shown to increase the rate of beta cell replication [53], but these observations are based mostly on in vitro studies and it is essentially unknown what drives changes in beta cell mitosis in vivo. However, it is known that regulatory components of the cell cycle are essential for normal beta cell replication, especially D-type cyclins and cell division protein kinase 4, CDK4 [36, 51, 76].

Inappropriate beta cell proliferation could lead to the development of endocrine tumors and, consequently, tumor-suppressive processes have evolved to recognize and counteract the malignant potential of beta cells with aberrant cell cycle characteristics. These mechanisms can direct inappropriately cycling beta cells toward distinct terminal states, including cell death via apoptosis (Figure 1.2) and an irreversible form of cell cycle arrest called cellular senescence, and thereby prevent tumor development. Promoting cell proliferation as a means to expand beta cell mass as a means of regeneration thus needs to overcome these built-in cancer-preventing mechanisms, yet do so in a regulated fashion so that tumor formation is avoided [15].

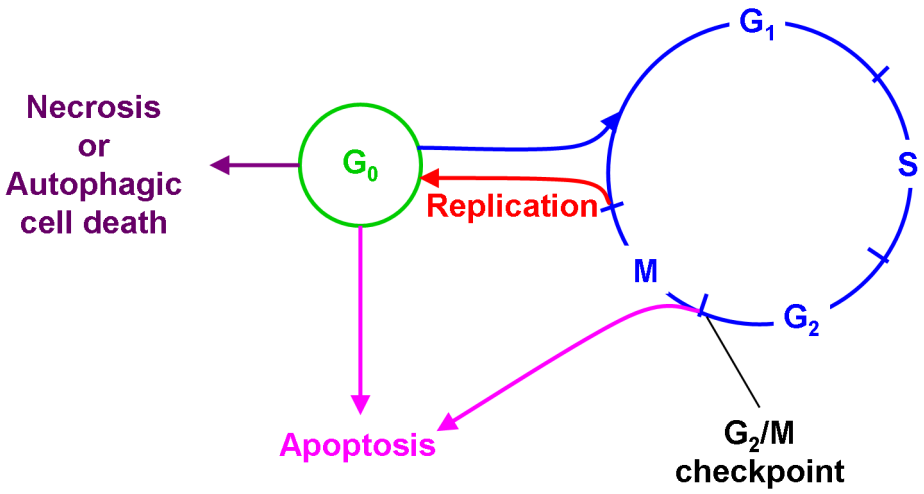

Figure 1.2: Cell cycle and cell death. Non differentiated beta cells driven from the non-dividing state, G_0, into the cell cycle will advance from G_1 and S states to the G_2/M checkpoint: here the cell decides either for replication (in red) through the M phase or apoptosis (in purple), depending on the environment of the cell. Beta cells from G_0 state may die by apoptosis, necrosis or autophagic cell death (in purple and violet).

Caution is required in interpreting studies of beta cell replication, not only because most of the studies have been undertaken in rodents, but also because the available techniques have limitations. Most of the analyses have relied on immunohistochemical or immunofluorescence techniques to quantify proliferation; these techniques include the bromodeoxyuridine (BrdU)-labeling index, and levels of the proliferating cell nuclear antigen (PCNA), phosphorylated histone H3 or replication marker Ki67. All the immunohistochemical or immunofluorescence techniques available have limitations. BrdU has been used to estimate the beta cell replication rate in rodents [31, 97], but this cannot be used in humans due to its toxic and mutagenic characteristics. Moreover BrdU as well as PCNA is expressed only in one phase (S phase) of the cell cycle and its use cannot distinguish cell replication from DNA repair [15]. Phosphorylated histone H3 is a reliable marker of the cell cycle, but very few cells are labelled, making quantification difficult [15]. Immunostaining of the nuclear protein Ki67 is an alternative method of quantifying the frequency of cell replication. Ki67 is expressed in all phases of the cell cycle except the resting phase (G_0) and for a short period at the beginning of the G_1 phase [15]. Ki67 is moreover not detectable during DNA repair. Therefore Ki67 labeling is the most sensitive and specific available technique to estimate the frequency of beta cell replication [15].

Sources other than Replication

In the immediate postnatal period beta cells can proliferate in rodents and humans, but this does not necessary mean that beta cell replication is the only responsible for generation of new beta cells. There may be other sources of beta cells other than beta cell replication. The extent to which there are potentially new sources of beta cells other than beta cell replication is controversial. It is plausible that beta cells arise from a single source, such as differentiation from a pancreatic stem pool [5, 70, 109], or from several sources. Bone marrow-derived stem cells [84], transdifferentiation of pancreatic acinar cells [54] and ductal cells [6, 7], and dedifferentiation [81] and then redifferentiation of pancreatic beta cells [38] have all been proposed. Although there has been controversy as to whether there is any source of beta cells other than duplication of existing beta cells, there is accumulating evidence in favour of such pool. For example, lineage studies reveal that pancreatic ductal cells can serve as precursors for subsequent formation of pancreatic islets or acinar cells, implying that duct cells include cells that are pluripotential [43, 103].

1.3 Beta Cell Loss

Beta cell may die either by apoptosis, necrosis or autophagic cell death. These are considered individually below.

Apoptosis

Apoptosis has come to be used synonymously with the phrase "programmed cell death" as it is a cell-intrinsic mechanism for suicide that is regulated by a variety of cellular signalling pathways. For cell death to be classified as apoptotic, nuclear condensation and fragmentation, cleavage of chromosomal DNA into internucleosomal fragments and packaging of the deceased cell into apoptotic bodies without plasma membrane breakdown must be observed (Figure 1.3, (c)). Apoptotic bodies are recognized and removed by phagocytic cells and thus apoptosis is also notable for the absence of inflammation around the dying cell. The morphologic features of apoptosis result from the activation of caspases (cysteine proteases) by either death receptor ligation or the release of apoptotic mediators from the mitochondria. Dying by apoptosis requires energy in the form of ATP; a tidy, regulated death does not come for free [27].

TdT-mediated dUTP nick-end labeling (TUNEL) determined either by immunohistochemistry or immunofluorescence is the most widely used approach to detect cell death and has the advantage in this regard, in that it detects apoptosis and necrosis in tissue samples [20, 37]. Alternative approaches to quantify apoptosis include detection of cleaved caspase-3 and annexin-V. TUNEL is usually preferred because the available antibodies for TUNEL have shown to be the most reproducibile, with those for caspase-3 being unreliable.

Necrosis

In contrast to apoptosis, necrosis has been traditionally thought to be a passive form of cell death with more similarities to a train wreck than a suicide. Necrosis is the end result of a bioenergetic catastrophe resulting from ATP depletion to a level incompatible with cell survival and was thought to be initiated mainly by cellular "accidents" such as toxic insults or physical damage. Necrosis is characterized morphologically by vacuolation of the cytoplasm, breakdown of the plasma membrane and an induction of inflammation around the dying cell attributable to the release of cellular contents and proinflammatory molecules (Figure 1.3, (d)). Cells that die by necrosis frequently exhibit changes in nuclear morphology, but not the organized chromatin condensation and fragmentation of DNA into 200 bp fragments that is characteristic of apoptotic cell death [27].

Autophagic Death

Autophagic cell death has recently been proposed as a third mechanism of cell death (Figure 1.3, (b)). It is found in certain human degenerative diseases [86]. Autophagy, under normal conditions, is an ATP-requiring regulated process in eukaryotic cells essential for cell survival that mitigates the degradation of protein complexes and organelles in their normal turnover [86]. Several autophagic genes (named *ATGs*) have been discovered that control the process of autophagy [86]. In detail, it was demonstrated that in *ATG*7 knock out mice beta cell mass and pancreatic insulin content are reduced because of increased apoptosis and decreased proliferation of beta cells [26, 46]. These results suggest that autophagy is necessary to maintain structure, mass, and function of beta cells, and its impairment causes insulin deficiency and hyperglycaemia because of abnormal turnover.

1.4 Beta Cell Size as a Contribution to Beta Cell Mass

Changes in individual beta cell size (volume) can contribute to the involution and expansion of beta cell mass [21, 56], however there is limited information as to the contribution that changes in beta cell size has in regulation of beta cell mass. It is also unknown whether a bigger beta cell actually means a larger capacity to produce, process, store, and/or secrete insulin, although this is often assumed to be the case. Physiological studies and electron microscopy analysis of big versus small beta cells are needed to address this last issue.

1.5 Beta Cells and the Pathogenesis of Diabetes

Both type 1 and type 2 diabetes are characterized by a deficit in beta cell mass and increased beta cell apoptosis [2, 13].

It is widely held that the deficit in beta cell mass in humans with T1DM is caused by autoimmune-mediated beta cell apoptosis [2]. Some data suggest that there are efforts to oppose this autoimmune-mediated destruction through increased beta cell formation. It has been noted in pancreata obtained at autopsy from patients who died shortly after development of type 1 diabetes that some islets are enlarged, with increased numbers of beta cells, compared with those in nondiabetic individuals [34]. In a case report of a man with a pancreatic tumor requiring partial pancreatectomy after relatively recent-onset type 1 diabetes, beta cell replication and beta cell

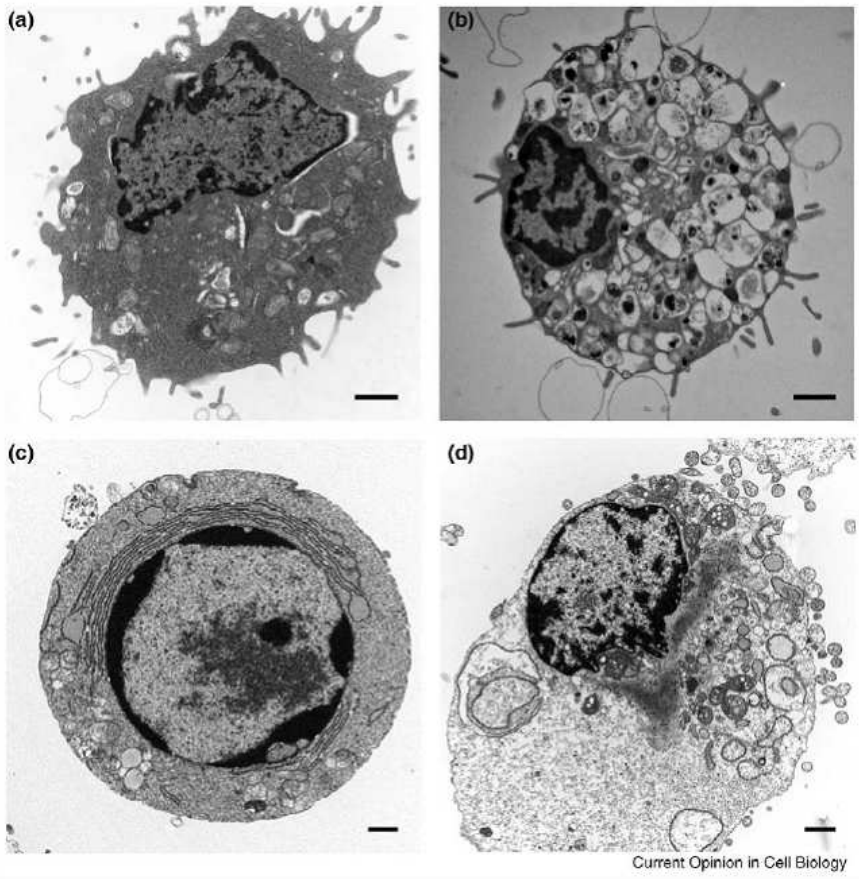

Figure 1.3: Morphological features of autophagic, apoptotic, and necrotic cells. (a) Normal, (b) autophagic, (c) apoptotic, and (d) necrotic cells. Whereas the morphological features of apoptosis are well defined, the distinction between necrotic and autophagic death is less clear. The bioenergetic catastrophe that culminates in cellular necrosis also stimulates autophagy as the cell tries to correct the decline in ATP levels by catabolising its constituent molecules. Thus, vacoulation of the cytoplasm is observed in both autophagic cells and in cells stimulated to undergo necrosis. By contrast, ATP levels are maintained in normal and apoptotic cells consistent with the limited number of autophagic vacuoles in their cytoplasm. The scale bar represents 1μm. Reproduced from [27].

apoptosis were concurrently increased [65]. Examination of pancreata from patients with long-standing T1DM often reveals a small number of beta cells accompanied by a low-grade immune infiltrate. These beta cells also have an increased frequency of apoptosis. These findings indirectly imply ongoing beta cell formation in long-standing type 1 diabetes [62]. Collectively these studies suggest that there is some capacity for beta cell formation in response to the injury of T1DM, but because the beta cell mass is approximately 80% deficient at diagnosis [34], the implication is that under these conditions beta cell formation fails to keep pace with accelerated beta cell loss.

During the cell cycle, at the G2/M checkpoint (Figure 1.2) damaged replicating cells tend to undergo apoptosis in order to avoid propagating damage [87]. A clear demonstration of this principle is the loss of small-bowel villi as a consequence of chemotherapy [105]. Villus epithelial cells are constantly shed and replaced by newly forming cells in the villus crypt. After a pulse of "proapoptotic" chemotherapy, villi collapse because cells attempting regeneration from the replicating progenitors in the villus crypt undergo a wave of apoptosis. The villus only recovers after the chemotherapy is discontinued (removing the proapoptotic signal) so that the progenitor cells in the villus crypt can replicate and regenerate the villus epithelial cells. One possibility for the failure of attempted beta cell replication to overcome beta cell apoptosis is therefore the increased vulnerability of replicating cells to apoptosis.

Whereas it is generally held that increased beta cell apoptosis in type 1 diabetes is autoimmunemediated, there is less agreement as to the primary mechanisms underpinning increased beta cell apoptosis in T2DM. Given the usual long delay between type 2 diabetes onset and diagnosis, there is, moreover, no information available from the pancreas in recent-onset type 2 diabetes in humans. In long-standing type 2 diabetes there is no adaptive increased beta cell replication despite hyperglycemia, although again this might be at least in part because of the increased vulnerability of replicating cells to apoptosis [13, 79]. Three genome-wide association studies published in 2007 that examined genetic variants predisposing to type 2 diabetes revealed several novel associations that include genes with a known role in cell development, implying that inadequate development of beta cell mass might be a risk factor for development of type 2 diabetes [85, 88, 108].

There is a wide range of beta cell mass in adult nondiabetic humans [78]. The extent of this range in obese nondiabetic humans [63] far exceeds the apparent capacity for adaptive expansion of beta cell mass in response to obesity, suggesting that the beta cell mass in an adult is dictated to a large extent by the growth during embryogenesis and childhood, although subtle differences in the rate of cell formation or loss over years could contribute to this variance. It has been suggested that the increased incidence of diabetes

in children with low birth weight might reflect inadequate expansion in beta cell progenitors during fetal development [3, 24]. The lower is the baseline beta cell mass, the smaller is the capacity to compensate for an increase in metabolic load and/or insulin demand as found in pregnancy and obesity. As such, a low beta cell mass could represent an increased risk of gestational diabetes, or progression to T2DM. In conclusion, insufficient growth of beta cell mass during development and infancy might have a role in predisposition to type 2 diabetes. Although there might be some attempted efforts at regeneration through increased beta cell replication in early-onset diabetes, these perhaps eventually fail because of the increased vulnerability of replicating cells to apoptosis.

This paragraph was partially extracted from [15].

Chapter 2

Measurements and Data

As described in *Chapter 1*, since the fundamental defect in both type 1 (T1DM) and type 2 diabetes (T2DM) is beta cell failure [2, 13], there is increasing interest in the capacity, if any, for beta cell regeneration. In this context quantitative analysis of beta cell turnover becomes important to permit an understanding of the variety of mechanisms that regulate it, including aging effects on beta cell mass, beta cell expansion during childhood, and beta cell ability to adapt to obesity. Ideally, to establish a model for beta cell turnover, beta cell mass and the rates of beta cell formation and loss would be measured in the same individual at several time points. However, it is currently not possible to measure beta cell mass, beta cell formation, and beta cell loss in vivo.

Therefore, the best approximation to this ideal currently plausible is to obtain pancreas, either after euthanasia in animals or autopsy in humans, from representative individuals in a relatively homogeneous population at different time points. The Larry Hillblom Islet Research Center (LHIRC) at University of California Los Angeles is the worldwide leading research group in this field. In this *Chapter*, LHIRC techniques to analyze pancreas morphology are described and the studies designed at the LHIRC to gain insights into beta cell turnover in rats, monkeys, and humans are shown. All data are represented as mean±SEM. Student's t-test ($P<0.05$) was performed to compare different groups.

2.1 Pancreatic tissue processing

Immediately after euthanasia or during autopsy, the complete pancreas is rapidly resected, all fat and non pancreatic tissue are trimmed, and the pancreas is weighed. A longitudinal section of the pancreas (tail through head in the flat plane of the pancreas) is fixed in formaldehyde and then embedded

in paraffin. Sections of pancreas are then taken through the fixed tissue in the plane of embedding so that a section of pancreas (head, body, and tail) through its maximal width is obtained with each section. When the complete pancreas is not available (it usually happens at autopsy), only a part of the pancreatic tissue is similarly processed. In this case, if the parenchymal volume is available by CT scan, the pancreatic weight is obtained from the volume assuming that $1cm^3$ of pancreas equals 1g. Otherwise, in humans the parenchymal volume is obtained by linear regression from age according to a population study described in [82].

2.2 Morphological Analysis

Pancreatic sections are stained for insulin (peroxidase staining) and hematoxylin to establish fractional beta cell area. As to replication and apoptosis, there are two immunostaining techniques considered equivalent: immunohistochemistry and immunofluorescence. The first requires double immunostaining for the marker of replication Ki67 (described in *Chapter 1*) and insulin, or for the TdT-mediated dUTP nick-end labeling (TUNEL) method for apoptosis (described in *Chapter 1*) and insulin (for the detailed primary antibodies see [13]). In the immunofluorescence technique pancreatic sections are stained for insulin, either Ki67 or TUNEL, and 4',6-diamidino-2-phenylindole dihydrochloride (DAPI) combined (for the detailed primary antibodies see [60, 63]).

Fractional Beta Cell Area

To determine the fractional beta cell area the entire pancreatic section is usually imaged at 40Xmagnification (4Xobjective). The ratio between beta cell area and exocrine area is digitally quantified as described in details in [13] using Image Pro Plus software.

Beta Cell Size

There are two ways to measure the mean volume of a beta cell, i.e. beta cell size. The first technique consists of scanning insulin-stained sections of pancreas (peroxidase staining) counterstained with hematoxylin/eosin by ScanScope XT System - Aperio (Vista, CA) at 20X magnification. 10 islets per case are usually selected. Each of these islets is then examined with ImageScope - Aperio software (Vista, CA) to identify 10 representative distances between the centers of adjacent beta cell nuclei. Selection criteria include clear presence of the nucleus within a beta cell, the ability to clearly

visualize nuclear boundaries, circular shape (similar dimensions in all directions), and the appearance to the observer that the nucleus had been sectioned through its maximum diameter. Once satisfied all these requirements, measurement of 100 distances is taken in each individual and the mean volume of a beta cell is calculated, considering that on average cells approximate a sphere [106]. In the second technique, the assumption that a beta cell has a spherical shape is again made, but the radius is calculated in a different way. 10 islets per each case stained for insulin and hematoxylin are selected at random and imaged at 400X (40X objective) and the mean individual beta cell cross sectional area is obtained by dividing the insulin positive area of each islet by the number of nuclei within the same insulin positive area. The mean radius of a beta cell is calculated from the resulting area.

Frequencies of Beta Cell Replication and Apoptosis

All beta cells per pancreatic section (usually two sections per individual) are examined in detail at 400X magnification (40X objective). In the section stained for insulin (marker for beta cells), Ki67 (marker for replication), and hematoxylin (marker for the nucleus in the immunohistochemistry technique) or DAPI (marker for the nucleus in the immunofluorescence technique), Ki67 and insulin positive cells are counted as well as insulin positive cells. The frequency of beta cell replication is obtained as the ratio between the number of Ki67 and insulin positive cells (i.e. replicated beta cells) and the total number of insulin positive cells in the section (i.e. beta cells). Similarly, in the section stained for insulin, TUNEL (marker for apoptosis), and hematoxylin or DAPI, TUNEL and insulin positive cells are counted as well as insulin positive cells. The frequency of beta cell apoptosis is obtained as the ratio between the number of TUNEL and insulin positive cells (i.e. apoptotic beta cells) and the total number of insulin positive cells in the section (i.e. beta cells).

Assessment of Beta Cell Mass and Number

The beta cell mass for each individual is obtained multiplying the fractional beta cell area by the pancreatic weight. Then, on the assumption that in aqueous organs, such as pancreas, 1g of weight equals $1cm^3$ of volume, in each individual the total number of beta cells is established as the ratio between beta cell mass and beta cell size.

2.3 Rat Study

In the rat study, the first purpose is to quantify beta cell turnover in wild type Sprague Dawley rats through their normal life span to address the questions: 1) is there ongoing beta cell turnover in adult rats? 2) what proportion of these cells are derived from duplication of existing beta cells versus derived from other sources of beta cells? Moreover, this study is designed to quantify beta cell turnover in a rodent model of type 2 diabetes, the HIP rat. The HIP rat is transgenic for human IAPP on a Sprague Dawley background. As previously described, this rat model of type 2 diabetes has endoplasmic reticulum stress induced beta cell apoptosis that leads to a progressive deficit in beta cell mass and develops both an anatomical (Figure 2.1) as well as functional islet phenotype comparable to that in humans with T2DM [12, 40, 60]. This study is finally designed to establish the mean age of a beta cell and the mean beta cell lifetime in WT and HIP rats.

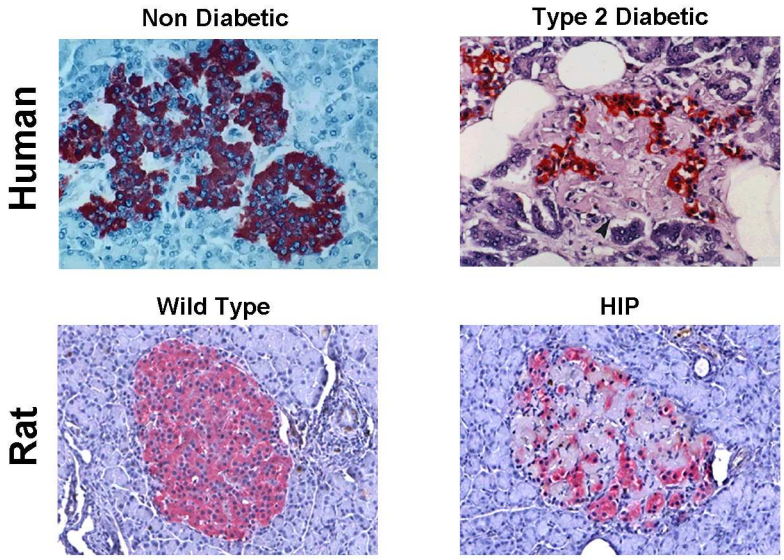

Figure 2.1: Representative pancreatic islets from non-diabetic (top left panel) and type 2 diabetic humans (top right panel) and from wild type (lower left panel) and HIP rats (lower right panel). Right panels stained for insulin (in red) show a relative loss of insulin-positive cells with amyloid deposits between cells (the pinkish material among beta cells). Reproduced from [12, 13].

Methods

Most pancreata studied here were obtained from a previously published study that reported the metabolic changes in the HIP rat versus wild type

controls from aged 2 to 10 months of age [60]. With the approval of the University of California Los Angeles - Institutional Animal Care and Use Committee, experiments were carried out in 20 wild type (WT) and 18 HIP rats, at 0.07 (i.e. 2 days), 2, 5, and 10 months of age (3-5 WT and HIP rats per type and age group). The beta cell mass and frequency of beta cell apoptosis in the 2, 5 and 10 months of age rats were included in [60]. No data from the 0.07 month rats and no beta cell replication data from any of the rats were included in that report.

Pancreatic tissues were processed as described in *Morphological Analysis* using immunohistochemistry to quantify the frequency of beta cell replication and immunofluorescence for apoptosis. These analyses were performed in a mean of 70 islets per rat. The mean beta cell size was estimated by the first technique illustrated in *Morphological Analysis - Beta Cell Size*.

Impaired Fasting Glucose by 5 Months of Age and Diabetes by 10 Months of Age in HIP Rats

The blood glucose values in the 2, 5 and 10 month old rats were previously reported [60]. Blood glucose was comparable in 2 day and 2 month old HIP and WT rats (102±2 *versus* 109±3 mg/dl in WT *versus* HIP rats). While fasting blood glucose concentrations remained unchanged in WT rats at 5 and 10 months of age (103±2 mg/dl and 100±2 mg/dl, respectively), by 5 months of age HIP rats had impaired fasting glucose (128±6 mg/dl), and by 10 months of age diabetes (185±25 mg/dl).

Decreased Beta Cell Mass and Increased Beta Cell Apoptosis by 2 Months of Age in HIP Rats

The beta cell mass and the frequencies of beta cell replication and apoptosis are shown in Figure 2.2. Beta cell mass in WT rats (Figure 2.2 - top left panel) increased from 0.9±0.2 mg at 0.07 months to 14.9±4.0 mg by 2 months. Thereafter it continued to increase: 19.2±3.5 mg at 5 months and 34.0±6.9 mg by 10 months. In HIP rats (Figure 2.2 - top right panel) beta cell mass increased similarly to WT rats until 2 months (1.9±0.6 mg at 0.07 months; 13.6±3.6 mg at 2 months), but thereafter it decreased when compared to that in WT rats: 9.9±0.8 mg ($P<0.04$) at 5 months and to 8.3±1.5 mg by 10 months ($P<0.01$).

The frequency of beta cell replication in WT rats (Figure 2.2 - middle left panel), declined from a highest value at 0.07 months of age (1.98±0.41 %), to 0.25±0.04% at 2 months, 0.24±0.05% at 5 months, and 0.13±0.07% by 10 months. The pattern was similar in HIP rats (Figure 2.2 - middle right panel): 2.0±0.9% at 0.07 months, 0.2±0.1% at 2 months, 0.5±0.1% at 5 months, and 0.2±0.0% at 10 months.

The frequency of beta cell apoptosis in WT rats (Figure 2.2 - lower left panel) was 0.21±0.08% at 0.07 months of age, decreasing to 0.03±0.02% by 2 months, thereafter remaining relatively low (0.07±0.02% at 5 months, and 0.07±0.03% by 10 months). The frequency of beta cell apoptosis was already increased in HIP *versus* WT rats by 0.07 months (0.40±0.20% at 0.07 months) and further increased by 2, 5, and 10 months: 0.18±0.04% 0.36±0.07%, 0.37±0.10% at 2, 5, and 10 months, all P<0.01 *versus* WT (Figure 2.2 - lower right panel).

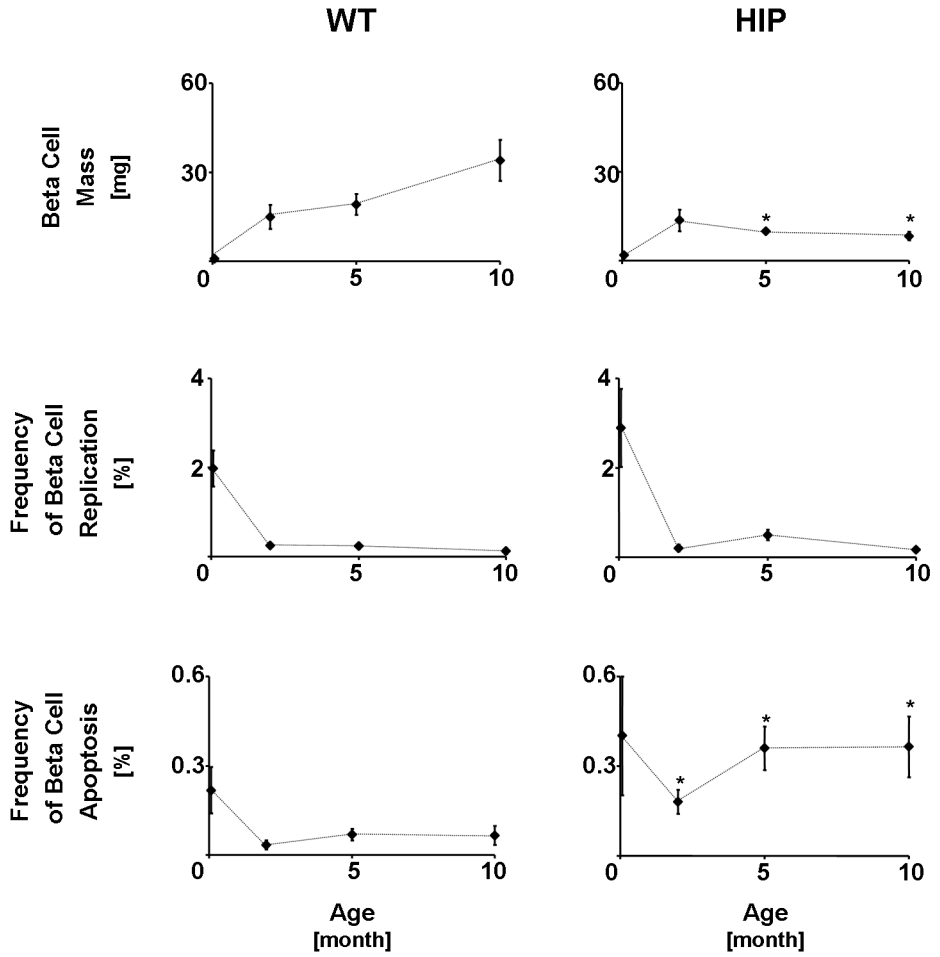

Figure 2.2: The mean beta cell mass (top panels), frequencies of beta cell replication (middle panels), and beta cell apoptosis (lower panels) in 20 WT (left panels) and 18 HIP (right panels) rats at 0.07, 2, 5, and 10 months of age. *: HIP *versus* WT, P<0.05. Bars represent SEM.

Total Beta Cell Number Showed a Pattern Similar to Beta Cell Mass

The mean individual beta cell size and the total beta cell number are shown in Figure 2.3. The mean individual beta cell size in WT rats (Figure 2.3 - top left panel) increased from 247±19 μm^3 at 0.07 months to 448±18 μm^3 by 2 months. Thereafter it remained almost constant: 416±4 μm^3 at 5 months and 443±20 μm^3 by 10 months. In HIP rats (Figure 2.3 - top right panel) the mean volume of a beta cell increased similarly to that in WT rats until 2 months (311±35 μm^3 at 0.07 months; 574±67 μm^3 at 2 months), it then decreased slightly to 486±22 μm^3 by 5 months and 10 months (460±6 μm^3).

The beta cell number, obtained by dividing beta cell mass by the average beta cell size, in WT rats (Figure 2.3 - lower left panel) increased from $(3.5\pm1.0)\cdot10^6$ at 0.07 months to $(32.3\pm7.6)\cdot10^6$ by 2 months, and thereafter it continued to increase: $(46.2\pm8.8)\cdot10^6$ at 5 months and $(78.2\pm13.3)\cdot10^6$ by 10 months. In HIP rats (Figure 2.3 - lower right panel) the number of beta cells increased similarly to that in WT rats until 2 months $(5.8\pm1.4)\cdot10^6$ at 0.07 months; $(24.7\pm6.4)\cdot10^6$ at 2 months), but thereafter decreased in comparison to WT rats: $(20.9\pm2.8)\cdot10^6$ ($P<0.03$) at 5 months and to $(18.1\pm3.0)\cdot10^6$ by 10 months ($P<0.02$).

In Figure 2.4, 100 beta cell sizes measured in a 2 day old WT rat are depicted: the reduced range of variation supports the hypothesis that beta cell size is homogeneous.

2.4 Monkey Study

The first aim of the monkey study is to address the following questions: 1) is there ongoing beta cell turnover in adult non human primates? and 2) what proportion of these cells are derived from duplication of existing beta cells versus derived from other sources of beta cells? Secondarily this study is designed to establish if there is any evidence of an adaptive increase in beta cell formation (regeneration) in a streptozotocin (STZ) model of type 1 diabetes in non human primates. Finally, the third purpose of the study is to establish the mean age of a beta cell and the mean beta cell lifetime in control and STZ monkeys.

Methods

Usually, to study beta cell turnover at non steady state, measurements of beta cell mass, beta cell replication, and beta cell apoptosis at multiple

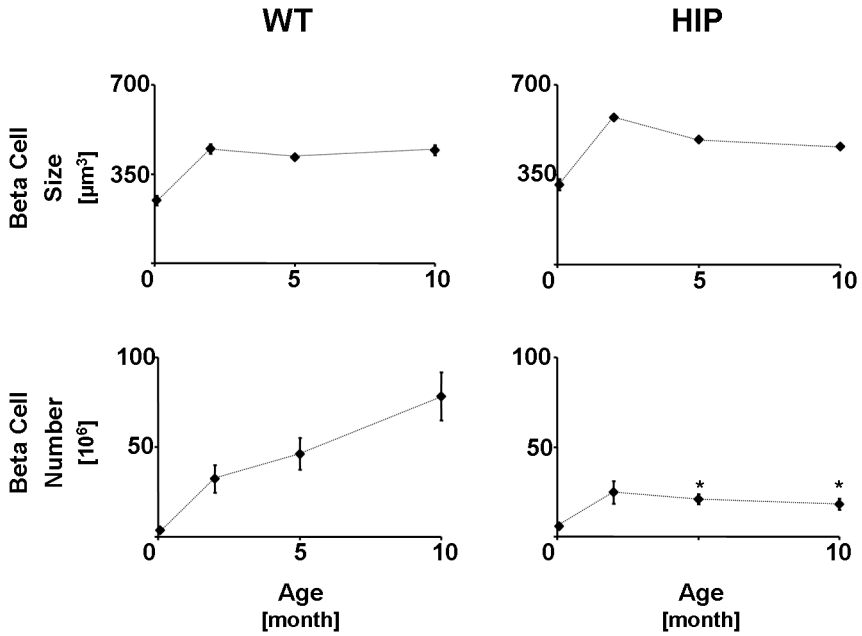

Figure 2.3: The mean individual beta cell size (top panels) and beta cell number (lower panels) in 20 WT (left panels) and 18 HIP (right panels) rats at 0.07, 2, 5, and 10 months of age. *: HIP *versus* WT, P<0.05. Bars represent SEM.

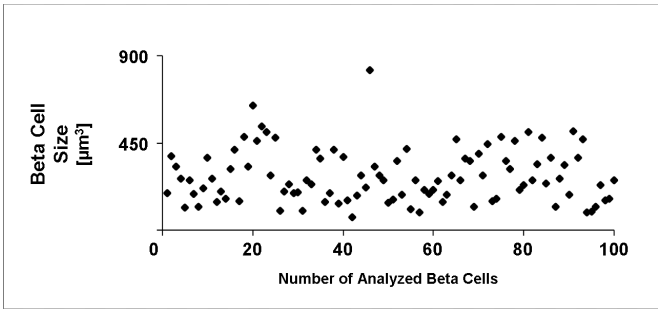

Figure 2.4: One hundred beta cell sizes measured in a 2 day old WT rat. The reduced range of variation supports the hypothesis that beta cell size is homogeneous.

different time points are required. Alternatively if beta cell turnover is at steady state, then a single time point is sufficient.

To assure that beta cell turnover was at steady state in both control monkeys and STZ diabetic monkeys, we obtained pancreas first by an open surgical biopsy and then subsequently at euthanasia from each animal. The first surgical sample was obtained one month after administration of either STZ (N=5) or saline (N=6), and the second euthanasia sample was obtained at between 2-5 months later as shown in Figure 2.5 (at euthanasia the entire pancreas was removed).

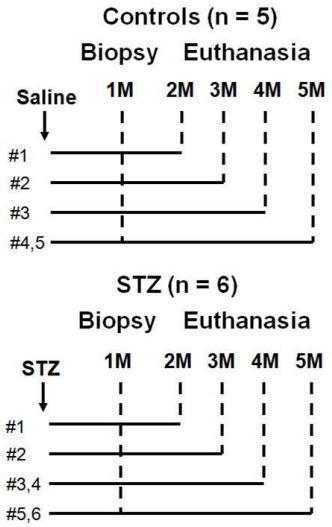

Figure 2.5: Monkey study: design protocol. Male vervet monkeys were treated with STZ (STZ group, N=6) or saline injection (control group, N=5). Pancreas open biopsy was conducted in all monkeys one month after the treatment. The same monkeys were then euthanized from 2 to 5 months after the treatment and the whole pancreas was collected.

All procedures involving animals were conducted in compliance with state and federal laws, standards of the US Department of Health and Human Services, and guidelines established by the Institutional Animal Care and Use Committee. Eleven male vervet monkeys (Chlorocebus pygerythrus, 6.4±0.2 years old) were imported from a multigenerational pedigreed colony at University of California Los Angeles Vervet Research Colony to the animal facility of Wake Forest University. All monkeys were fed on a standard chow diet (PMI Nutrition International, Brentwood, MO) and were acclimatized to place and staff prior to study. The animals were randomly divided into a control group and STZ-treated group.

To induce diabetes, monkeys were given a single dose of STZ (45 mg/kg i.v., Zanosar, SICOR Pharmaceutics, Irvine, CA) under sedation with ketamine. Control animals were manipulated similarly and given similar in-

jections (approximately 0.3 ml) of saline rather than STZ. Plasma glucose was measured 24 and 48 h hyperglycemia. All monkeys treated with STZ developed fasting hyperglycemia (>144 mg/dl) within 48 h. After induction of diabetes, we maintained post prandial glucose concentrations in the range of 200-300 mg/dl by twice daily insulin injections (70% intermediate-acting [e.g., NPH], 30% short-acting [e.g., regular] insulin, Novolin 70/30, Novo Nordisk USA, Prinston, NJ). The dose of insulin was adjusted according to biweekly postprandial whole blood glucose measurements obtained by a tail stick of non-sedated animals, and measured by a glucometer. Daily exogenous insulin requirements in the STZ group were 15.6±2.4 units (range 7 to 23 units). Control monkeys were treated with 0.2 ml of saline injected subcutaneously twice daily at the same time as diabetic monkeys received insulin.

To determine pancreas parenchymal volume, abdominal CT scans were performed at baseline, 1 month after treatment (before pancreas biopsy) and before euthanasia. There was no differences in total or parenchymal pancreas volumes in the control and STZ groups (6.7±0.3 *versus* 6.3±0.5 cm^3, P=0.5 and 5.1±0.3 *versus* 4.9±0.4 cm^3, P=0.7, respectively). The pancreas parenchymal volume did not change during the study in control or STZ groups. The mean pancreas parenchymal volume of the three measurements in each monkey was used to calculate beta cell mass.

After collection of pancreas by surgery or at euthanasia, pancreatic tissues were processed as described in *Morphological Analysis* using immunofluorescence to quantify the frequencies of beta cell replication and apoptosis. To this purpose a minimum of 100 islets per case was analyzed at biopsy; due to the smaller number of beta cells in STZ group, 5 sections (circa 500 islets) were examined at euthanasia. A total of 29895 beta cells in the control group and 8336 beta cells in STZ group were counted and included in evaluation of beta cell replication. Similarly, total 73535 beta cells in control group and 13462 beta cells in STZ group were analyzed to determine the frequency of beta cell apoptosis. The mean beta cell size was estimated by the second technique illustrated in *Morphological Analysis - Beta Cell Size*.

Induction of Diabetes

Before STZ treatment fasting plasma glucose levels were comparable in control and STZ groups (73±2 *versus* 65±5 mg/dl, control *versus* STZ groups, P=0.2). Two days after STZ injection, all monkeys in the STZ group were hyperglycemic (257±55 mg/dl) and they remained diabetic throughout the study. The HbA1c was increased in the STZ versus control group (8.1±0.3 *versus* 4.7±0.1%, one month after STZ or saline, P<0.001). Body weight did not significantly change during the study in control or STZ groups.

Decreased Beta Cell Mass in STZ monkeys

Beta cell mass was unchanged in the control group during the five month period of observation (115±22 mg *versus* 104±11 mg, biopsy *versus* euthanasia, P=0.7, Figure 2.6), assuring that beta cell mass was at steady state. As expected the STZ group had a marked (circa 90%) deficit in beta cell mass one month after STZ (12±5 mg *versus* 115±22 mg, STZ *versus* control, P<0.001, Figure 2.6), the deficit being unchanged during the subsequent five months when pancreas was procured by euthanasia (Figure 2.6).

No Differences in Frequencies of Beta Cell Replication and Apoptosis in Control *versus* STZ Monkeys

The frequency of beta cell replication was comparably low in control monkeys at both biopsy and euthanasia (0.10±0.04% *versus* 0.08±0.04%, Figure 2.7 - top panel) . Beta cell replication was also comparably low and not different between biopsy and euthanasia in STZ monkeys (0.397±0.278% *versus* 0.011±0.007%, Figure 2.7 - lower panel), although with more variance in the biopsy sample likely because of the smaller number of beta cells available to evaluate. There was no evidence of a compensatory increase in beta cell replication in response to the beta cell deficit induced by STZ (P=0.4 at biopsy; P=0.07 at euthanasia).

The frequency of beta cell apoptosis was comparable in the STZ and control monkeys one month after STZ or saline, assuring that the STZ actions to promote beta cell apoptosis were no longer present. Intriguingly the frequency of beta cell apoptosis was not influenced by the glucose concentrations of circa 200-300 mg/dl in the STZ monkeys since they remained comparable to that of the control monkeys throughout the 5 months of study (0.12±0.03% *versus* 0.12±0.06% (at biopsy, P=0.9) and 0.07±0.02% *versus* 0.08±0.04% (at euthanasia, P=0.9) in control *versus* STZ, respectively).

Total Beta Cell Number Showed a Pattern Similar to Beta Cell Mass

Beta cell size was decreased in STZ monkeys with respect to controls (419±31 μm^3 *versus* 890±65 μm^3 at biopsy; 478±34 μm^3 *versus* 839±40 μm^3 at euthanasia, P<0.0001, Figure 2.8 - top panel). Despite this, the beta cell number, obtained by dividing beta cell mass by the average beta cell size, was still higher in control *versus* STZ monkeys: $(133\pm55)\cdot10^6$ *versus* $(25\pm11)\cdot10^6$ at biopsy; $(124\pm12)\cdot10^6$ *versus* $(14\pm5)\cdot10^6$ at euthanasia, P<0.01 (Figure 2.8 - lower panel).

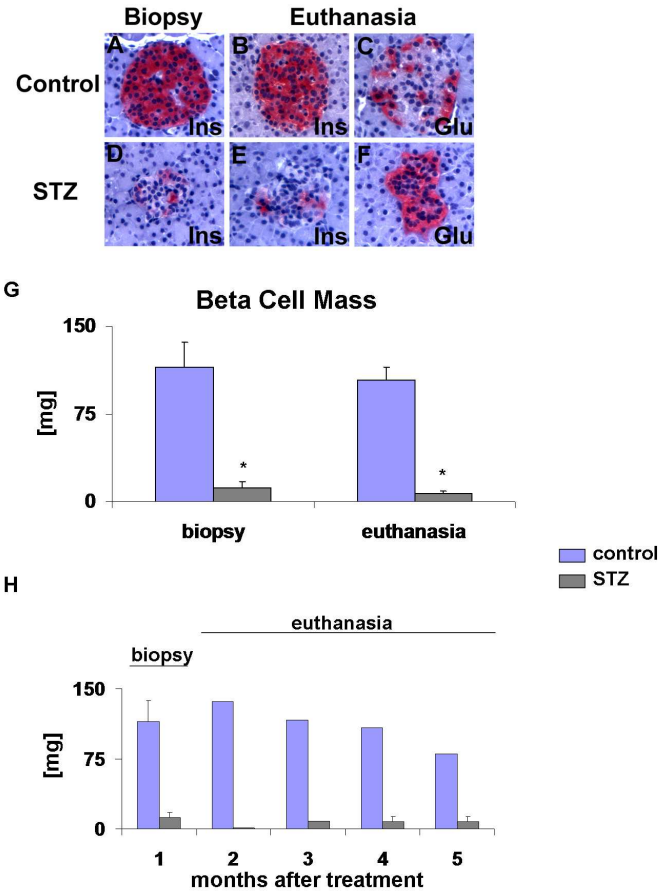

Figure 2.6: Monkey study: islet morphology and beta cell mass. A - F: islet morphology of control (top panels) and STZ groups (lower panels). 40X objective. As expected, there was no change in islet morphology between biopsy and euthanasia pancreas in control group (panels A and B; insulin in pink, nuclei in blue). In contrast, there was a marked reduction in the number of beta cells in biopsy pancreas of STZ group (panels D and E; insulin in pink, nuclei in blue) and this islet morphology with few beta cells and most alpha cells (panels C for controls and F for STZ monkeys; glucagon in pink, nuclei in blue) did not change in euthanasia pancreas. G: reduced beta cell mass in STZ monkeys (in grey) compared to controls (in azure). H: changes in beta cell mass during the study. The beta cell mass was circa 90% decreased in biopsy pancreas (1 month after the treatment) of STZ group compared to that of control group. This decreased beta cell mass did not recover during the study. * $P<0.001$ STZ *versus* control.

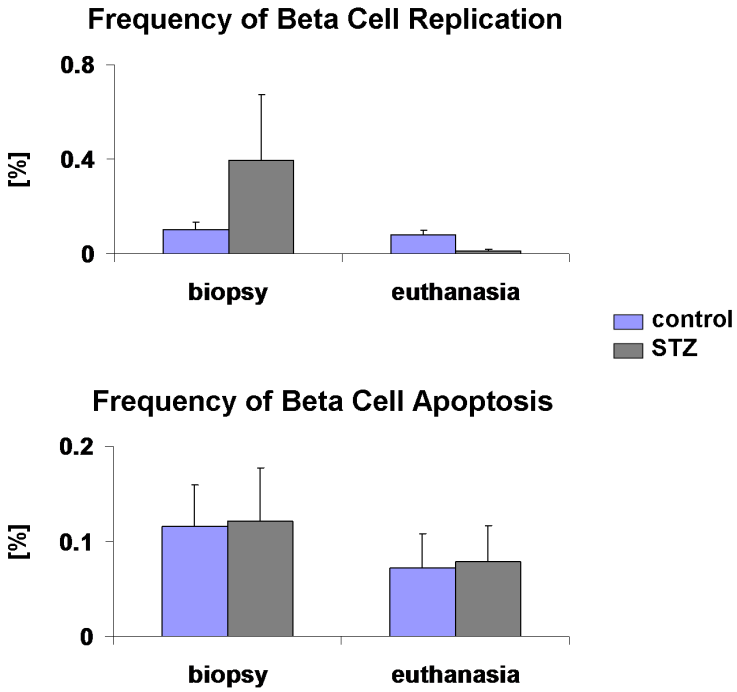

Figure 2.7: Monkey study: frequencies of beta cell replication (top panel) and apoptosis (lower panel). Despite the marked hyperglycemia, similar frequencies of beta cell replication and apoptosis were observed in STZ group (in grey) compared to control group (in azure).

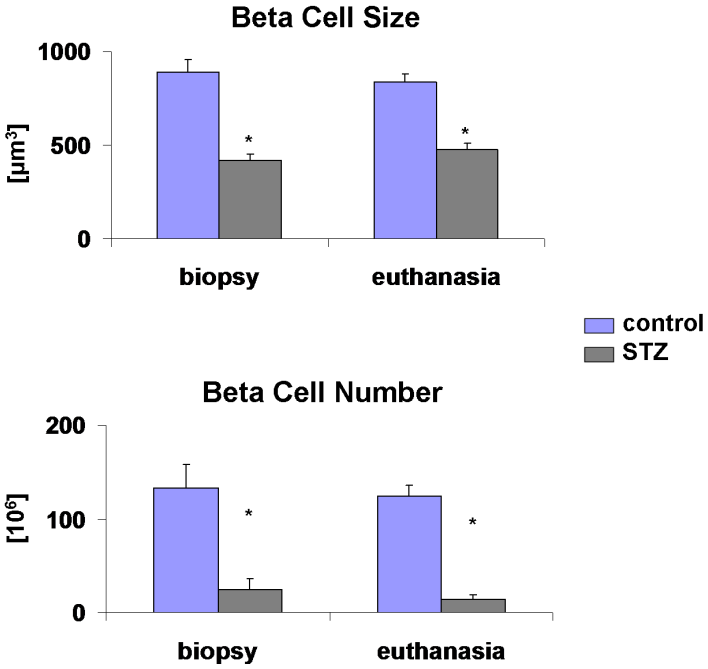

Figure 2.8: Monkey study: beta cell size and number. Mean beta cell size (top panel) and number (lower panel) were decreased in STZ group (in grey) compared to controls (in azure). * P<0.01 STZ *versus* control.

2.5 Young Human Study

In the young human study, human pancreata at autopsy from non-diabetic subjects (2 weeks-21 years of age) were examined to establish the extent, timing, and predominant source of new beta cell formation as well as the mean age of a beta cell and the mean beta cell lifetime during normal growth.

Methods

Ideally beta cell mass would be measured in vivo, but this is still not technically feasible in humans. Therefore we obtained pancreas at autopsy from 45 individuals, aged 2 weeks to 21 years, mean BMI: 17.9±0.7 kg/m^2 ([63]). Potential cases were identified by retrospective analysis of the Mayo Clinic autopsy database. To be included, cases were required to have: 1) had a full autopsy within 24 h of death and 2) pancreatic tissue stored that was of adequate size and quality. Cases were excluded if pancreatic tissue had undergone autolysis or showed evidence of acute pancreatitis. None of the individuals had a history of diabetes or any other diseases affecting the pancreas.

At autopsy pancreas is not routinely dissected free from retroperitoneal tissues to permit measurement of pancreas weight. To address this we calculated parenchymal volume from age basing on the population analysis [82]. Beta cell mass was then computed as the product of fractional beta cell area and pancreas weight under the assumption that 1g of weight equals 1cm^3 of volume.

Pancreatic tissues were processed as described in *Morphological Analysis* using immunofluorescence to quantify the frequency of beta cell replication (Figure 2.9) and immunohistochemistry for beta cell apoptosis. The mean beta cell size was estimated by the first technique illustrated in *Morphological Analysis - Beta Cell Size*.

Beta Cell Mass Increased with Age, Frequency of Replication Decreased, and Frequency of Apoptosis was Very Low

Beta cell mass (Figure 2.10 - top panel) was calculated as 35 mg in the youngest case (male, 2 weeks of age) and increased gradually to 594 mg in the oldest case (female, 21 years of age).

Frequency of beta cell replication (Figure 2.10 - middle panel) was highest in the youngest case (2.6% beta cells positive for Ki67) and substantially decreased thereafter.

Frequency of beta cell apoptosis (Figure 2.10 - lower panel) was not detectable or very low at all ages (range: 0-0.2% beta cells positive for TUNEL).

Total Number of Beta Cells Showed a Pattern Similar to Beta Cell Mass

Beta cell size (Figure 2.11 - top panel) was almost unchanged from 2 weeks ($748\mu m^3$) to 21 years of age ($692\mu m^3$).

The resulting total number of beta cells (Figure 2.11 - lower panel), calculated as the ratio between beta cell mass and beta cell size, showed a pattern similar to beta cell mass ($0.05 \cdot 10^9$ in the youngest case; $0.86 \cdot 10^9$ in the oldest case).

2.6 Adult Human Study

In the adult human study human pancreata at autopsy from adult non-diabetic subjects were examined to address the following questions: 1) is there ongoing beta cell turnover in adult humans? If so, what is the rate of turnover and source of newly formed beta cells? 2) does beta cell mass increase in response to obesity? 3) does beta cell mass change with age? 4)

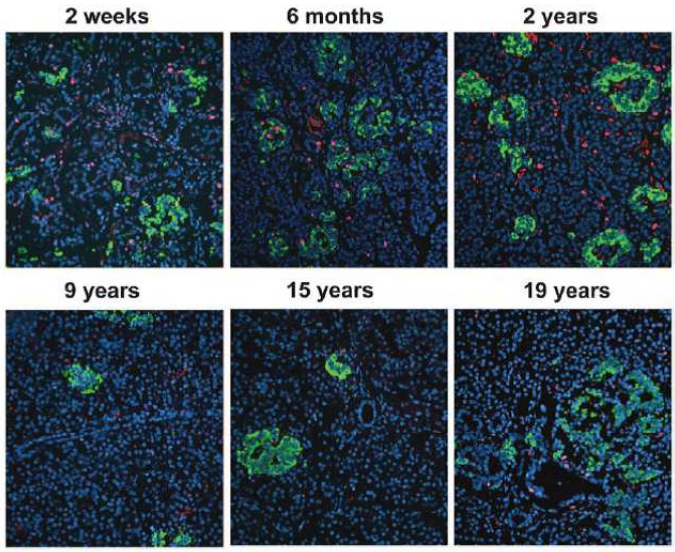

Figure 2.9: Young human study: representative pancreatic sections stained for insulin (green), Ki67 (red), and 4',6-diamidino-2-phenylindole dihydrochloride (DAPI) (blue) from six children aged 2 weeks to 19 years. Images were taken at 200X magnification (20X objective). Reproduced from [63].

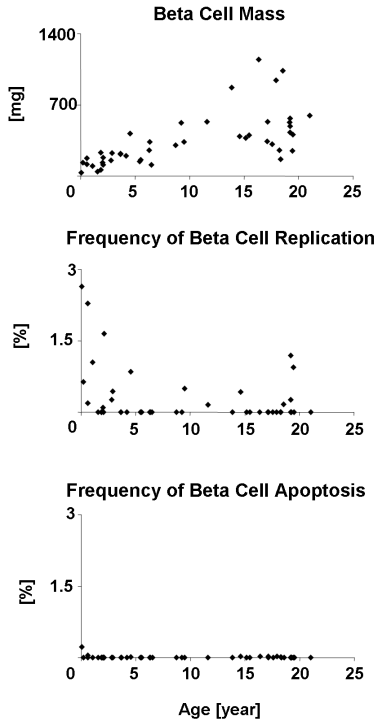

Figure 2.10: Young human study: beta cell mass (top panel) and frequencies of beta cell replication (middle panel) and apoptosis (lower panel) in 45 young humans, aged 2 weeks-21 years.

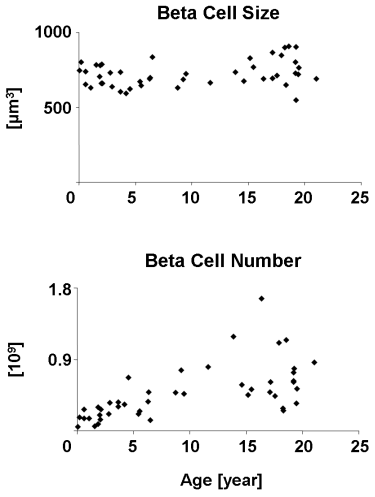

Figure 2.11: Young human study: beta cell size (top panel) and total number of beta cells (lower panel) in 45 young humans, aged 2 weeks-21 years.

how do the mean age of a beta cell and the mean beta cell lifetime change with obesity and aging?

Methods

Similarly to what was performed in the young human study, pancreata were obtained from autopsy in total 42 cases (a subgroup of the subjects reported in [82]) with a well-characterized clinical record and well-preserved pancreas suitable for morphological evaluation. The 42 subjects were divided into three groups basing on age and BMI:

- Young adult lean group: N=14; age: 20-39 years; mean BMI: 21.7 kg/m^2;
- Young adult obese group: N=13; age: 24-39 years; mean BMI: 32.8 kg/m^2;
- Elderly lean group: N=15; age: 73-97 years; mean BMI: 21.3 kg/m^2;

to study obesity (young adult obese *versus* young adult lean) and aging (elderly lean *versus* young adult lean) effects.

Parenchymal volume from age basing on the population analysis [82] was calculated. According to [82], the pancreas parenchymal volume reaches a plateau from 20 to 90 years old in lean non-diabetics (N=106, P=0.7), as well as in obese non-diabetics (N=61, P=0.2) in the range of age 20-50 years (the corresponding beta cell mass did not change with age, Figure 2.12). Beta cell mass was then computed as the product of fractional beta cell area and pancreas weight.

Pancreatic tissues were processed as described in *Morphological Analysis* using immunofluorescence to quantify the frequencies of beta cell replication and apoptosis. Total 578452 beta cells (6288±346 beta cells per section) were assessed for this analysis. The mean beta cell size was estimated by the second technique illustrated in *Morphological Analysis - Beta Cell Size*.

Increased Beta Cell Mass in Obese Young *versus* Lean Young Humans

Beta cell mass was increased by circa 50% with obesity: 751±69 mg in young adult lean *versus* 1249±131 mg in young adult obese humans ($P<0.01$); while it did not change with age: 866±168 mg in elderly lean humans (Figure 2.13 - top panel).

The frequency of beta cell replication (Figure 2.13 - middle panel) was neither altered by obesity (0.063±0.026% in young adult lean *versus*

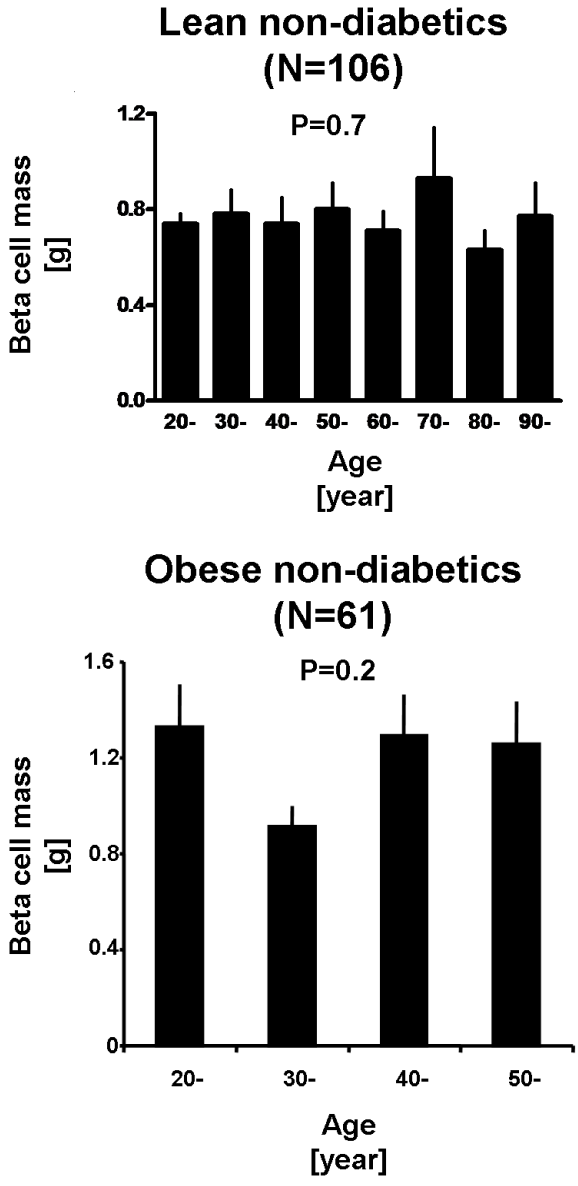

Figure 2.12: Adult human study: beta cell mass does not change with age in both lean (top panel) and obese non-diabetics (lower panel). Bars represent SEM. Reproduced from [82].

0.021±0.005% in young adult obese humans) or aging (0.022±0.008% in elderly lean humans).

Similarly, the frequency of beta cell apoptosis (Figure 2.13 - lower panel) was neither altered by obesity (0.069±0.015% in young adult lean *versus* 0.131±0.037% in young adult obese humans) or aging (0.104±0.031% in elderly lean humans).

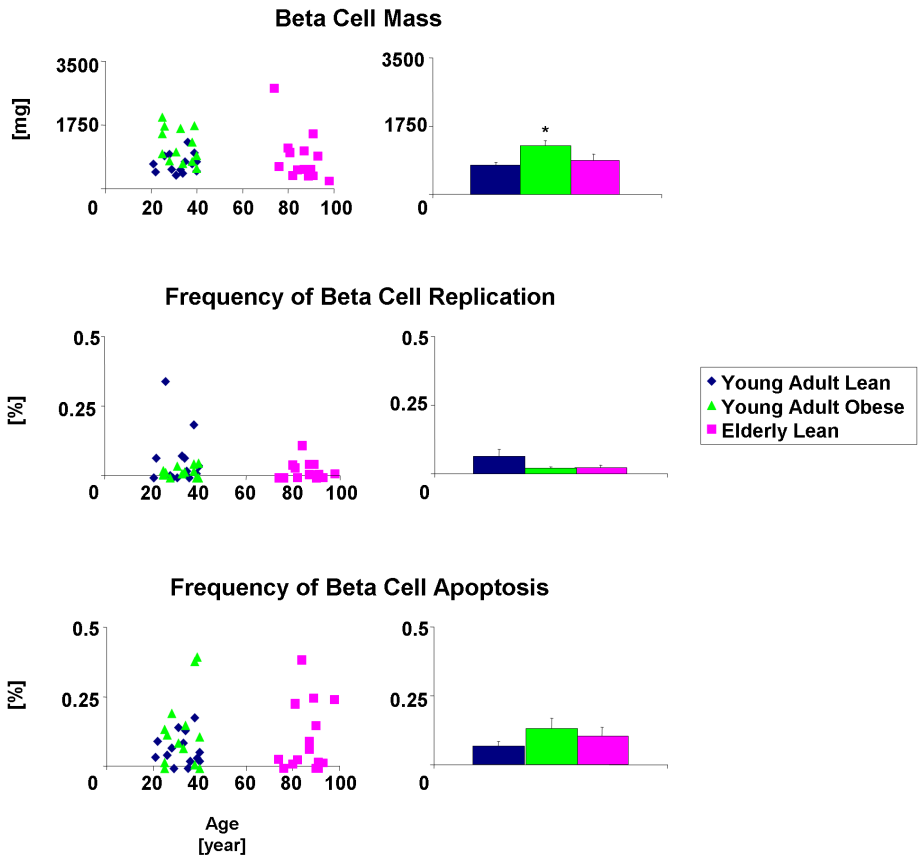

Figure 2.13: Adult human study: beta cell mass (top panels) and frequencies of beta cell replication (middle panels) and apoptosis (lower panels) in 14 young adult lean (in blue), 13 young adult obese (in green), and 15 elderly lean (in pink) humans. *: obese young *versus* lean young, P<0.05. Bars represent SEM.

Total Beta Cell Number Showed a Pattern Similar to Beta Cell Mass

Beta cell volume was increased by circa 30% with aging: 931±63 μm^3 in young adult lean *versus* 1188±94 μm^3 in elderly lean humans (P<0.05); while it did not change with obesity: 947±89 μm^3 in young adult obese

humans (Figure 2.14 - top panel).

The total number of beta cell showed a pattern similar to beta cell mass (Figure 2.14 - lower panel), i.e. there was an obesity effect on beta cell number: $(0.86\pm0.10)\cdot10^9$ in young adult lean *versus* $(1.44\pm0.20)\cdot10^9$ in young adult obese humans ($P<0.05$). Despite the significant increase in beta cell size with age, total beta cell number did not change with aging.

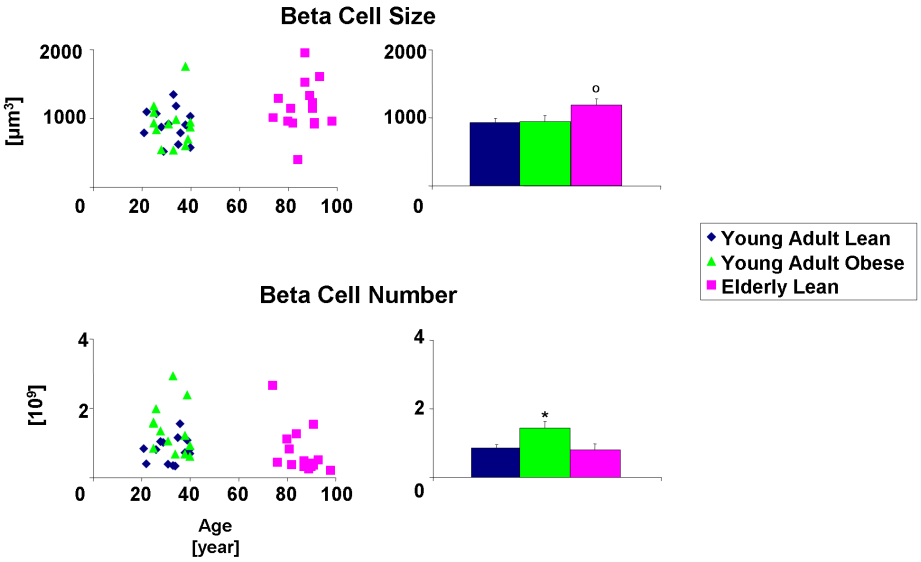

Figure 2.14: Adult human study: beta cell size (top panels) and total number (lower panels) in 14 young adult lean (in blue), 13 young adult obese (in green), and 15 elderly lean (in pink) humans. *: young adult obese *versus* young adult lean, $P<0.05$. ○: elderly lean *versus* young adult lean, $P<0.05$. Bars represent SEM.

Chapter 3

Factors to Convert Frequency to Event Rate for Beta Cell Replication and Apoptosis

To develop models to quantify beta cell mass turnover from pancreas tissue, beta cell replication and apoptosis must be expressed as rates (mass/time). Unfortunately, the available techniques offer measurements of frequency of beta cell replication (fractional replicated beta cells) and apoptosis (fractional apoptotic beta cells). This obstacle was addressed by use of islets isolated from 1 month old rats by quantifying the relationship between the event rate of beta cell replication (fractional replicated beta cells/time) observed directly by time-lapse video microscopy (TLVM) and the frequency of beta cell replication in the same islets detected by immunohistochemistry using antibodies against Ki67 and insulin in the same islets fixed immediately after TLVM. Similarly, the event rate of beta cell apoptosis (fractional apoptotic beta cells/time) was quantified by TLVM as well as the frequency of apoptosis in the same islets using TUNEL and insulin. Conversion factors (1/time) from frequency to event rate were estimated by linear regression analysis.

3.1 Assumptions

To develop conversion factors from frequency to event rate by the combination of TLVM and immunostaining techniques, the following conditions are required:

1. Steady-state event rates of beta cell replication or apoptosis present for 24 h in pilot experiments using INS-1 cells (i.e. tumor cells obtained by different levels of cytokine (toxic) mix) and isolated islets.

2. Reproducibility in identifying beta cells during TLVM from the subsequent immunostaining of islets (for insulin).

3. Observation of beta cell replication and apoptosis at a variety of event rates and frequencies to establish a relationship between these two parameters. This is particularly challenging for beta cell replication in islets, since, even in rodent islets, beta cell replication is rare in adults. The challenge was overcome by use of islets from rats at 1 month of age, when the postnatal expansion of beta cell numbers through beta cell replication is still present.

3.2 Measurements

Having established these conditions, we studied 10 sets of juvenile rat islets (5 for replication, 5 for apoptosis) under steady-state conditions of beta cell replication and beta cell apoptosis and then immunostained these same cells with Ki67 and insulin or TUNEL and insulin, respectively. From the resulting merged images, we established the relationship between the steady-state event rate of beta cell replication (by TLVM) and frequency of insulin and Ki67 positive cells by immunofluorescence. Similarly, we set up the relationship between the event rate of beta cell apoptosis (by TLVM) and the frequency of TUNEL positive beta cells by immunofluorescence. The frequency of TUNEL positive beta cells in isolated islets (0.20±0.06%) was low compared with the frequency of Ki67 positive beta cells (5.9±1.4%). Therefore, we also used a cytotoxin-treated beta cell line (cytokine mix: 0%, 50%, 100%, and 200%) to increase the event rate of apoptosis and provide a wider range of apoptosis rates to more reliably establish a relationship between the frequency of TUNEL positive cells and the observed event rate of beta cell apoptosis by TLVM.

For the detailed protocol see [83].

TLVM Images

Time-lapse images were merged into a movie and then evaluated for identification of each replication or apoptosis event. The total number of islet cells in each field was counted at the beginning of the study, and then the change in the total number of beta cells during the movie was accounted for the number of replication events subtracted by the number of apoptosis events. Replication was judged to have occurred when a single islet cell divided into

two daughter cells (Figure 3.1 - A and B). Apoptosis was judged to have occurred when an islet cell rounded up, the nucleus condensed and subsequently fragmented, and the cell cytoplasm disintegrated via cytoplasmic blebs into apoptotic bodies (Figure 3.1 - C and D). Thus the event rates of replication and apoptosis were calculated as the number of events per total number of cells per hour × 100 (%events/h). Because, in preliminary studies, most cells that spread from the islet in culture were subsequently shown to be fibroblast-like and insulin negative, we analyzed only the cells within the islet that spread in the monolayer. Although most of the islet cells within these fields subsequently proved to be beta cells, a small proportion were not. To address this issue, we determined the frequency of replication and apoptosis in beta and non-beta cells within these fields of islet cells. Given these data, we adjusted the event rates (replication and apoptosis) observed in these islet fields by TLVM by the ratio of beta cells to non-beta cells and the ratio of the frequency of events in beta cells *versus* non-beta cells determined by immunostaining in each experiment.

In INS-1 cell study, each measurement was replicated 4 times to define the event rate law of error.

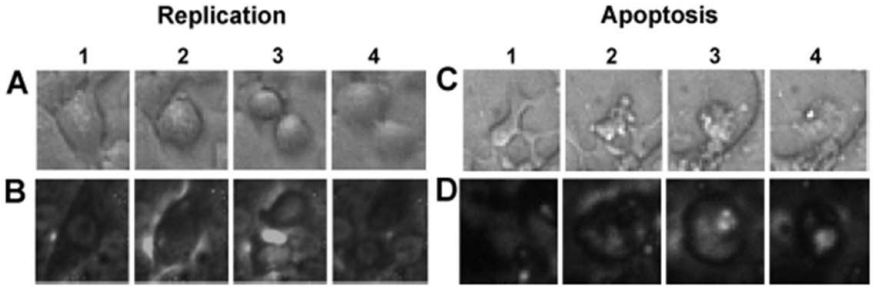

Figure 3.1: Detection of replication and apoptosis during time-lapse video microscopy. A and B: sequential images of an INS-1 cell and a rat islet cell, respectively, undergoing replication. C and D: sequential images of an INS-1 cell and a rat islet cell, respectively, undergoing apoptosis. Replication was judged to have occurred when 1 cell divided into 2 daughter cells (1-4). Apoptosis was judged to have occurred when a cell rounded up (2 and 3), the nucleus condensed and subsequently fragmented, and the cell cytoplasm disintegrated via cytoplasmic blebs into apoptotic bodies (4). Reproduced from [83].

Frequencies of Beta Cell Replication and Apoptosis

After completion of TLVM studies, culture chambers or dishes were immediately processed to obtain immunostaining images. For all 5 experiments, replication (Figure 3.2 - A) was analyzed by counting Ki67 positive beta cells in each islet (5037±220 cells analyzed per experiment), and expressed as frequency, i.e. percentage of replicated beta cells. Similarly, in the other

5 experiments, apoptosis (Figure 3.2 - B) was analyzed by counting TUNEL positive beta cells in each islet (4358±350 cells analyzed per experiment), and expressed as frequency, i.e. percentage of dead beta cells. The same approach was applied to analyze the frequency of apoptosis in a mean of 2213±218 INS-1 cells per kind of cytokine mix.

Furthermore, in INS-1 cell study each measurement was replicated 4 times to define the frequency law of error.

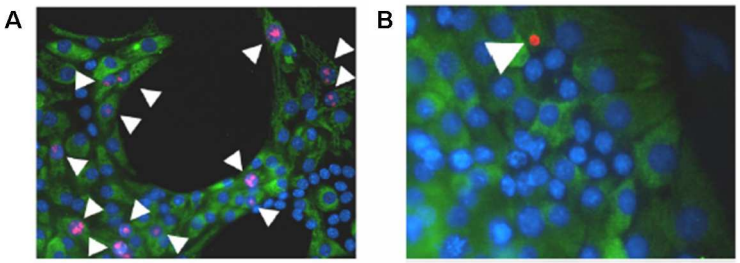

Figure 3.2: Immunostaining of rat islets for Ki67 (A) and TUNEL (B) after TLVM. Green: insulin; red: Ki67 or TUNEL; blue: nuclear 4',6-diamidino-2-phenylindole (DAPI). Most of the islet cells were insulin positive; cells that spread out from islets were most often insulin negative. Ki67 positive cells were frequently seen, and most Ki67 positive cells were insulin positive (arrowheads in C). TUNEL positive beta cells were more rare (arrowhead in D). Reproduced from [83].

3.3 Data Analysis

Values are means±SEM, except as otherwise noted. All the following algorithms were implemented by MATLAB, Version 7.6.0 (Mathworks, Natick, MA).

Laws of Error for Frequency and Event Rate

A generic law of error that links a datum D to its standard deviation SD is:

$$SD^2 = a + b \cdot D^c, \tag{3.1}$$

where a, b, and c are parameters that can assume different values. For example, when a is a constant different from zero, but b and c are zero, the law of error described by Eq. (3.1) becomes: $SD^2 = a$. That is, the standard deviation is constant, i.e. it does not depend on the datum.

Errors were assessed from replicated measurements (i.e. each datum results from the mean of 4 replicates) and then the estimates for a, b, and

c were obtained by a Non Linear Least Squares (NLLS) analysis performed on TLVM and immunofluorescence data.

Conversion Factors from Frequency to Event Rate

To determine the conversion factors from frequency to event rate a Weighted Total Least Squares (WTLS) algorithm for fitting a straight line [50] was implemented. This algorithm takes into account the errors of measurement affecting both frequency and event rate.

In details, a linear relation between the event rate (y) measured by TLVM (in %/h), and the frequency (x) measured by immunofluorescence (in %) was supposed, that is:

$$y = \alpha \cdot x. \tag{3.2}$$

where α (1/h) is the slope of the line. The intercept was set to zero, because if a 0% frequency is measured after TLVM, that event rate is 0%/h. Deming [22] faced the problem of fitting a straight line to data with errors in both coordinates by minimizing the sum:

$$\chi^2 = \sum_{k=1}^{n} \left[\frac{(x_k - X_k)^2}{{SD_{x,k}}^2} + \frac{(y_k - Y_k)^2}{{SD_{y,k}}^2} \right], \tag{3.3}$$

where (x_k,y_k) denote the given n data pairs with corresponding standard deviations ($SD_{x,k}$,$SD_{y,k}$); (X_k,Y_k) indicate points of the straight line represented by Eq. (3.2).

Although general solutions for Eq. (3.3) can be find in literature, Krystek and Anton [50] suggest a parameterization of the problem that consists in estimating the slope angle β instead of the slope α. The function to be minimized is still Eq. (3.3), but through the parameterization is possible to obtain the solution by the MATLAB function *lsqnonlin*. This function requires a user-defined vector V, so that the sum of the squares of its elements is the quantity to minimize.

According to the parameterization, the straight line to be fitted is:

$$y \cdot cos\beta - x \cdot sin\beta = 0. \tag{3.4}$$

Therefore, χ^2 has to be minimized under the constrains:

$$Y_k \cdot cos\beta - X_k \cdot sin\beta = 0, \quad for \quad k = 1, \ldots, n, \tag{3.5}$$

which is equivalent to minimizing the functional:

$$Q = \sum_{k=1}^{n} \left[\frac{(x_k - X_k)^2}{{SD_{x,k}}^2} + \frac{(y_k - Y_k)^2}{{SD_{y,k}}^2} - \lambda_k \cdot (Y_k \cdot cos\beta - X_k \cdot sin\beta) \right]. \quad (3.6)$$

A necessary condition for a minimum is that the partial derivatives of Q with respect to X_k, Y_k, and the Langrange multipliers λ_k vanish:

$$\frac{\partial Q}{\partial X_k} = \frac{\partial Q}{\partial Y_k} = \frac{\partial Q}{\partial \lambda_k} = 0, \quad for \quad k = 1, \ldots, n. \quad (3.7)$$

After some manipulations, this leads to the following expression for χ^2:

$$\chi^2 = \sum_{k=1}^{n} \left(\frac{v_k}{g_k} \right)^2, \quad (3.8)$$

where the abbreviations:

$$v_k = y_k \cdot cos\beta - x_k \cdot sin\beta, \quad (3.9)$$

$$g_k = \sqrt{SD_{x,k}^2 \cdot sin^2\beta + SD_{y,k}^2 \cdot cos^2\beta}, \quad (3.10)$$

have been introduced. Eq. (3.8) can be easily implemented by the function *lsqnonlin* considering as elements of the vector V: v_k/g_k, for $k = 1, \ldots, n$.

Once the parameter β is estimated together with its precision SD_β by minimizing the Eq. (3.8), the slope α and its uncertainty SD_α are obtained by:

$$\alpha = tan\beta, \quad (3.11)$$

$$SD_\alpha = \frac{SD_\beta^2}{cos^4\beta}. \quad (3.12)$$

3.4 Results

Law of Error for Event Rate

The general model for the law of error described by Eq. (3.1) was applied to event rate data of INS-1 cells. The following estimates for the unknown

parameters were obtained: a=0, b=1.2$(\%/h)^{-3}$, and c=5 (fit is shown in Figure 3.3). So, the resulting law of error was:

$$SD_{er}^2 = 1.2 \cdot (event \quad rate)^5, \tag{3.13}$$

where SD_{er} (%/h) is the standard deviation of TLVM measurements and $event \quad rate$ (%/h) is the event rate measurement.

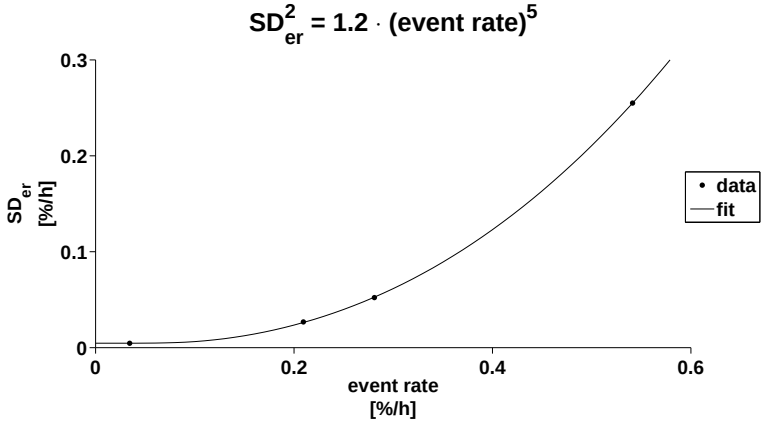

Figure 3.3: Law of error for event rate data determined on INS-1 cells. On the horizontal scale is depicted the $event \quad rate$ (%/h), on the vertical scale its standard deviation SD_{er} (%/h). Dots represent data of INS-1 cells, the continuous line is the fit obtained by the model equation shown on the top.

Law of Error for Frequency

The general model for the law of error described by Eq. (3.1) was applied to frequency data of INS-1 cells. The following estimates for the unknown parameters were obtained: a=0, b=0.11%, and c=1 (fit is shown in Figure 3.4). So, the resulting law of error was the well-known Poisson's law:

$$SD_f^2 = 0.11 \cdot frequency, \tag{3.14}$$

where SD_f (%) is the standard deviation of frequency measurements and $frequency$ (%) is the frequency measurement.

Since from Figure 3.4 SD_f seems to be linked to $frequency$ in a linear fashion, we also tried a linear model, that is:

$$SD_f = m \cdot frequency + q, \tag{3.15}$$

where m (dimensionless; value: 0.011) is the slope of the line and q (%; value: 0.061) is the intercept. The resulting Akaike indices, $2.37 \cdot 10^{10}$ for the

general model (Eq. (3.14)) and $4.21{\cdot}10^{10}$ for the linear model (Eq. (3.15)), decreed that the best model is the first.

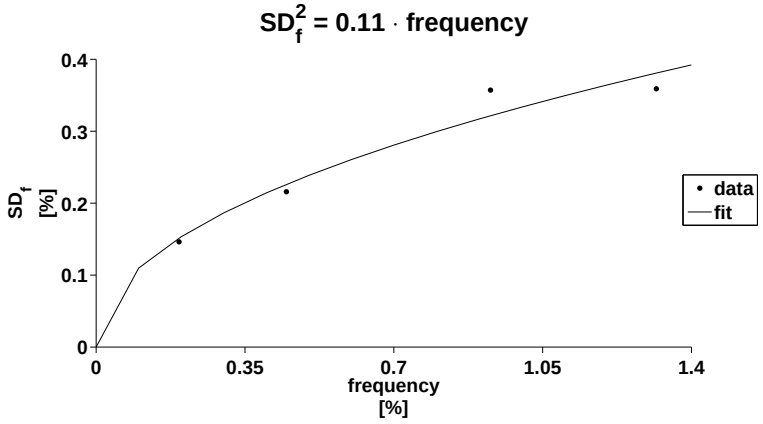

Figure 3.4: Law of error for frequency data determined on INS-1 cells. On the horizontal scale is depicted the $frequency$ (%), on the vertical scale its standard deviation SD_f (%). Dots represent data of INS-1 cells, the continuous line is the fit obtained by the model equation shown on the top.

Conversion Factor from Frequency to Event Rate for Beta Cell Replication

The relationship between the event rate (%/h) and the frequency (%) of beta cell replication evaluated on isolated islets was obtained by applying the WTLS algorithm to Eq. (3.2) ($r^2 = 0.87$, P<0.01; Figure 3.5). The resulting conversion factor from frequency to event rate for beta cell replication was:

$$\alpha_R = (0.025 \pm 0.003)h^{-1} \tag{3.16}$$

The conventional approach for error analysis, which considers errors affecting only one variable (i.e., frequency or event rate) leads to biased estimates. The conversion factor for replication is 0.028 h^{-1} when only errors in frequency are considered and event rate is assumed error free, and 0.023 h^{-1} in the reciprocate situation.

According to the conversion factor defined by Eq. (3.16), if the frequency of Ki67 positive beta cells was 1%, the corresponding event rate of replication would be 0.025%/h. These results imply that, on average, beta cell undergoing replication is Ki67 positive for circa 40 h, comparable to the duration of replication observed for other cell types [32, 33, 47, 80, 91, 100, 107]. Interestingly, this time period is similar to the doubling time of INS-1 cells, in which 100% of cells are in the active cell cycle (G1 to M phase). Moreover, Russ *et al.* [81] reported that circa 30% of human

islet cells cultured in vitro with doubling time of 7 days (circa 150 h) were positive for Ki67, which is consistent with the present conversion factor. Swenne [92, 93] reported that the cell cycle length of fetal islet cells is 14.9 h. Our estimated cell cycle length of juvenile beta cells (i.e., time during which they are Ki67 positive) was circa 40 h. This discrepancy is likely due to different techniques. Swenne used [^{3}H]thymidine to label DNA synthesis after synchronization of fetal islets by hydroxyurea to estimate cell cycle length. Since [^{3}H]thymidine incorporation occurs in DNA synthesis during the cell cycle and also with DNA repair, to the extent that the latter is present, cell replication is overestimated and computed cell length is underestimated. Using time-lapse microscopy, we previously reported that the cell cycle length of rat insulinoma cells is circa 30 h [66, 79].

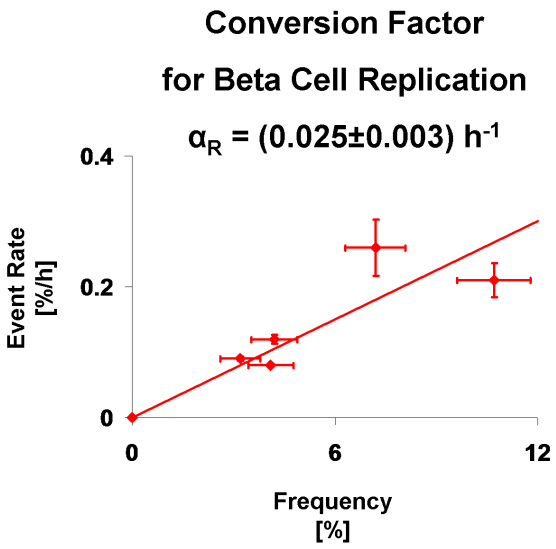

Figure 3.5: Conversion factor from frequency to event rate for beta cell replication evaluated in isolated rat islets. Data are mean±SD. Standard deviation for each datum was determined by the resulting laws of error based on INS-1 experiment (see Eqs. (3.13) and (3.14)). The continuous line was obtained by applying the WTLS algorithm to Eq. (3.2) on replication data.

Conversion Factor from Frequency to Event Rate for Beta Cell Apoptosis

The relationship between the event rate (%/h) and the frequency (%) of beta cell apoptosis evaluated on isolated islets was obtained by applying the WTLS algorithm to Eq. (3.2) ($r^2 = 0.77$, P<0.01; Figure 3.6). The resulting conversion factor from frequency to event rate for beta cell apoptosis was:

$$\alpha_A = (0.41 \pm 0.05)h^{-1} \tag{3.17}$$

The conventional approach for error analysis, which considers errors affecting only one variable (i.e., frequency or event rate) generally leads to slightly biased estimates. The conversion factor for apoptosis is 0.41 h^{-1} when only errors in frequency are considered and event rate is assumed error free, and 0.39 h^{-1} in the reciprocate situation.

The resulting conversion factor for beta cell apoptosis (Eq. (3.17)) were confirmed in INS-1 cells ($\alpha_{A,INS-1cells} = (0.38 \pm 0.05)h^{-1}$). In INS-1 cells exposed to 0-200% cytokine mix, the rate of apoptosis increased in a dose-dependent manner, while the rate of replication declined (for details see [83]), confirming that cell exposed to proapoptotic signals preferentially undergo apoptosis, rather than mitosis [28, 66].

From Eq. (3.17), if the frequency of TUNEL positive beta cells was 1%, the corresponding event rate of beta cell apoptosis would be 0.4%/h. This relationship implies that, on average, a beta cell undergoing apoptosis is TUNEL positive for circa 2.5 h, a finding that is consistent with published data from other cell types undergoing apoptosis [1, 4, 19, 29, 33, 72, 75].

Although the duration of the process of programmed cell death by apoptosis can be 12-24 h from initiation to cell disintegration, the duration of the final execution phase corresponding to nuclear condensation by light microscopy is several hours on the basis of morphological observation of the epithelial lining of the small intestine in vivo [1, 75]. TUNEL detects only this final execution phase of apoptosis (nuclear fragmentation) and is consistent with our calculated period of 2.5 h.

On a technical note, it is important to emphasize that, in this study and in those in which we have reported the frequency of apoptosis in tissues, we consider a cell to be TUNEL positive only if the nucleus is clearly positive for TUNEL staining and the cell is still distinguishable as a cell. When the rate of apoptosis is high, it is not unusual to observe TUNEL positive nuclear debris that is no longer within the confines of a cell. This debris presumably remains for variable periods after cell death, depending on the time taken for it to be cleared by macrophages. If this TUNEL positive debris is included in counts of apoptosis, the conversion factors provided here would not be valid, and the calculated rates of apoptosis would be greatly exaggerated.

The relatively short duration of the TUNEL positive final commitment phase of apoptosis implies that the frequency of TUNEL positive cells in most tissues is low. Even a relatively modest increase in frequency of TUNEL positive cells can correspond to a very significant increase in cell death through apoptosis. In addition, the relatively low frequency of apoptosis determined by TUNEL implies that it is important to evaluate a large

cell sample size to minimize sampling and counting errors, since these will be multiplied by the conversion factor. Also, since TUNEL is also positive in necrotic tissue, it is particularly important to obtain tissue that is rapidly fixed after removal. In occasional reports of frequency of apoptosis as high as 3%, the explanation would imply an explosive loss of tissue or, perhaps more likely, the presence of postmortem autolysis.

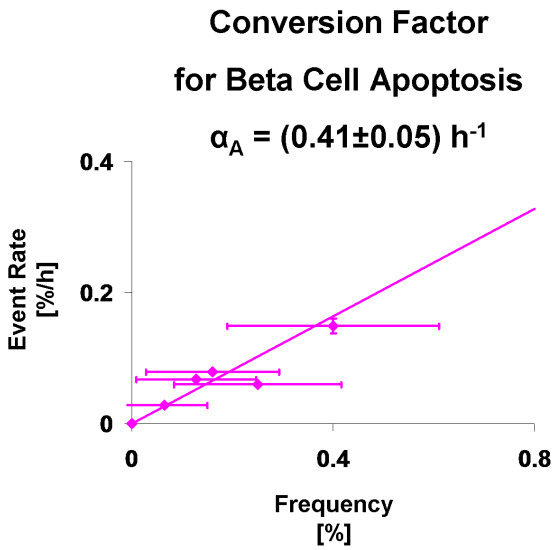

Figure 3.6: Conversion factor from frequency to event rate for beta cell apoptosis evaluated in isolated rat islets. Data are mean±SD. Standard deviation for each datum was determined by the resulting laws of error based on INS-1 experiment (see Eqs. (3.13) and (3.14)). The continuous lines was obtained by applying the WTLS algorithm to Eq. (3.2) on apoptosis data.

Chapter 4

Dynamic Models for Beta Cell Turnover and Life Span

As described in *Chapter 1*, beta cell mass results from the balance between beta cell formation and loss. Beta cells are added either by replication of existing beta cells or by other sources of beta cells, and they are mainly lost through beta cell apoptosis (Figure 4.1). Changes in individual beta cell size (volume) can also contribute to the involution and expansion of beta cell mass [21, 56], however there are no studies in literature demonstrating that its role is comparable to the contributions from beta cell formation and loss. In this chapter dynamic models to describe beta cell turnover considering changes either in beta mass or in total beta cell number are presented and the impact of beta cell size on beta cell turnover is evaluated. Finally, to assess the mean age of a beta cell and the mean beta cell lifetime, a variation of the classical McKendrick-von Foerster equation is applied considering total beta cell number as a variegated population of cells that differ each other by age.

4.1 Assumptions

To develop dynamic models for beta cell turnover the following assumptions are required.

1. The net balance of beta cells (beta cell mass or number) at any given time is a function of the rate of beta cell formation and beta cell loss.

2. Beta cell formation can be considered as the sum of beta cell formation from the duplication of existing beta cells (i.e. beta cell replication)

and the formation of beta cells from all other sources of beta cells.

3. In vivo beta cell loss is through beta cell apoptosis. Theoretically, beta cells may be lost through beta cell apoptosis, necrosis or autophagic cell death. As necrosis and autophagic death are relatively rare compared to apoptosis under physiological conditions [27], beta cell apoptosis is used as a synonym of beta cell death, where not otherwise specified.

4. Beta cell turnover is homogeneously distributed; this implies that duration of beta cell replication (apoptosis) is the same among individual beta cells and all beta cells have the same probability to replicate [8, 94] or die.

5. Changes in beta cell size (volume) are homogeneous.

6. The conversion factors for beta cell replication (Eq. (3.16)) and apoptosis (Eq. (3.17)) are applicable across the population of beta cells and are not changed by age, species, or development of diabetes. Macrophage function declines with hyperglycemia in diabetes [59] that may reduce the clearance rate of apoptotic cells and theoretically alter the conversion factor from the frequency to the rate of beta cell apoptosis. However, by design the LHIRC only counts cells as beta cells undergoing apoptosis if the cell is positive for TUNEL, the cytoplasm is positive for insulin and the cell is intact. Macrophage clearance

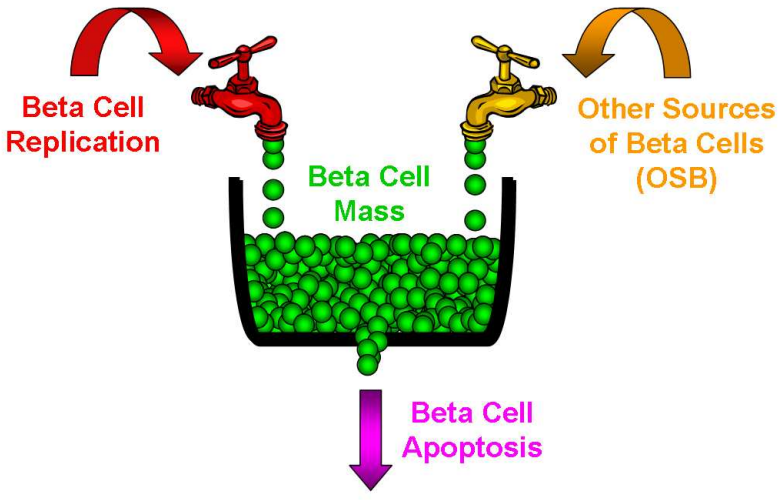

Figure 4.1: The beta cell mass depends on the balance of beta cell formation either by replication of existing beta cells (red tap) or, eventually, by other sources (orange tap), and beta cell loss (pink drain) through beta cell apoptosis.

removes cellular debris (apoptotic bodies) that is not included in our evaluation of beta cell apoptosis.

7. Since it is impossible to obtain data on beta cell turnover from an individual at multiple time points we have to assume that the behavior of a group of individuals examined at a variety of time points can be used to predict beta cell turnover over time in the population from which those individuals were sampled.

4.2 A Model for Beta Cell Mass Turnover

The model of beta cell turnover (Figure 4.1) describes beta cell mass as the balance between beta cell formation and loss. Beta cells are added either by replication of existing beta cells or by other sources of beta cells and are lost through beta cell apoptosis. The model equation is thus:

$$\frac{dM(t)}{dt} = RR(t) - RA(t) + OSB(t), \tag{4.1}$$

where: $dM(t)/dt$ (mass/time) is the mass derivative, i.e. rate of change in beta cell mass, $M(t)$ (mass); $RR(t)$ (mass/time) and $RA(t)$ (mass/time) are, respectively, rates of beta cell replication and apoptosis.

$OSB(t)$ (mass/time) indicates the contribution of Other Sources of Beta cells, i.e. from sources different from beta cell replication, to beta cell mass; t (time) is the age of an individual.

The rates of beta cell replication and apoptosis, $RR(t)$ and $RA(t)$, are respectively derived from the frequencies of beta cell replication $R(t)$ (fraction of replicated beta cells) and apoptosis $A(t)$ (fraction of apoptotic beta cells) each multiplied by the respective conversion factors (i.e. α_R (1/time) and α_A (1/time) defined in Eqs. (3.16) and (3.17)) and by beta cell mass, that is:

$$RR(t) = \alpha_R \cdot R(t) \cdot M(t), \tag{4.2}$$

$$RA(t) = \alpha_A \cdot A(t) \cdot M(t). \tag{4.3}$$

Since all model parameters in Eq. (4.1) can be quantified with the exception of the formation of beta cells from other sources than duplication of existing beta cells, it is possible to solve for this unknown. It is important to stress that the term 'other sources of beta cells' (OSB) is a mathematical term, not a term that identifies the source (or sources) of these cells.

If the frequencies of beta cell replication and apoptosis and beta cell mass are known from age t_1 to age t_2, by integrating Eq. (4.1) from t_1 to t_2, the overall OSB over the same period can be expressed as:

$$AUC_{OSB} = \Delta M - AUC_{RR} + AUC_{RA}, \tag{4.4}$$

where AUC_{OSB}, AUC_{RR}, and AUC_{RA} (mass) are the areas under OSB, RR, and RA curves, and ΔM (mass) is the change in beta cell mass from t_1 to t_2.

The time course of OSB contribution can also be determined from Eq. (4.1), rewritten as:

$$OSB(t) = \frac{dM(t)}{dt} - RR(t) + RA(t), \tag{4.5}$$

but this equation requires that the rate of change in beta cell mass is calculated.

When beta cell mass turnover is in steady state, i.e. $dM(t)/dt = 0$, $RR(t) = RR$, $RA(t) = RA$, and $OSB(t) = OSB$, Eq. (4.5) becomes:

$$OSB = -RR + RA. \tag{4.6}$$

4.3 A Model for Beta Cell Number Turnover

In Eq. (4.1) the term $OSB(t)$ includes change in beta cell mass due to both the change in number of beta cells as well as changes in the mean beta cell size (volume). Since our primary interest is the turnover of beta cells, we further refined Eq. (4.1) to focus on turnover of beta cell number as in the following equation.

$$\frac{dN(t)}{dt} = RR_N(t) - RA_N(t) + OSB_N(t), \tag{4.7}$$

where: $dN(t)/dt$ (number of beta cells/time) is the rate of change in beta cell number, $N(t)$ (number of beta cells); $RR_N(t)$ (number of beta cells/time) and $RA_N(t)$ (number of beta cells/time) are, respectively, rates of beta cell replication and apoptosis; $OSB_N(t)$ (number of beta cells/time) indicates the contribution of other sources to changes in beta cell number.

The total beta cell number, $N(t)$, is obtained by the ratio between beta cell mass $M(t)$ and the individual beta cell size (volume), assuming that in aqueous organs, such as pancreas, 1g of weight equals $1cm^3$ of volume (*Chapter 2*).

The rates of beta cell replication and apoptosis, $RR_N(t)$ and $RA_N(t)$, are respectively derived from the frequencies of beta cell replication $R(t)$ (fraction of replicated beta cells) and apoptosis $A(t)$ (fraction of apoptotic beta cells) each multiplied by the respective conversion factors (i.e. α_R (1/time) and α_A (1/time) defined in Eqs. (3.16) and (3.17), *Chapter 3*) and by beta cell number, that is:

$$RR_N(t) = \alpha_R \cdot R(t) \cdot N(t), \tag{4.8}$$

$$RA_N(t) = \alpha_A \cdot A(t) \cdot N(t). \tag{4.9}$$

In order to derive the overall contribution of OSB_N to the balance of beta cell number as well as its time course, equations similar to Eqs. (4.4) and (4.5) can be derived, that is:

$$AUC_{OSB_N} = \Delta N - AUC_{RR_N} + AUC_{RA_N}, \tag{4.10}$$

$$OSB_N(t) = \frac{dN(t)}{dt} - RR_N(t) + RA_N(t). \tag{4.11}$$

When beta cell number turnover is in steady state, i.e. $dN(t)/dt = 0$, $RR_N(t) = RR_N$, $RA_N(t) = RA_N$, and $OSB_N(t) = OSB_N$, the Eq. (4.11) becomes:

$$OSB_N = -RR_N + RA_N. \tag{4.12}$$

4.4 Impact of Beta Cell Size on Beta Cell Turnover

Since the total beta cell number, $N(t)$, is obtained by the ratio between beta cell mass $M(t)$ and the individual beta cell size, $V(t)$ (volume), beta cell mass can be written as:

$$M(t) = N(t) \cdot V(t). \tag{4.13}$$

The time derivative of Eq. (4.13), is:

$$\frac{dM(t)}{dt} = \frac{dN(t)}{dt} \cdot V(t) + N(t) \cdot \frac{dV(t)}{dt}. \tag{4.14}$$

Substituting Eq. (4.7) in Eq. (4.14) and expressing $RR_N(t)$ and $RA_N(t)$ as in Eqs. (4.8) and (4.9), it results:

$$\begin{aligned}\frac{dM(t)}{dt} &= \alpha_R \cdot R(t) \cdot N(t) \cdot V(t) - \alpha_A \cdot A(t) \cdot N(t) \cdot V(t) \\ &+ OSB_N(t) \cdot V(t) + \frac{dV(t)}{dt} \cdot N(t) \\ &= RR(t) - RA(t) + OSB_N \cdot V(t) + \frac{dV(t)}{dt} \cdot N(t). \end{aligned} \tag{4.15}$$

From Eq. (4.15), it results clear that $OSB(t)$ contains the contribution of changes in beta cell size to changes in beta cell mass, i.e.:

$$OSB(t) = OSB_N \cdot V(t) + \frac{dV(t)}{dt} \cdot N(t). \tag{4.16}$$

4.5 A Model for the Mean Age of a Beta Cell and the Mean Beta Cell Lifetime

Considering total beta cell number as a variegated population of beta cells that differ each other by age, a variation of the classical McKendrick-von Foerster equation was applied to the components of beta cell turnover to assess the mean age of a beta cell as well as the mean beta cell lifetime.

4.5.1 The McKendrick-von Foerster Equation

Let us denote as $n(a,t)$ (number of cells/time) the density of a population of beta cells of age a (time) for an individual of age t (time): death (apoptosis) results in the loss of some beta cells during the interval $(t, t+dt)$. Let $\mu(a,t)$ (1/time) denote the *per capita* death rate at age a for an individual of age t. Then:

$$n(a+dt, t+dt) - n(a,t) = -\mu(a,t) \cdot n(a,t)dt. \tag{4.17}$$

If $n(a+dt, t+dt)$ is expanded in a Taylor series and terms of order dt^2 and higher are ignored:

$$n(a+dt, t+dt) \simeq n(a,t) + \frac{\partial n}{\partial a}dt + \frac{\partial n}{\partial t}dt. \tag{4.18}$$

By using Eq. (4.18), Eq. (4.17) becomes:

$$\frac{\partial n(a,t)}{\partial a} + \frac{\partial n(a,t)}{\partial t} = -\mu(a,t) \cdot n(a,t). \tag{4.19}$$

Eq. (4.19) is the McKendrick-von Foerster equation [17]. It can be used to express the dynamics of the population of beta cells under the impact of aging and death, but does not include new beta cell formation. This component appears as a boundary (renewal) condition, defining the abundance of aged zero beta cells: $n(0,t)$ (number of cells/time).

It is possible also to define the initial age distribution, $n(a,0)$ (number of cells/time), which describes the density of beta cells of age a in an individual of age zero, i.e. at birth.

The total number of beta cells clearly equals:

$$N(t) = \int_0^\infty n(a,t)\, da. \tag{4.20}$$

For an individual of age t the ratio between the density $n(a,t)$ and the total number of beta cells $N(t)$:

$$pdf_n(a,t) = \frac{n(a,t)}{\int_0^\infty n(a,t)\, da}, \tag{4.21}$$

is the probability density function (1/time) and describes the age-based heterogeneity of beta cell population, i.e. how beta cells are distributed basing on their age.

The general relationship between the *per capita* death rate at age a for an individual of age t, $\mu(a,t)$, and the rate of beta cell apoptosis defined in Eq. (4.9) is:

$$RA_N(t) = \int_0^\infty \mu(a,t) \cdot n(a,t)\, da. \tag{4.22}$$

To estimate the mean age of a beta cell as well as the mean beta cell lifetime from the available data, the following assumptions are required (in addition to those defined in *Chapter 4 - Assumptions of Beta Cell Turnover Models*).

1. After an event of beta cell replication, one daughter cell retains the age of the parent cell and one is considered new. This implicates that the quantity $n(0,t)$ equals the new beta cell formation rate $B(t)$ (number of cells/time), i.e. the sum between the rate of beta cell replication (Eq. (4.8)) and the other sources of beta cells different from beta cell replication (Eq. (4.11)). Thus:

$$n(0,t) \equiv B(t) = RR_N(t) + OSB_N(t). \tag{4.23}$$

2. All the beta cells have the same probability to die, i.e. to undergo apoptosis. This implicates that $\mu(a,t)$ is independent from a, that is: $\mu(a,t) = \mu(t)$. Substituing this quantity into Eq. (4.22), it results:

$$RA_N(t) = \mu(t) \cdot \int_0^\infty n(a,t)\, da = \mu(t) \cdot N(t). \tag{4.24}$$

Thus:

$$\mu(t) = \alpha_A \cdot A(t). \tag{4.25}$$

That is, the quantity $\mu(t)$ equals the product of the conversion factor for beta cell apoptosis (Eq. (3.17)) by the frequency of beta cell apoptosis (expressed as fractional apoptotic beta cells).

3. Since no information is available on the initial age distribution $n(a,0)$, once option is to hypothesize that this variable has a known distribution (e.g. Gaussian, gamma, or lognormal distribution). The alternative and more convenient approach is to define plausible conditions that correspond to make this quantity negligible. In detail, considering the data described in *Chapter 2*, two different scenarios are developed.

   (a) In an aging study, when multiple data points are available, it is reasonable to assume that $t = 0$ corresponds at the start of gestation, instead of at birth. With this hypothesis $n(a,0)$, $N(0)$, $B(0)$, and $\mu(0)$ plausibly equal zero. The unknown profiles for $N(t)$, $B(t)$, and $\mu(t)$ from zero to the first available sample can be easily reconstructed by a linear, cubic spline, or piecewise cubic Hermite interpolation.

   (b) Another plausible condition occurs when $t \gg 0$ as in adulthood: in this case it is reasonable to think that the beta cells present at birth (or at the start of gestation) are dead at time t, concluding that $n(a,0)$ is negligible.

With these assumptions the McKendrick-von Foerster equation and its boundary conditions become:

$$\begin{cases} \frac{\partial n(a,t)}{\partial a} + \frac{\partial n(a,t)}{\partial t} = -\mu(t) \cdot n(a,t) \quad when \quad a,t \geq 0 \\ n(0,t) = B(t) \\ n(a,0) = 0 \end{cases} \tag{4.26}$$

4.5.2 Solution to the McKendrick-von Foerster Equation

The solution to the system (4.26) is obtained by the method of characteristics.

If $n(a,t)$ is a solution of the system (4.26), then at each point on the surface $S \equiv \{(a,t,n(a,t))\}$, the vector $(1,1,-\mu(t)\cdot n(a,t))$ of the characteristic curves must lie in the tangent plane to the surface S. Consequently, to find the solution $n(a,t)$, letting $z(r,s) = n(a(r,s),t(r,s))$, the partial differential equation in the system (4.26) is reduced to the following system of characteristic ordinary differential equations:

$$\begin{cases} \frac{da}{dr}(r,s) = 1 \\ \\ \frac{dt}{dr}(r,s) = 1 \\ \\ \frac{dz}{dr}(r,s) = -\mu \cdot z \end{cases} \tag{4.27}$$

with initial conditions:

$$\begin{cases} a(0,s) = 0 \\ \\ t(0,s) = s \\ \\ z(0,s) = B(s) \end{cases} \tag{4.28}$$

The system (4.27) is solved as follow:

$$\begin{cases} a(r,s) = r + c_1(s) \\ \\ t(r,s) = r + c_2(s) \\ \\ z(r,s) = z_0 \cdot e^{-\int_{r_0}^{r} \mu(r,s)\, dr} \end{cases} \tag{4.29}$$

Now, using the initial conditions (4.28), it is possible to define $c_1(s)$, $c_2(s)$, and z_0. Thus the system (4.29) becomes:

$$\begin{cases} a(r,s) = r \\ \\ t(r,s) = r + s \\ \\ z(r,s) = B(s) \cdot e^{-\int_{r_0}^{r} \mu(r,s)\, dr} \end{cases} \tag{4.30}$$

From the first equation of (4.30), we see that $a = r$, and therefore, $s = t - a$. Consequently, letting $n(a,t) = z(r,s)$ and using the third assumption described in the previous paragraph, the solution to (4.26) is given by:

$$n(a,t) = \begin{cases} B(t-a) \cdot e^{-\int_0^a \mu(t-x)\,dx} & when \quad 0 \le a < t \\ \\ 0 & when \quad a \ge t \ge 0 \end{cases} \tag{4.31}$$

Alternatively, the solution to (4.26) can be numerically calculated by MATLAB software, but this option was not taken into account in this thesis.

4.5.3 Mean Age of a Beta Cell

The mean age of a beta cell for an individual of age t (or at time t where t is the start of gestation) is the normalized first order momentum of the density $n(a,t)$, that is:

$$\begin{aligned} \bar{a}(t) &= \frac{\int_0^\infty a \cdot n(a,t)\,da}{\int_0^\infty n(a,t)\,da} \\ &= \frac{\int_0^t a \cdot B(t-a) \cdot e^{-\int_0^a \mu(t-a)\,da}\,da}{\int_0^t B(t-a) \cdot e^{-\int_0^a \mu(t-a)\,da}\,da}. \end{aligned} \tag{4.32}$$

When beta cell turnover is in steady state, i.e. $N(t) = N$, $B(t) = B$, and $\mu(t) = \mu$, the mean age of a beta cell (Eq. (4.32)) becomes:

$$\bar{a} = lim_{t\to\infty} \frac{\int_0^t a \cdot B \cdot e^{-\mu \cdot a}\,da}{\int_0^t B \cdot e^{-\mu \cdot a}\,da} = \frac{1}{\mu}. \tag{4.33}$$

4.5.4 Mean Beta Cell Lifetime

The probability of a beta cell surviving till age a for an individual of age t (or at time t, where $t = 0$ is the start of gestation) is given by the survivor function [52]:

$$S(a,t) = \int_a^\infty pdf_n(x,t)\,dx. \tag{4.34}$$

The *per capita* beta cell death rate $\mu(a,t)$ is related to the probability density function $pdf_n(a,t)$ and to the survivor function $S(a,t)$ by [52]:

$$\mu(a, t-a) = \frac{pdf_n(a,t)}{S(a,t)}. \tag{4.35}$$

Since $pdf_n(a,t) = -S'(a,t)$ (Eq. (4.34)), Eq. (4.35) implies that:

$$\mu(x, t-x) = -\frac{\partial}{\partial a} log S(x,t). \tag{4.36}$$

Thus:

$$log S(x,t)|_0^a = -\int_0^a \mu(x, t-x)\, dx, \tag{4.37}$$

and, since $S(0,t) = 1$, it results that:

$$S(a,t) = e^{-\int_0^a \mu(x,t-x)\, dx}. \tag{4.38}$$

According to the second assumption (i.e. all the beta cells have the same probability to die), Eq. (4.38) becomes:

$$S(a,t) = e^{-\int_0^a \mu(t-x)\, dx}. \tag{4.39}$$

We can note that the quantity that multiply $B(t-a)$ in the solution (4.31) is the survivor function: thus, this solution states that the density of beta cells of age a for an individual of age t (or at time t, where t is the start of gestation) is constituted by those beta cells born at time $t-a$ that survive till age a.

The mean beta cell lifetime (time) in an individual of age t (or at time t, where $t = 0$ is the start of gestation) is:

$$\bar{l}(t) = \int_0^t S(a,t)\, da = \int_0^t e^{-\int_0^a \mu(t-x)\, dx}\, da. \tag{4.40}$$

In steady state conditions, the mean beta cell lifetime is:

$$l = lim_{t\to\infty} \int_0^t e^{-\mu \cdot a}\, da = \frac{1}{\mu}, \tag{4.41}$$

which corresponds to the mean age of a beta cell (Eq. (4.33)).

It is important to note that all the analysis related to the mean age of a beta cell and to the mean beta cell lifetime is consistent as long as the new beta cell formation and the *per capita* beta cell death rate are different from zero.

Chapter 5

Implementation

To apply the models introduced in *Chapter 4* to rat, monkey, and human data (*Chapter 2*) some implementing solutions must be established considering the heterogeneity of the different datasets. Moreover, dynamic models for beta cell turnover (Eqs. (4.1) and (4.7)) require that we calculate the rate of change in beta cell mass and number: for this purpose a new algorithm based on a stochastic regularization method [23] is presented.

5.1 Smoothing and Time-Derivative in One Step

Eqs. (4.1) and (4.7) require that the rate of change in beta cell mass and number are calculated. For this purpose a new algorithm developed by Prof. Giovanni Sparacino (Department of Information Engineering, University of Padova) and based on a stochastic regularization method [23] is applied.

Traditional methods evaluate the derivative using a two-step process, i.e., the data is first smoothed followed by numerical estimation of the derivative. In contrast the new algorithm, by simultaneously performing both data regularization and calculation of the derivative, provides an estimate of the derivative together with its uncertainty on a uniform, arbitrarily defined grid.

To obtain $OSB(t)$ ($OSB_N(t)$) on the same fine grid, smoothed mean profiles for $RR(t)$ ($RR_N(t)$) and $RA(t)$ ($RA_N(t)$) are evaluated using the same algorithm.

5.1.1 Simultaneous Smoothing and Time-Derivative Calculation as a Deconvolution Problem

Let $c(t)$ and $u(t)$ be two continuous-time signals with:

$$u(t) = \frac{dc(t)}{dt}. \tag{5.1}$$

For a generic t_0, the following integral equation holds:

$$c(t) = c(t_0) + \int_{t_0}^{t} u(\tau)\, d\tau. \tag{5.2}$$

Assuming for simplicity that t_0=0 and $c(0)$=0, we can rewrite Eq. (5.2) as:

$$c(t) = \int_{0}^{t} g(t-\tau) \cdot u(\tau)\, d\tau = g(t) * u(t), \tag{5.3}$$

where $g(t)$ is the step function, i.e. $g(t)$=0 for $t < 0$ and $g(t)$=1 for $t \geq 0$, and the symbol $*$ denotes the convolution. Eq. (5.3) represents a convolution integral. The problem of recovering $u(t)$ from the time-series $\{y_k\}$, k=1, ..., n, of the noisy samples of $c(t)$, is a deconvolution problem.

Deconvolution is known to be an ill-conditioned problem and there are several approaches that can be used. These methods can be divided into two families referred to as parametric and non-parametric deconvolution. Parametric deconvolution assumes the analytic expression for the input to be known expect for a small number of parameters, so that the deconvolution problem becomes a parameter estimation problem [101, 102]. The second family of deconvolution methods does not require the assumption of a analytic form of the input. The most widely used non-parametric approach goes under the name of regularization, traces back to the historical works by Phillips [73] and Tikhonov [96], and presents a huge number of variants and implementations at a different stage of sophistication, e.g. [23, 39, 41, 57].

5.1.2 Algorithm

Among the various deconvolution approaches available in the literature, a modification of the regularization approach presented in [23] was implemented. In regularization, to preserve the regularity of $\hat{u}(t)$, $\hat{c}(t) = g(t)*\hat{u}(t)$, evaluated at the sampling instants, does not fit exactly the noisy $c(t)$ samples, $\{y_k\}$, with the distance determined by the value of a scalar parameter called the regularization parameter. In other words, in regularization $\hat{c}(t) = g(t) * \hat{u}(t)$ is a smoothed version of the measured time-series $\{y_k\}$. Therefore, regularization allows to estimate simultaneously the function which smoothes the original time-series and its first time-derivative.

Let $\Omega_S = \{t_1, t_2, \ldots, t_n\}$ be the sampling grid which the samples of the time-series $\{y_k\}$ have been collected over, and $\Omega_V = \{T_1, T_2, \ldots, T_N\}$

an arbitrary, much finer ($N \gg n$), uniform grid, called the virtual grid; Ω_V must contain Ω_S. The virtual grid is so fine that, over it, the unknown input $u(t)$ can arbitrarily be described well by a piecewise constant function. Let $c_V(T_K)$ denote the ideal noise-free sample of $c(t)$ at time T_K, belonging to the virtual grid. Assuming that $u(t)$ is piecewise constant within each time interval of the virtual grid, from Eq. (5.3) it follows that:

$$\begin{aligned} c_V(T_K) &= \int_0^{T_K} g(T_K - \tau) \cdot u(\tau)\, d\tau \\ &= \sum_{i=1}^{k} u_i \cdot \int_{T_{i-1}}^{T_i} g(T_K - \tau)\, d\tau \end{aligned} \tag{5.4}$$

where T_0=0. Adopting a matrix notation it results: $c_V = G_V \cdot u$, where c_V and u are N-dimensional vectors obtained by sampling $c(t)$ and $u(t)$ on the virtual grid, and G_V is a NXN lower triangular matrix. Defining G the nXN matrix obtained by removing from G_V those rows that do not correspond to sampled output data, the measurement vector $y = [y_1, y_2, \ldots, y_n]^T$ is thus:

$$y = G \cdot u + v, \tag{5.5}$$

where $v = [v_1, v_2, \ldots, v_n]^T$ is the n-dimensional measurement error vector and $u = [u_1, u_2, \ldots, u_N]^T$ is the N-dimensional vector so that its elements are the values of $u(t)$ on the virtual grid. The vector v of error of measurements is random and some information on its statistics is usually available. Often v is Gaussian, zero mean and with covariance matrix Σ_v which can be usefully described by: $\Sigma_v = \theta^2 \cdot B$, where B is a nXn positive definite matrix assumed to be known and θ^2 is a scale factor that can be unknown. Often measurement errors are independent so that B is diagonal. For example, assuming a constant coefficient of variation for the measurement error, CV (dimensionless), thus: $B = diag(y_1^2, y_2^2, \ldots, y_n^2)$ and $\theta = CV$. Otherwise, if the standard deviation of the measurement error, SD, is constant, thus: $B = I_n$ and $\theta = SD$, where I_n is the n-dimension identity matrix.

The regularization method provides an estimate of u from y of Eq. (5.5) by solving the optimization problem:

$$min_{\hat{u}}(y - G \cdot \hat{u})^T \cdot B^{-1} \cdot (y - G \cdot \hat{u}) + \gamma \cdot \hat{u}^T \cdot F^T \cdot F \cdot \hat{u}, \tag{5.6}$$

where F is a NXN penalty matrix (see below) and γ is a real non negative parameter. Problem defined by Eq. (5.6) is quadratic and its solution:

$$\hat{u} = (G^T \cdot B^{-1} \cdot G + \gamma \cdot F^T \cdot F)^{-1} \cdot G^T \cdot B^{-1} \cdot y, \tag{5.7}$$

linearly depends on the data vector y.

The cost function in Eq. (5.6) is made up of two terms. The first one penalizes the distance, weighted by the inverse of B, between model predictions $\hat{c} = G \cdot \hat{u}$ (the reconvolution vector) and data. The second contribution, i.e. $\hat{u}^T \cdot F^T \cdot F \cdot \hat{u}$, is a term that penalizes the "roughness" of the estimate of $u(t)$ measured by the energy of its $m-th$ order time-derivative. Theory on how to choose m is not available in the literature, but since this choice is commonly recognized to be not a major issue, $m = 1$ or $m = 2$ are normally used (the user finds out *a posteriori* which is the most appropriate value). These values correspond to select $F = D^m$, where D is a NXN lower-triangular Toepliz matrix whose first column is: $[1, -1, 0, \ldots, 0]^T$.

In Eq. (5.6) the relative weight given to data fit and solution regularity is governed by the so called regularization parameter γ. The choice of the regularization parameter is known to be crucial: too high values of γ would lead to very smooth estimates of $\hat{u}$ which may be not able to explain the data y (over-smoothing), while too small values of γ would lead to ill-conditioned solutions $\hat{u}$ that accurately fit the data y, but exhibit spurious oscillations due to their sensitivity to noise (under-smoothing).

One of the possible strategies to fix the regularization parameter on a sound statistical basis resorts to Maximum Likelihood (ML) and can be applied in both the known and unknown θ^2 cases [23]. Let $WRSS = (y - G \cdot \hat{u})^T \cdot B^{-1} \cdot (y - G \cdot \hat{u})$ and $WESS = \hat{u}^T \cdot F^T \cdot F \cdot \hat{u}$ denote the weighted residuals sum of squares and the weighted estimates sum of squares, respectively, and $q(\gamma) = trace(G \cdot (G^T \cdot B^{-1} \cdot G + \gamma \cdot F^T \cdot F)^{-1} \cdot G^T \cdot B^{-1})$ indicate the equivalent degrees of freedom associated with γ. The regularization parameter should be fixed as follows:

- When θ^2 is known, tune γ until:

$$WESS = \theta^2 \cdot \frac{q(\gamma)}{\gamma}; \tag{5.8}$$

- When θ^2 is unknown, tune γ until:

$$\frac{WRSS}{n - q(\gamma)} = \gamma \cdot \frac{WESS}{q(\gamma)}; \tag{5.9}$$

  and estimate *a posteriori* θ^2:

$$\hat{\theta}^2 = \frac{WRSS}{n - q(\gamma)}. \tag{5.10}$$

In [23], it is shown that, as the virtual grid gets finer and finer (i.e. $N \to \infty$) an estimate of $u(t)$ asymptotically continuous up to any desired

order of time-derivatives is eventually obtained, even when the available data are collected on a sparse (non uniform) sampling grid. The degree of continuity reflects the value of the integer parameter m selected by the user in the definition of the penalty matrix F. For instance, the typical choices of $m = 2$ or $m = 1$ lead to estimates of $u(t)$ asymptotically continuous at least up to the third or first time-derivatives, respectively. At the same time, since in our problem $g(t)$ is a step function, the corresponding estimates of $c(t)$ will be continuous at least up to the fourth or second time-derivatives, respectively.

5.2 Rat Study

Experiments were carried out in 20 WT and 18 HIP rats, at 0.07 (i.e. 2 days), 2, 5, and 10 months of age (3-5 WT and HIP rats per type and age group). As described in *Chapter 4*, we have to assume that the behavior of a group of individuals examined at a variety of time points can be used to predict beta cell turnover over time in the population from which those individuals were sampled. Beta cell mass (M), number (N), rates of beta cell replication (RR and RR_N) and apoptosis (RA and RA_N) were obtained by averaging the corresponding data at each time point. The rates of beta cell replication (RR and RR_N) and apoptosis (RA and RA_N) were obtained by Eqs. (4.2), (4.8), (4.3), and (4.9).

Working on the mean data, in both WT and HIP rats it was possible to assess:

- *The overall contributions to beta cell mass and number turnovers.* The net change in beta cell mass ΔM equaled the difference between beta mass at ages 10 and 0.07 months (i.e. $\Delta M = M(10) - M(0.07)$). Similarly, the net change in beta cell number ΔN equaled the difference between beta number at ages 10 and 0.07 months (i.e. $\Delta N = N(10) - N(0.07)$). The overall contributions from rates of beta cell replication and apoptosis (AUC_{RR} and AUC_{RR_N}; AUC_{RA} and AUC_{RA_N}) were calculated as areas under the corresponding curves by the trapezoid method. Finally, the overall contributions to beta cell mass and number from other sources of beta cells (AUC_{OSB} and AUC_{OSB_N}) were obtained by Eqs. (4.4) and (4.10), respectively.

- *The time profiles of the contributions to beta cell mass and number turnovers.* The new algorithm proposed at the beginning of this *Chapter* was applied to beta cell mass (number) mean data in the period 0.07-10 months to obtain a smoothed profile for beta cell mass (number) and an estimate of beta cell mass (number) derivative together with its uncertainty on a uniform grid (step of the virtual grid: 0.01

month). On the same fine grid, smoothed mean profiles for rates of beta cell replication and apoptosis were evaluated using the same algorithm. Finally, the time profile for OSB (OSB_N) resulted from Eq. (4.5) (Eq. (4.11)).

All the smoothed profiles were obtained by assuming that the measurement error equals the standard deviation (i.e. inter-rat variability) associated to each mean datum. Then, the approach of propagation of errors to establish the variance in the computed OSB (OSB_N) was used; taking this variance into account the hypothesis that OSB was different from zero was tested.

To verify the consistency between the overall contribution from other sources of beta cells over the period of the study, i.e. AUC_{OSB} (AUC_{OSB_N}), and OSB (OSB_N), the area under the curve of the latter was calculated by the trapezoid method and compared to AUC_{OSB} (AUC_{OSB_N}).

- *The impact of beta cell size on beta cell turnover.* Beta cell turnover was compared by two models: the first considering beta cell mass (Eq. (4.4)), where the term AUC_{OSB} includes changes in beta cell mass due to both the change in number of beta cells by other sources and changes in the mean beta cell size (*Chapter 4*), and the second based on beta cell number (Eq. (4.10)). To make possible this comparison, the overall contributions from beta cell replication, apoptosis, and other sources of beta cells defined in Eqs. (4.4) and (4.10) were expressed as percentage of ΔM and ΔN, respectively. Then, the percent relative differences between these overall contributions from mass and number were obtained. For example, considering beta cell replication, the resulting percent relative difference was:

$$\frac{\frac{AUC_{RR}}{\Delta M} - \frac{AUC_{RR_N}}{\Delta N}}{\frac{AUC_{RR_N}}{\Delta N}} X 100. \tag{5.11}$$

Based on the values assumed by these percent relative differences, it was possible to define the role of beta cell size.

- *The mean age of a beta cell and the mean beta cell lifetime.* As described in *Chapter 4*, to estimate the mean age of a beta cell and the mean beta cell lifetime from the available data it was reasonable to assume that $t = 0$ corresponds to the start of gestation. In a rat, the mean period of gestation is circa 21 days (i.e. 0.7 month). To calculate the mean age of a beta cell the following steps were required:

  1. The mean smoothed profiles of total number of beta cells, $N(t)$ (Eq. (4.7)), new beta cell formation, $B(t)$ (Eq. (4.23)), and the

per capita beta cell death rate, $\mu(t)$ (Eq. (4.25)), were interpolated from t=0 to t corresponding to the first available sample (t=0.7+0.07 month). Three different kinds of interpolations were tested: linear, cubic spline, and piecewise cubic Hermite; the one(s) which provided strange profiles was(were) excluded.

2. The interpolations of the new beta cell formation and the *per capita* beta cell death rate were used to calculate the density $n(a,t)$ of beta cells of age a at time t according to Eq. (4.31). The density was obtained for all t in the range: 0-10.7 months. Similarly, the probability density function $pdf_n(a,t)$ was calculated by Eq. (4.21) from $n(a,t)$ and $N(t)$.
3. The obtained density $n(a,t)$ was used to calculate the mean age of a beta cell by Eq. (4.32).

The mean beta cell lifetime was calculated as the integral of the survivor function $S(a,t)$ according to Eq. (4.40).

The integrals defined in Eqs. (4.21), (4.31), (4.32), and (4.40) were obtained as areas under the corresponding integrating functions by the trapezoid method.

To verify the impact of the assumptions of the model, the profile of the total number of beta cells ($N(t)$) was compared to the area under the curve of the density $n(a,t)$ according to Eq. (4.20).

5.3 Monkey Study

Usually, to study beta cell turnover at non steady state, measurements of beta cell mass, beta cell replication, and beta cell apoptosis at multiple different time points were required. Alternatively if beta cell turnover is at steady state, then a single time point is sufficient. To assure that beta cell turnover was at steady state in both the control monkeys and STZ diabetic monkeys, we obtained pancreas first by an open surgical biopsy and then subsequently at euthanasia from each animal. The first surgical sample was obtained one month after administration of either STZ (N=5) or saline (N=6), and the second euthanasia sample was obtained at between 2-5 months later as shown in Figure 2.5. Having established that beta cell turnover was at steady state over the period of observation (Figures 2.6, 2.7, and 2.8), beta cell mass (M), number (N), rates of beta cell replication (RR and RR_N) and apoptosis (RA and RA_N) were obtained by averaging the corresponding data at biopsy and euthanasia. The rates of beta cell replication (RR and RR_N) and apoptosis (RA and RA_N) were obtained by Eqs. (4.2), (4.8), (4.3), and (4.9).

In both control and STZ monkeys it was possible to assess:

- *The contributions to beta cell mass and number turnovers.* Since steady state conditions were verified, the rates of change in beta cell mass $dM(t)/dt$ and number $dN(t)/dt$ were set to zero. The contributions from other sources of beta cells (OSB and OSB_N) to beta cell mass and number were respectively obtained by Eqs. (4.6) and (4.12) in each monkey.

- *The mean age of a beta cell and the mean beta cell lifetime.* Since the monkeys were adults (mean age: circa 6.5 years), it was reasonable to assume that beta cells present at birth are almost dead at the time of the study (*Chapter 4*). The total number of beta cells (N), the new beta cell formation (B), and the *per capita* beta cell death rate (μ) were obtained by averaging the data at biopsy and euthanasia in each monkey. The mean age of a beta cell and the mean beta cell lifetime were calculated as the reciprocal of the *per capita* beta cell death rate according to Eqs. (4.33) and (4.41). For STZ monkeys number two and five it was not possible to determine these variables since *per capita* beta cell death rate was zero.

  The density $n(a,t)$ of beta cells of age a in a monkey of age t was calculated in each monkey according to Eq. (4.31). Similarly, the curves of the probability density function $pdf_n(a,t)$ were obtained by Eq. (4.21). For STZ monkeys number two and five it was not possible to determine the density $n(a,t)$ and the probability density function $pdf_n(a,t)$ since both the new beta cell formation and the *per capita* beta cell death rate were zero. To verify the impact of the model assumptions, the total number of beta cells (N) was compared to the area under the curve of the density $n(a,t)$ according to Eq. (4.20).

It is important to note that there was not an impact of beta cell size on beta cell turnover since steady state conditions were verified.

5.4 Young Human Study

To establish the extent, timing, and predominant source of new beta cell formation during normal growth in humans, the young human (range of age: 2 weeks-21 years) and the lean young adult human (range of age: 20-39 years) datasets were put together. The rates of beta cell replication (RR and RR_N) and apoptosis (RA and RA_N) were obtained by Eqs. (4.2), (4.8), (4.3), and (4.9). In this study, in contrast to the rat one, it was not possible to work on mean data since we did not have a group of individuals at each time point. Thus, working on the single data, it was feasible to assess:

- *The time profiles of the contributions to beta cell mass and number turnovers.* The new algorithm proposed at the beginning of this chapter was applied to beta cell mass (number) data in the period 2 weeks-39 years to obtain a smoothed profile for beta cell mass (number) and an estimate of beta cell mass (number) derivative together with its uncertainty on a uniform grid (step of the virtual grid: 0.1 years). On the same fine grid, smoothed mean profiles for rates of beta cell replication and apoptosis were evaluated using the same algorithm. Finally, the time profile for OSB (OSB_N) resulted from Eq. (4.5) (Eq. (4.11)).

  All the smoothed profiles were obtained by assuming a constant standard deviation for the data error estimated *a posterior*: the resulting standard deviations are shown in Table 5.1. The approach of propagation of errors to establish the variance in the computed OSB (OSB_N) was used; taking this variance into account the hypothesis that OSB was different from zero was tested through the 95% confidence intervals.

	Standard Deviation
M	223 mg
RR	210 mg/year
RA	682 mg/year
N	$0.30{\cdot}10^9$
RR_N	$0.29{\cdot}10^9$/year
RR_A	$0.72{\cdot}10^9$/year

Table 5.1: Standard deviations for the data error estimated *a posterior*. Data: beta cell mass M, rates of beta cell replication RR and apoptosis RA, beta cell number N, and rates of beta cell replication RR_N and apoptosis RA_N referred to number.

- *The overall contributions to beta cell mass and number turnovers in 2week-20 year and 20-39 year periods.* The net change in beta cell mass in the period 2weeks-20 years of age equaled the difference between the smoothed beta mass at age 20 years and at 2 weeks (i.e. $\Delta M = M(20) - M(0)$). Similarly, the net change in beta cell number ΔN over the same period equaled the difference between the smoothed beta number at age 20 years and at 2 weeks (i.e. $\Delta N = N(20) - N(0)$). The overall contributions from rates of beta cell replication and apoptosis (AUC_{RR} and AUC_{RR_N}; AUC_{RA} and AUC_{RA_N}) were calculated as areas under the corresponding smoothed curves in the period 2weeks-20 years by the trapezoid method. Finally, the overall contributions to beta cell mass and number from other sources of beta cells (AUC_{OSB} and AUC_{OSB_N}) were obtained by Eqs. (4.4) and (4.10), respectively. Similarly calculi were done to obtained the overall contributions to

beta cell mass and number turnovers in 20-39 year period.

- *The impact of beta cell size on beta cell turnover.* As performed in the rat study, the impact of beta cell size was quantified by comparing the turnovers of beta cell mass and beta cell number. To make this comparison possible, the overall contributions of beta cell replication, apoptosis, and other sources of beta cells defined in Eqs. (4.4) and (4.10) were expressed as percentage of ΔM and ΔN in the period 2weeks-40 years of age respectively. Then, the percent relative differences between these overall contributions from mass and number were obtained (Eq. (5.11)).

- *The mean age of a beta cell and the mean beta cell lifetime.* As performed in the rat study, to estimate the mean age of a beta cell and the mean beta cell lifetime from the available data, it was reasonable to assume that t corresponds to the start of gestation. In an individual, the mean period of gestation is circa 9 months (i.e. 0.8 year). To calculate the mean age of a beta cell the following steps were required:

  1. The smoothed profiles of total number of beta cells, $N(t)$ (Eq. (4.7)), new beta cell formation, $B(t)$ (Eq. (4.23)), and the *per capita* beta cell death rate, $\mu(t)$ (Eq. (4.25)), were interpolated from t=0 to t corresponding to the first available sample (t=0.8+0 year). Three different kinds of interpolations were tested: linear, cubic spline, and piecewise cubic Hermite; the one(s) which provided strange profiles was(were) excluded.
  2. The interpolations of the new beta cell formation and the *per capita* beta cell death rate were used to calculate the density $n(a,t)$ of beta cells of age a at time t according to Eq. (4.31). The density was obtained for all t in the range: 0-39.7 years. Similarly, the probability density function $pdf_n(a,t)$ was calculated by Eq. (4.21) from $n(a,t)$ and $N(t)$.
  3. The obtained density $n(a,t)$ was used to calculate the mean age of a beta cell by Eq. (4.32).

  The mean beta cell lifetime was calculated as the integral of the survivor function $S(a,t)$ according to Eq. (4.40).

  The integrals defined in Eqs. (4.21), (4.31), (4.32), and (4.40) were obtained as areas under the corresponding integrating functions by the trapezoid method.

  To verify the impact of the assumptions of the model to estimate the mean age of a beta cell, the profile of the total number of beta cells ($N(t)$) was compared to the area under the curve of the density $n(a,t)$ according to Eq. (4.20).

5.5 Adult Human Study

Usually, to study beta cell turnover at non steady state, measurements of beta cell mass, beta cell replication, and beta cell apoptosis at multiple different time points were required. Alternatively if beta cell turnover is at steady state, then a single time point is sufficient. In adult human study the steady state conditions were verified in both lean and obese adults (Figure 2.12).

The rates of beta cell replication and apoptosis were obtained by Eqs. (4.2), (4.8), (4.3), and (4.9) in each individual.

In all the three groups it was possible to assess:

- *The contributions to beta cell mass and number turnovers.* Since steady state conditions were verified, the rates of change in beta cell mass $dM(t)/dt$ and number $dN(t)/dt$ were set to zero. The contributions from other sources of beta cells (OSB and OSB_N) to beta cell mass and number were respectively obtained by Eqs. (4.6) and (4.12) in each individual.

- *The mean age of a beta cell and the mean beta cell lifetime.* Since the individuals are adults, it was reasonable to assume that beta cells present at birth are almost dead at the time of the study (*Chapter 4*). The total number of beta cells (N), the new beta cell formation (B), and the *per capita* beta cell death rate (μ) were obtained in each individual. The mean age of a beta cell and the mean beta cell lifetime were calculated as the reciprocal of the *per capita* beta cell death rate according to Eqs. (4.33) and (4.41). For young lean individuals number five and twelve, for young obese individuals number one and six, and for elderly lean individuals number two, ten, and eleven it was not possible to determine these variables *per capita* beta cell death rate was zero.

  The density $n(a,t)$ of beta cells of age a in an individual of age t was calculated in each individual according to Eq. (4.31). Similarly, the curves of the probability density function $pdf_n(a,t)$ were obtained by Eq. (4.21). For young lean individuals number five and twelve, for young obese individuals number one and six, and for elderly lean individuals number two, ten, and eleven it was not possible to determine the density $n(a,t)$ and the probability density function $pdf_n(a,t)$ since both the new beta cell formation and the *per capita* beta cell death rate were zero. To verify the impact of the model assumptions, the total number of beta cells (N) was compared to the area under the curve of the density $n(a,t)$ according to Eq. (4.20).

It is important to note that there was not an impact of beta cell size on beta cell turnover since steady state conditions were verified.

Chapter 6

Results

The beta cell turnover models described in *Chapter 4* were applied to the rat, monkey, and human data presented in *Chapter 2*. Using the same data, the impact of beta cell size on beta cell turnover was also evaluated. The mean age of a beta cell and the mean beta cell lifetime were assessed by the model introduced in *Chapter 4*.

Considering the heterogeneity of the datasets different implementing solutions were adopted (*Chapter 5*).

All the analysis was realized with MATLAB software, version 7.6.0 (Mathworks, Natick, MA). Student's t-test ($P<0.05$) was performed to compare different groups.

6.1 Rat Study

A Major Role of Other Sources of Beta Cells

A graph to depict overall contributions to beta cell mass turnover (Eq. (4.4)) in WT and HIP rats is shown in Figure 6.1. In WT rats, to account for the net increase in beta cell mass ($\Delta M = 33$ mg) from 0.07 to 10 months of age, a contribution of OSB ($AUC_{OSB} = 61$ mg) was required, with only a smaller contribution of beta cell formation from beta cell replication ($AUC_{RR} = 7$ mg). Formation of 68 mg of beta cells total (90% from OSB and 10% from beta cell replication) was required to permit the net increase in beta cell mass in the face of 35 mg of beta cell apoptosis (AUC_{RA}) during the same period. In HIP rats, the net increase in beta cell mass from age 0.07 to 10 months ($\Delta M = 7$ mg) was more modest. However, given the much greater loss of beta cells from apoptosis ($AUC_{RA} = 88$ mg) and the relatively minor contribution of new beta cells from replication of existing beta cells ($AUC_{RR} = 6$ mg, 7% of beta cell formation), we computed that the contribution of

new beta cells from OSB in the HIP rat was 89 mg (AUC_{OSB}, 93% of new beta cells formed).

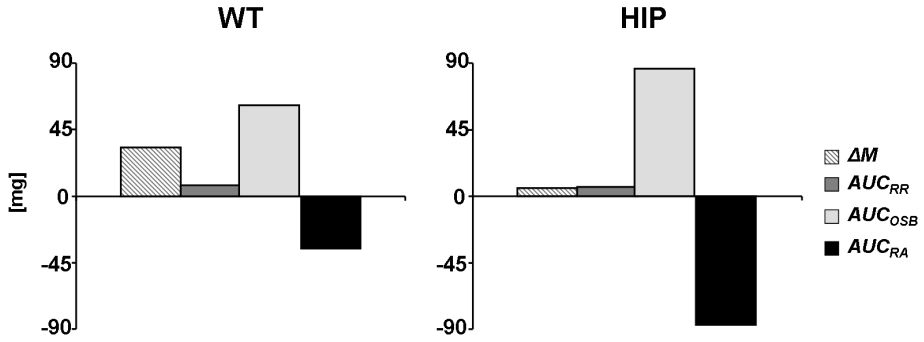

Figure 6.1: Beta cell mass turnover: overall contributions in WT (left panel) and HIP rats (right panel) aged 0.07-10 months. Hatched bars represent the net change in beta cell mass (ΔM) from age 0.07 to 10 months. Dark gray and light gray bars show, respectively, the overall contributions to beta cell mass formation from replication of existing beta cells (AUC_{RR}) and from other sources (AUC_{OSB}). Black bars represent the loss due to beta cell apoptosis (AUC_{RA}).

A similar overall pattern of findings was obtained considering beta cell number instead of beta cell mass (Figure 6.2). In WT rats, the net increase in beta cell number ($\Delta N = 75{\cdot}10^6$) during the study period was mostly dependent on the contribution from OSB ($AUC_{OSB_N} = 141{\cdot}10^6$, 89% of new cells formed), with a much smaller contribution from beta cell replication ($AUC_{RR_N} = 18{\cdot}10^6$, 11% of new cells formed). These newly formed beta cells permitted a net expansion of beta cell number despite the concurrent loss of $84{\cdot}10^6$ cells through apoptosis (AUC_{RA_N}). In contrast, in HIP rats, whereas the overall variation in beta cell number ($\Delta N = 12{\cdot}10^6$) over the 10-month observation period was less than that in WT rats, because of a much higher number of beta cells lost through apoptosis ($AUC_{RA_N} = 180{\cdot}10^6$) and again a quite modest (7%) contribution of newly forming cells from beta cell replication ($AUC_{RR_N} = 13{\cdot}10^6$), the contribution from OSB was $179{\cdot}10^6$ (AUC_{OSB_N}), or 93% of newly formed cells. Clearly, in the absence of OSB, HIP rats would have had a much more marked deficit in beta cells at an earlier age.

In Figure 6.3, the time profiles of rate of change in beta cell mass (dM/dt), rate of beta cell replication (RR), rate of beta cell apoptosis (RA), and the calculated OSB (Eq. (4.5)) are shown in WT (Figure 6.3 - left panel) and HIP rats (Figure 6.3 - right panel). In WT rats, OSB played an important role in permitting the relatively high rate of change of beta cell mass during the first month (7 mg/month at 0.07 month). OSB decreased in 2- to 4-month period when the rate of expansion of beta cell mass (dM/dt)

slows. Finally, OSB again increased by 10 months of age to 9 mg/month, counterbalancing a gradual increase in the rate of beta cell apoptosis in the older animals. In HIP rats, OSB was comparatively even more important than in WT rats. If it was not for the high rate of OSB, the mass (or number) of beta cells would have rapidly declined to nearly zero by 5 months of age. The overall conclusions were essentially the same when beta cell number rather than beta cell mass was considered (Figure 6.4).

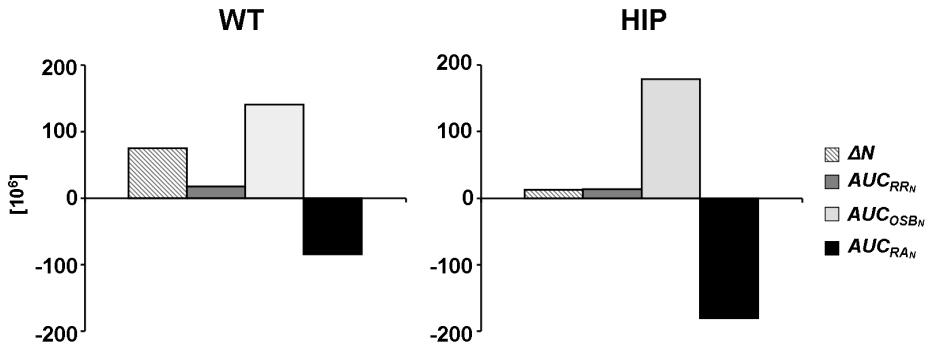

Figure 6.2: Beta cell number turnover: overall contributions in WT (left panel) and HIP rats (right panel) aged 0.07-10 months. Hatched bars represent the net change in beta cell number (ΔN) from age 0.07 to 10 months. Dark gray and light gray bars show, respectively, the overall contributions to beta cell number from replication of existing beta cells (AUC_{RR_N}) and from other sources (AUC_{OSB_N}). Black bars represent the loss due to beta cell apoptosis (AUC_{RA_N}).

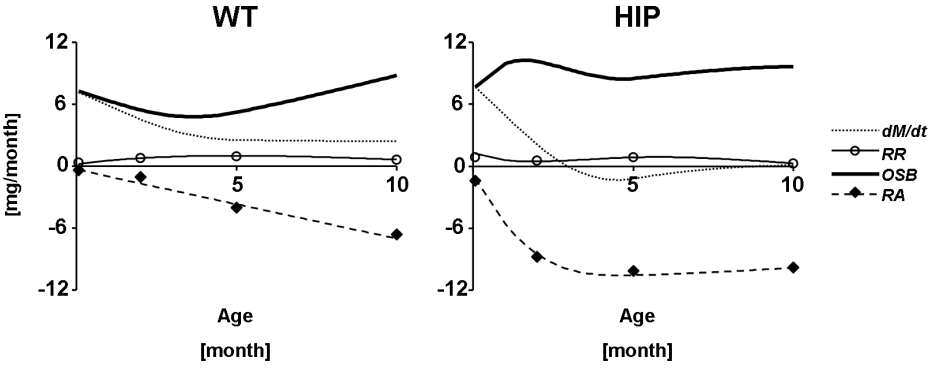

Figure 6.3: Time profiles of rate of change in beta cell mass dM/dt (dashed thin line), rate of beta cell replication RR (data: circles; smoothed profile: continuous thin line), other sources of beta cells OSB (continuous line), and rate of beta cell apoptosis RA (data: rhombuses; smoothed profile: dashed line) in WT (left panel) and HIP rats (right panel), aged 0.07-10 months.

We used the approach of propagation of errors to establish the variance in the computed OSB. Even when taking into account the sum of the variance of individual measurements required to compute OSB, the hypothesis that OSB is different from zero was consistently proven (Figure 6.5), implying that OSB is not simply a result of sample variance.

To verify the consistency between the overall OSB over the period of the study, i.e. AUC_{OSB}, Eq. (4.4), and the OSB profile obtained by Eq. (4.5), we evaluated the AUC of the latter by the trapezoid method and compared

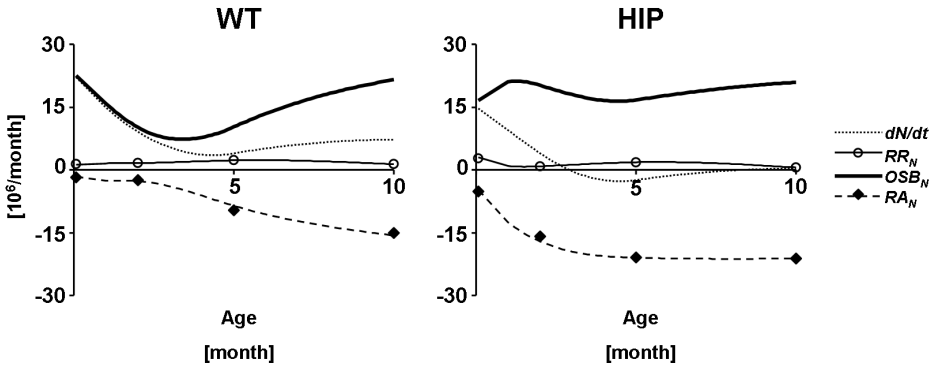

Figure 6.4: Time profiles of rate of change in beta cell number dN/dt (dashed thin line), rate of beta cell replication RR_N (data: circles; smoothed profile: continuous thin line), other sources of beta cells OSB_N (continuous line), and rate of beta cell apoptosis RA_N (data: rhombuses; smoothed profile: dashed line) in WT (left panel) and HIP rats (right panel), aged 0.07-10 months.

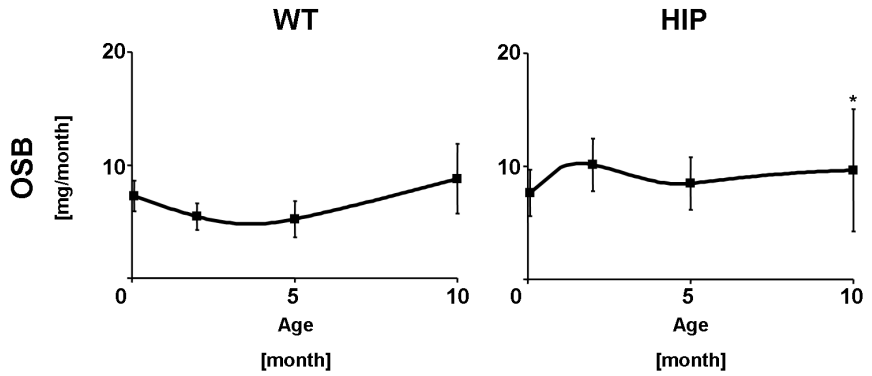

Figure 6.5: Uncertainty of the calculated other sources of beta cell mass. Time profile of OSB in WT (left panel) and HIP rats (right panel). Error bars are SEM of OSB obtained by propagating the inter-rat variability. OSB was significantly different from 0 at all time points except at 10 months of age in HIP rats (P=0.1), when variance was high. *OSB *versus* 0, P<0.05.

it to AUC_{OSB}. In both WT and HIP rats, the percent relative differences between the two approaches were less than 4%, confirming that the applied smoothing procedure did not introduce bias into the results.

Marginal Role of Changes in Beta Cell Size

To examine the role of individual beta cell size (volume) in involution and expansion of beta cell mass we compared beta cell turnover by two models: the first by considering beta cell mass (Eq. (4.1)), where OSB includes changes in beta cell mass due to both the change in number of beta cells by other sources and changes in the mean beta cell size, and the second based on beta cell number (Eq. (4.7)). The small percent relative differences (Eq. (5.11)) shown in Table 6.1 revealed that the cell size did not much influence the estimation of beta cell turnover with beta cell mass data in the WT or HIP rats with aging.

	$AUC_{massturnover}$ (% of ΔM)		$AUC_{numberturnover}$ (% of ΔN)		ΔAUC (%)	
	WT	HIP	WT	HIP	WT	HIP
replication	22	98	24	110	-8	-11
OSB	185	1369	189	1467	-2	-7
apoptosis	-107	-1367	-113	-1477	-5	-7

Table 6.1: Differences between beta cell mass and beta cell number turnovers in WT and HIP rats over the period 0.07-10 months. $AUC_{massturnover}$ and $AUC_{numberturnover}$ represent respectively the overall contributions (from either replication or OSB or apoptosis) to ΔM (net change in beta cell mass) and ΔN (net change in beta cell number). ΔAUC is the percent relative difference between $AUC_{massturnover}$ and $AUC_{numberturnover}$. The first four columns report the total contributions from replication, other sources of beta cells, and apoptosis to beta cell mass (number) over the period 0.07-10 months in WT and HIP rats. These quantities are expressed as percentage of the net change in beta cell mass (or number) over the same period in order to make possible the comparisons. The last two columns contain the values of this comparison, i.e. percent relative difference.

The Mean Age of a Beta Cell and The Mean Beta Cell Lifetime were Higher in WT compared to HIP rats

As described in *Chapter 4*, to estimate the mean age of a beta cell and the mean beta cell lifetime from the available data it was reasonable to assume that $t = 0$ corresponds to the start of gestation. In a rat, the mean period of gestation is circa 21 days (i.e. 0.7 month).

The mean smoothed profiles of total number of beta cells, $N(t)$ (Eq. (4.7)), the new beta cell formation, $B(t)$ (Eq. (4.23)), and the *per capita*

beta cell death rate, $\mu(t)$ (Eq. (4.25)) interpolated from t=0 to t corresponding to the first available sample (t=0.7+0.07 month) are shown in Figure 6.6. Three different kinds of interpolations were tested: linear, cubic spline, and piecewise cubic Hermite. While the first and the third interpolations provided reliable curves for N, B, and μ from zero to t corresponding to the first available sample, the cubic spline interpolation presented negative values for N in both WT and HIP rats. For this reason it was no longer considered in the following.

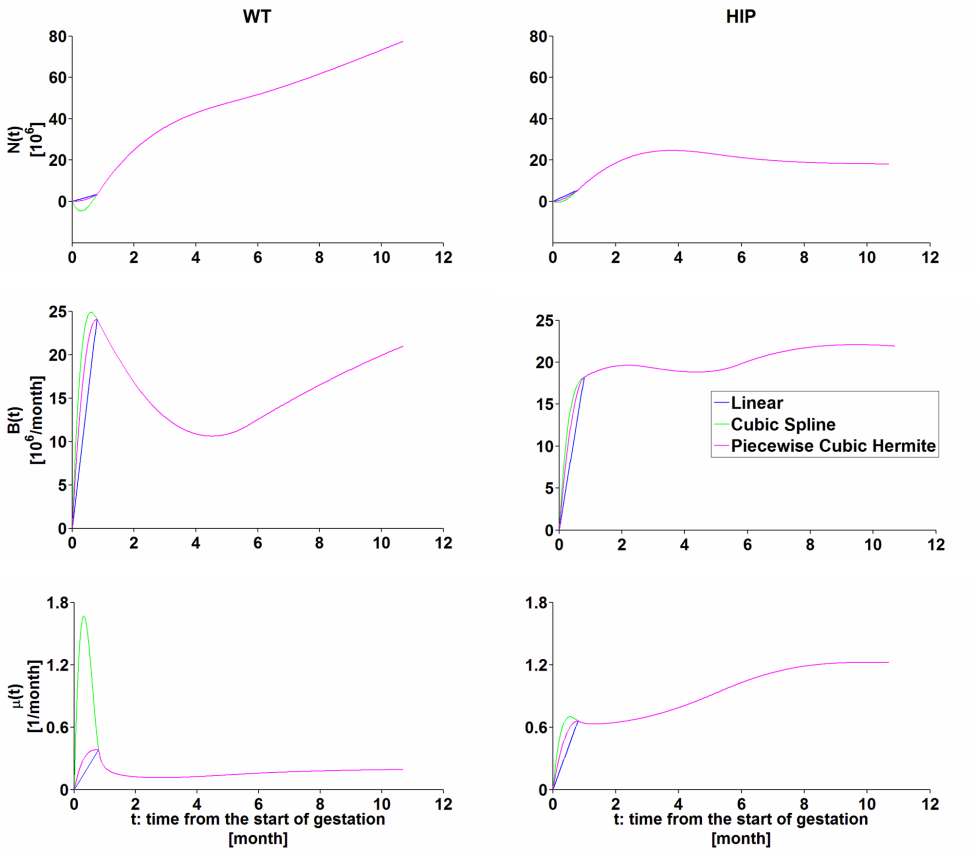

Figure 6.6: The total number of beta cells $N(t)$ (top panels), the new beta cell formation $B(t)$ (middle panels), and the *per capita* beta cell death rate $\mu(t)$ (lower panels) in WT (left panels) and HIP rats (right panels). These profiles were obtained by performing either a linear (in blue), cubic spline (in green) or a piecewise cubic Hermite (in pink) interpolation from zero (t=0 is the start of gestation that lasts circa 0.7 month in rats) to t corresponding to the first available sample (t=0.7+0.07 month).

The linear interpolations of the new beta cell formation and the *per capita* beta cell death rate were used to calculate the density $n(a,t)$ of beta cells of age a at time t according to Eq. (4.31). Figure 6.7 - top panels

depicts the resulting $n(a,t)$ for WT and HIP rats. Figure 6.7 - lower panels shows the probability density function $pdf_n(a,t)$ for t corresponding to 0.07, 2, 5, and 10 months of age. In WT rats (Figure 6.7 - lower left panel) at birth there was a high probability density of new born beta cells (3.1 month^{-1}); this quantity decreased and became more uniform thereafter (around 0.3 month^{-1}). In HIP rats (Figure 6.7 - lower right panel) at birth there was again a high probability density of new born beta cells (3.2 month^{-1}), but it remained relatively high for new born beta cells thereafter (range 0.8-1.2 month^{-1}). The overall conclusions were essentially the same when the piecewise cubic Hermite rather than linear interpolation was considered.

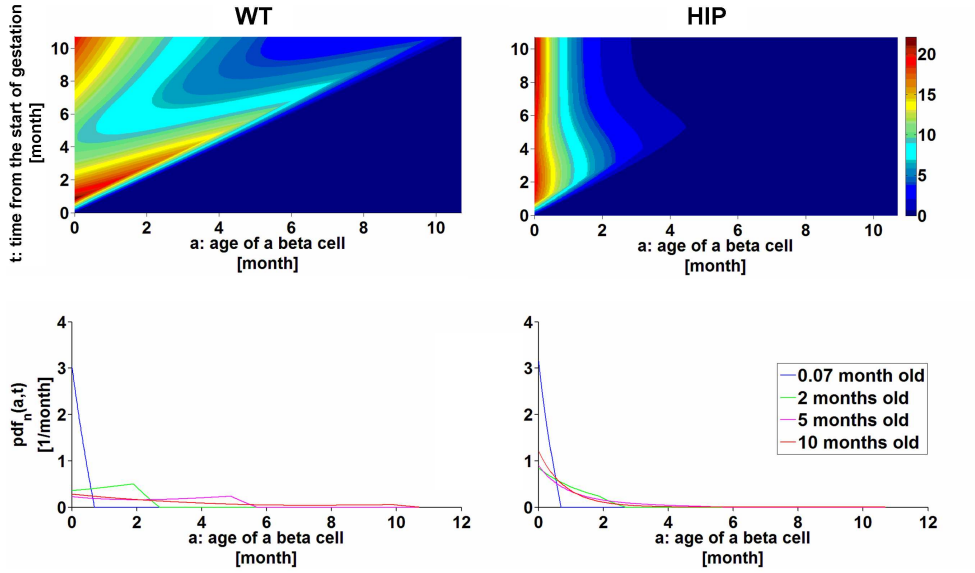

Figure 6.7: The density $n(a,t)$ (10^6/month) of beta cells of age a at time t in WT (top left panel) and HIP rats (top right panel). The density was obtained for all t in the range 0-10.7 months by substituting the linear interpolations of the new beta cell formation and the *per capita* beta cell death rate into Eq. (4.31). Light colors correspond to high values of $n(a,t)$, dark colors to low values. Lower panels show the curves of the probability density function $pdf_n(a,t)$ for t corresponding to 0.07, 2, 5, and 10 months of age. These curves describe how beta cells are distributed basing on their own age.

The obtained density $n(a,t)$ was used to calculate the mean age of a beta cell by Eq. (4.32). Figure 6.8 shows the mean age of a beta cell as a function of the time t from the start of gestation (period 0-10.7 months). In WT rats (Figure 6.8 - left panel) the mean age of a beta cell was in the range 0-3.6 months (average: 2.2 months), while in HIP rats (Figure 6.8 - left panel) in the range 0-1.2 months (average: 0.9 month). The profiles of the mean age of a beta cell obtained by either linear or piecewise cubic Hermite interpolations of the new beta cell formation and the *per capita*

beta cell death rate were similar.

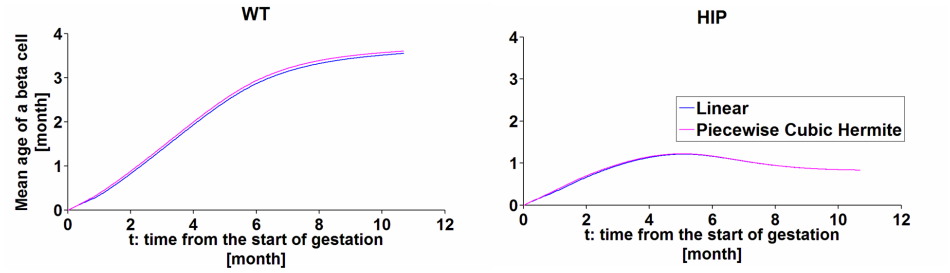

Figure 6.8: The mean age of a beta cell in WT (left panel) and HIP rats (right panel) obtained by either linear (in blue) or piecewise cubic Hermite interpolations (in pink) of the new beta cell formation and the *per capita* beta cell death rate.

The *per capita* beta cell death rate was used to calculate the mean beta cell lifetime according to Eq. (4.40). Figure 6.9 shows the mean beta cell lifetime as a function of the time t from the start of gestation (period 0-10.7 months). In WT rats (Figure 6.9 - left panel) the mean beta cell lifetime was in the range 0-4.6 months (average: 3.2 months), while in HIP rats (Figure 6.9 - left panel) in the range 0-1.3 months (average: 1.0 month). The profiles of the mean beta cell lifetime obtained by either linear or piecewise cubic Hermite interpolation of the *per capita* beta cell death rate were similar.

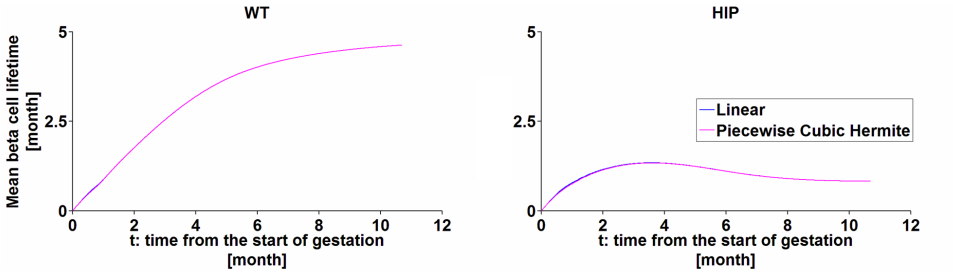

Figure 6.9: The mean beta cell lifetime in WT (left panel) and HIP rats (right panel) obtained by either linear (in blue) or piecewise cubic Hermite interpolation (in pink) of *per capita* beta cell death rate.

To verify the impact of the assumptions of the model to estimate the mean age of a beta cell and the mean beta cell lifetime, the profile of the total number of beta cells ($N(t)$) was compared to the area under the curve of the density $n(a,t)$ according to Eq. (4.20). In both WT and HIP rats, the profiles were similar (Figure 6.10) and the percent relative differences between the two quantities were less than 9%, assuring that the model assumptions did not introduce a relevant bias into the results.

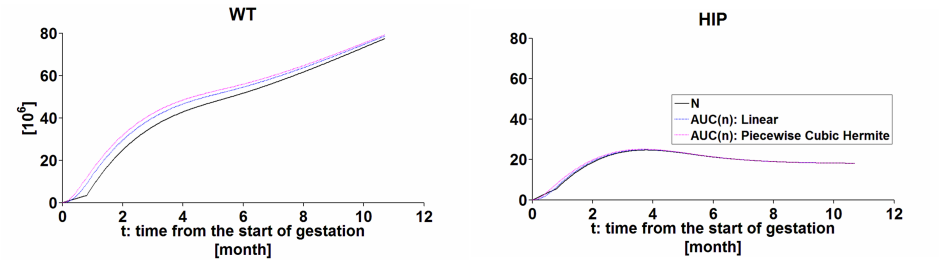

Figure 6.10: The total number of beta cells (black line) *versus* the areas under the curve of the density $n(a,t)$ in WT (left panel) and HIP rats (right panel) obtained either by linear (blue dashed line) of piecewise cubic Hermite interpolation (pink dashed line) of the new beta cell formation and the *per capita* beta cell death rate.

6.2 Monkey Study

Significant Beta Cell Turnover

Figure 6.11 shows the contributions to beta cell mass turnover from beta cell replication, apoptosis, and other sources of beta cells in control and STZ monkeys calculated by Eq. (4.6) under steady state conditions. In control monkeys the rate of beta cell apoptosis (31.7±7.1 mg/month) far exceeded the rate of beta cell replication (1.5±0.6 mg/month), implying that for steady state beta cell mass to prevail, the majority of newly forming beta cells must be derived independently from beta cell replication, i.e. OSB (30.2±7.4 mg/month) (Figure 6.11 - left panel). The pattern was comparable in STZ monkeys (Figure 6.11 - right panel) even if the total rate of beta cell formation was markely decreased with respect to controls ($P<0.05$). In detail, in STZ monkeys the rate of beta cell apoptosis was 5.2±2.3 mg/month, the rate of beta cell replication was 0.5±0.3 mg/month, and OSB was 4.7±2.1 mg/month.

Since the size of beta cells was decreased by circa 30% in the STZ group compared to the control group (Figure 2.8 - top panel), we also assessed beta cell turnover by adapting the model to compute the turnover of beta cell numbers rather than mass (Eq. (4.12)). The pattern of beta cell turnover was comparable to that in the mass calculation, although as expected the gap between the two groups decreased (Figure 6.12). In the control group using the cell number approach the rates of beta cell apoptosis and replication were $(37.1\pm8.0)\cdot10^6$ and $(1.9\pm0.8)\cdot10^6$ beta cells per month, with a computed OSB_N of $(35.2\pm8.1)\cdot10^6$ beta cells per month. In the STZ group using the cell number approach the rates of beta cell apoptosis and replication were $(11.1\pm4.8)\cdot10^6$ and $(1.2\pm0.7)\cdot10^6$ beta cells per month, with a computed OSB_N of $(9.9\pm4.5)\cdot10^6$ beta cells per month.

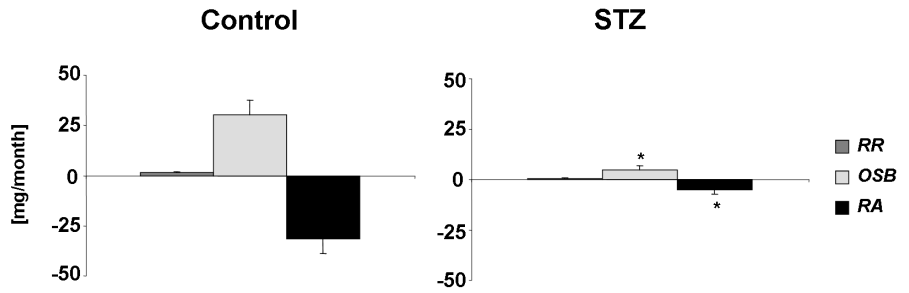

Figure 6.11: Beta cell mass turnover in control (left panel) and STZ monkeys (right panel). Dark gray and light gray bars show, respectively, the contributions to beta cell mass formation from replication of existing beta cells (RR) and from other sources (OSB). Black bars represent the loss due to beta cell apoptosis (RA). The contribution from changes in beta cell mass was zero since steady state conditions were verified. *: STZ *versus* control, P<0.05. Bars represent SEM.

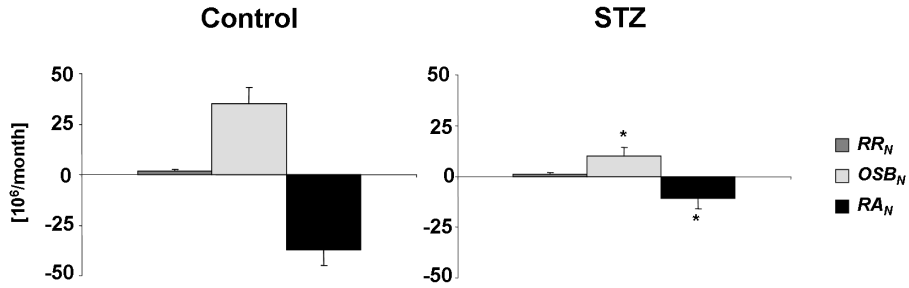

Figure 6.12: Beta cell number turnover in control (left panel) and STZ monkeys (right panel). Dark gray and light gray bars show, respectively, the contributions to beta cell formation from replication of existing beta cells (RR_N) and from other sources (OSB_N). Black bars represent the loss due to beta cell apoptosis (RA_N). The contribution from changes in beta cell number was zero since steady state conditions were verified. *: STZ *versus* control, P<0.05. Bars represent SEM.

The Mean Age of a Beta Cell and The Mean Beta Cell Lifetime were Lower in STZ Compared to Control Monkeys

Since the monkeys were adults (mean age: circa 6.5 years), it was reasonable to assume that beta cells present at birth are mostly dead at the time of the study.

The total number of beta cells (N), the new beta cell formation (B), and the *per capita* beta cell death rate (μ) were obtained by averaging the data at biopsy and euthanasia. These quantities were used to calculate the density $n(a,t)$ in each monkey according to Eq. (4.31) (Figure 6.13 - top panels). Similarly, the curves of the probability density function $pdf_n(a,t)$ were obtained in each monkey by Eq. (4.21). Figure 6.13 - lower left panel depicts the resulting probability density function for control monkeys. These animals presented a high probability density of new born beta cells (3.8±0.5 $year^{-1}$), except for the control monkey number five, where the density of new born beta cells was 1.1 $year^{-1}$. STZ monkeys (Figure 6.13 - lower right panel) showed a higher probability density of new born beta cells (6.4±0.6 $year^{-1}$) with respect to controls, except for the STZ monkey number one, where the probability density of new born beta cells was 1.4 $year^{-1}$. For STZ monkeys number two and five it was not possible to determine the density $n(a,t)$ and the probability density function $pdf_n(a,t)$ since both the new beta cell formation and the *per capita* beta cell death rate were zero.

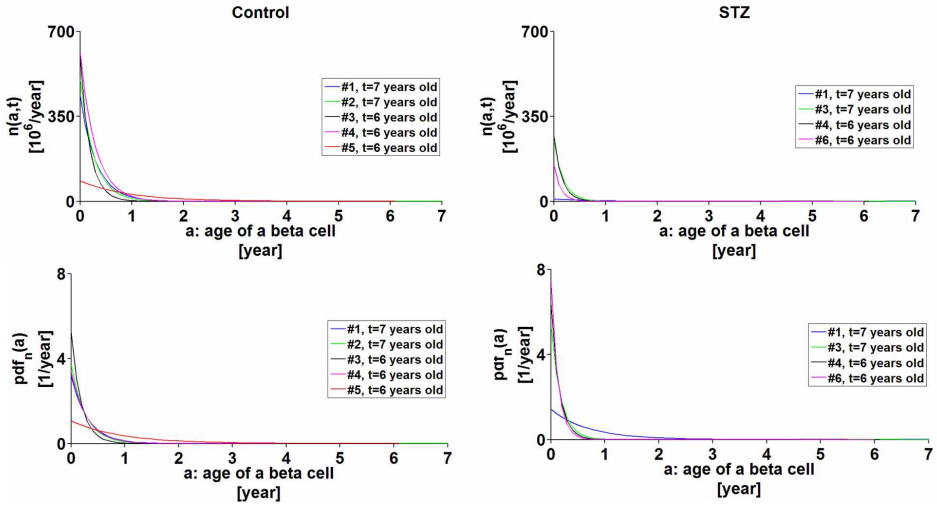

Figure 6.13: The density $n(a,t)$ (top panels) and the probability density function $pdf_n(a,t)$ (lower panels) of beta cells of age a in control (left panels) and STZ monkeys (right panels) of age t. For STZ monkeys number two and five it was not possible to determine the density $n(a,t)$ and the probability density function $pdf_n(a,t)$ since both the new beta cell formation and the *per capita* beta cell death rate were zero.

The mean age of a beta cell and the mean beta cell lifetime were calculated as the reciprocal of the *per capita* beta cell death rate according to Eqs. (4.33) and (4.41). In control monkeys these variables were 4.8±1.6 months, while in STZ monkeys 1.9±0.2 months (P=0.6, STZ *versus* control monkeys; Figure 6.14). For STZ monkeys number two and five it was not possible to determine these variables since *per capita* beta cell death rate was zero.

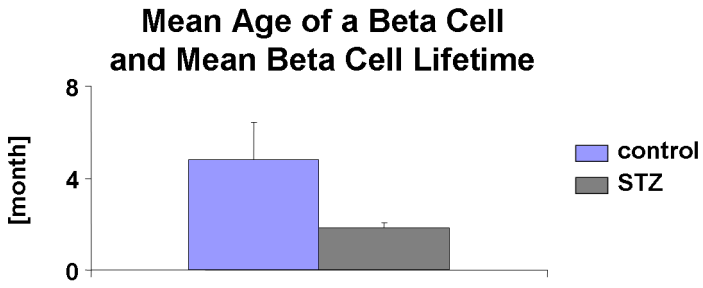

Figure 6.14: The mean age of a beta cell and the mean beta cell lifetime in control (azure) and STZ monkeys (grey). Bars represent SEM.

To verify the impact of the model assumptions, the total number of beta cells (N) was compared to the area under the curve of the density $n(a,t)$ according to Eq. (4.20). In both control and STZ monkeys, the percent relative differences between the two quantities were less than 4%, assuring that the model assumptions did not introduce a relevant bias into the results.

6.3 Young Human Study

To establish the extent, timing, and predominant source of new beta cell formation during normal growth in humans, the young human (range of age: 2 weeks-21 years) and the lean young adult human (range of age: 20-39 years) datasets were put together.

A Major Role of Beta Cell Replication in Childhood

In Figure 6.15 the individual data and the smoothed profiles of beta cell mass (M), rate of change in beta cell mass (dM/dt), and rates of beta cell replication (RR) and apoptosis (RA) are depicted. Beta cell mass (Figure 6.15 - top panel) gradually increased from 40 mg at 2 weeks of age to 854 mg at 39 years of age. The rate of change in beta cell mass (Figure 6.15 - middle-top panel) was most pronounced in the youngest ages (around 35 mg/year in the range 2 weeks-10 years of age) and gradually declined thereafter (13

mg/year at 39 years of age). The rate of beta cell replication (Figure 6.15 - middle-lower panel) was highest in the youngest age (240 mg/year at 2 weeks of age) and gradually declined thereafter (87 mg/year at 39 years of age). The rate of beta cell apoptosis (Figure 6.15 - lower panel) was very low in the youngest ages (around 90 mg/year in the range 2 weeks-15 years of age) and considerably increased thereafter (2087 mg/year at 39 years of age). The overall conclusions were essentially the same when beta cell number rather than beta cell mass was considered (Figure 6.16).

In Figure 6.17 the time profiles of the rate of change in beta cell mass, the rate of beta cell replication and apoptosis, and the calculated OSB (Eq. (4.5)) are shown. In the youngest ages the replication of existing beta cells played a major role in the new beta cell formation, while both rate of beta cell apoptosis and OSB were almost negligible (the latter resulted negative in the range 0-12 years of age, but not significantly different from zero). Around 20 years of age the contribution of other sources of beta cells other than beta cell replication became important in counterbalancing the increase in the rate of beta cell apoptosis that occurred at this age. The overall conclusions were essentially the same when beta cell number rather than beta cell mass was considered (Figure 6.18).

The overall contributions to beta cell mass and number turnover in 2 week-20 year and 20-39 year periods were calculated on the smoothed profiles according to Eqs. (4.4) and (4.10). This analysis confirmed the major role in beta cell formation from replication of existing beta cells in childhood and that the contribution of other sources of beta cells other than beta cell replication became important in counterbalancing the considerable increase in the rate of beta cell apoptosis in adulthood (Figures 6.19 and 6.20).

Marginal Role of Changes in Beta Cell Size

As performed in the rat study, the impact of beta cell size was quantified by comparing the beta cell mass and number turnovers. To permit this comparison, the overall contributions from beta cell replication, apoptosis, and other sources of beta cells defined in Eqs. (4.4) and (4.10) were respectively expressed as percentage of ΔM and ΔN in the period 2weeks-40 years of age. Then, the percent relative differences between these overall contributions from mass and number were obtained (Eq. (5.11)). The small percent relative differences shown in Table 6.2 revealed that the cell size did not much influence the estimation of beta cell turnover with beta cell mass data in young humans with aging.

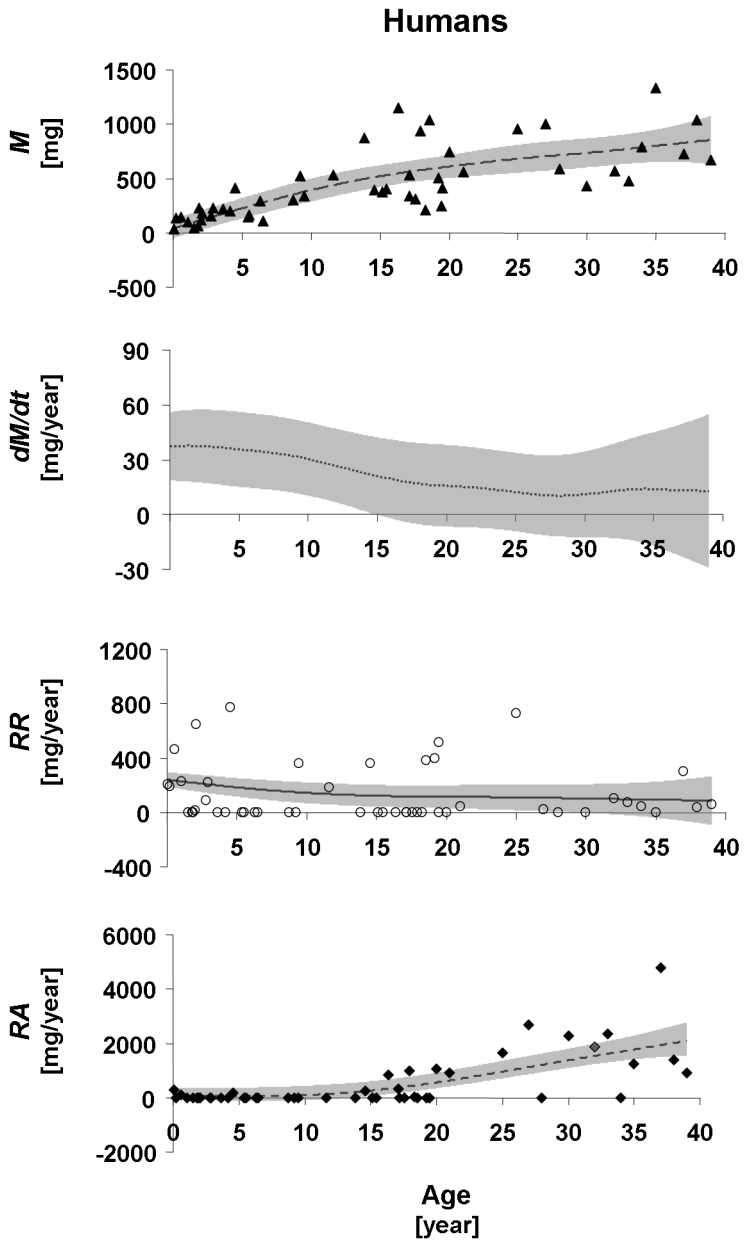

Figure 6.15: Beta cell mass M (top panel; data: triangles; smoothed profile: long-dashed line), rate of change in beta cell mass dM/dt (middle-top panel; dashed thin line), and rates of beta cell replication RR (middle-lower panel; data: circles; smoothed profile: continuous thin line) and apoptosis RA (lower panel; data: rhombuses; smoothed profile: dashed line) in young humans, aged 2 weeks-39 years. The grey bands stay for the 95% confidence intervals.

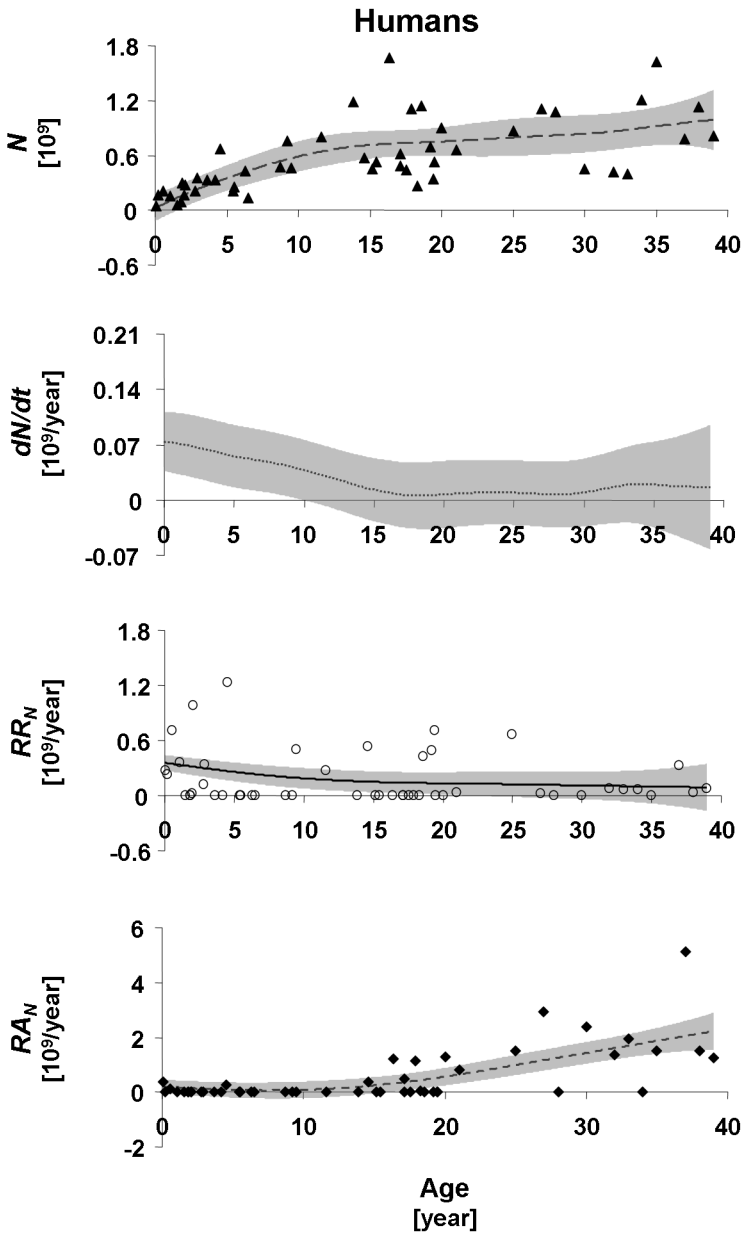

Figure 6.16: Beta cell number N (top panel; data: triangles; smoothed profile: long-dashed line), rate of change in beta cell number dN/dt (middle-top panel; dashed thin line), and rates of beta cell replication RR_N (middle-lower panel; data: circles; smoothed profile: continuous thin line) and apoptosis RA_N (lower panel; data: rhombuses; smoothed profile: dashed line) in young humans, aged 2 weeks-39 years. The grey bands stay for the 95% confidence intervals.

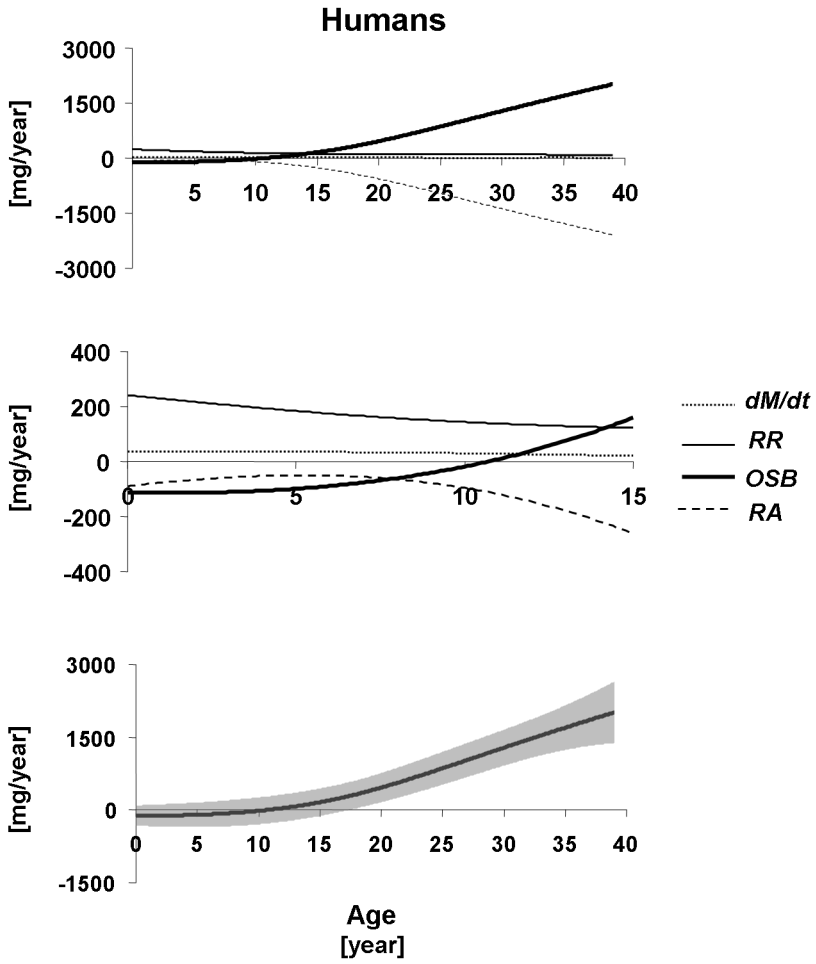

Figure 6.17: Top panel: rate of change in beta cell mass dM/dt (dashed thin line), rates of beta cell replication RR (continuous thin line) and apoptosis RA (dashed line), and other sources of beta cell mass OSB (continuous line) in young humans, aged 2 weeks-39 years. Middle panel: zoom in 2weeks-15 years of age. Lower panel: OSB and its 95% confidence intervals (grey band).

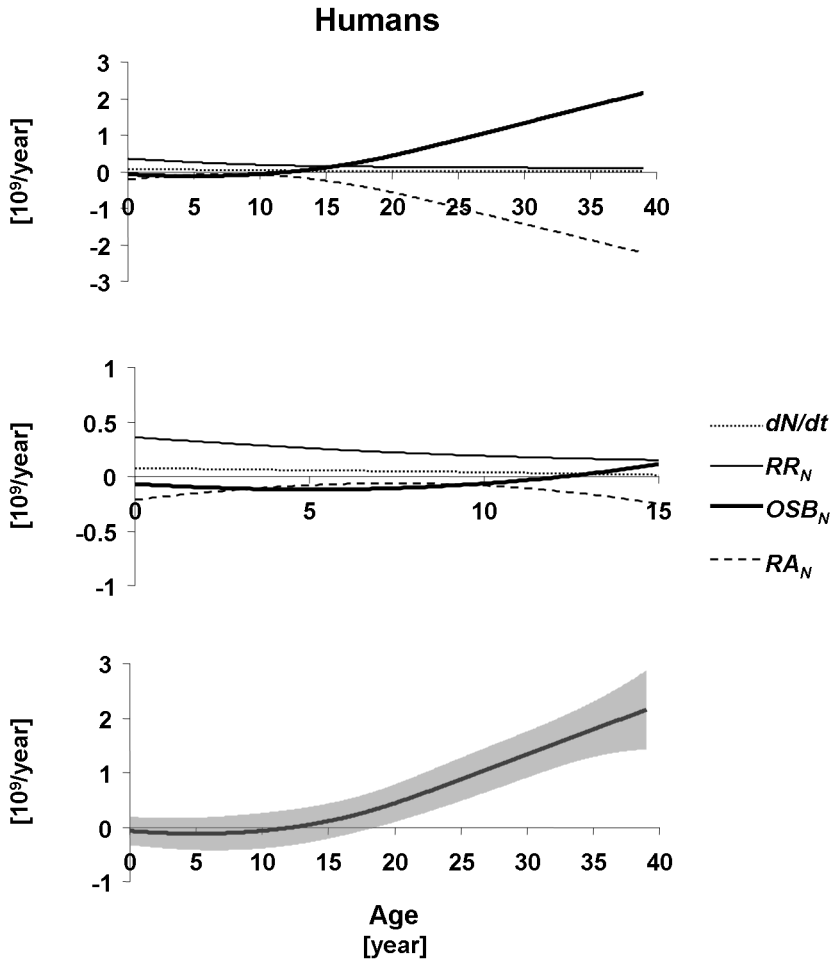

Figure 6.18: Top panel: rate of change in beta cell number dN/dt (dashed thin line), rates of beta cell replication RR_N (continuous thin line) and apoptosis RA_N (dashed line), and other sources of beta cells OSB_N (continuous line) in young humans, aged 2 weeks-39 years. Middle panel: zoom in 2weeks-15 years of age. Lower panel: OSB_N and its 95% confidence intervals (grey band).

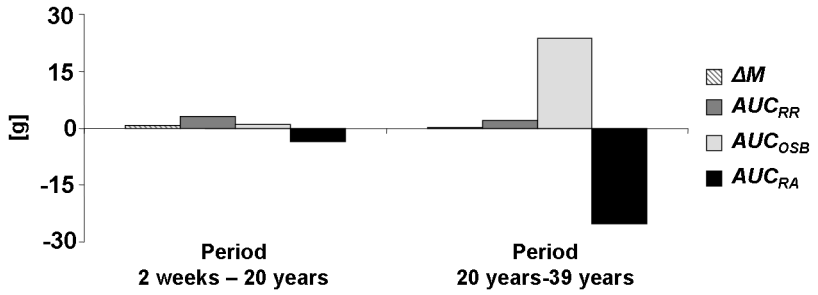

Figure 6.19: Beta cell mass turnover: overall contributions in young humans in the periods 2 weeks-20 years (left panel) and 20 years-40 years of age (right panel). Hatched bars represent the net change in beta cell mass (ΔM) over the periods. Dark gray and light gray bars show, respectively, the overall contributions to beta cell mass formation from replication of existing beta cells (AUC_{RR}) and from other sources (AUC_{OSB}). Black bars represent the loss due to beta cell apoptosis (AUC_{RA}).

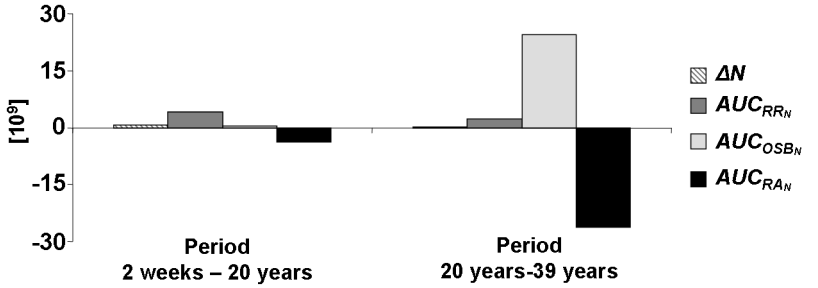

Figure 6.20: Beta cell number turnover: overall contributions in young humans in the periods 2 weeks-20 years (left panel) and 20 years-40 years of age (right panel). Hatched bars represent the net change in beta cell number (ΔN) over the periods. Dark gray and light gray bars show, respectively, the overall contributions to beta cell mass formation from replication of existing beta cells (AUC_{RR_N}) and from other sources (AUC_{OSB_N}). Black bars represent the loss due to beta cell apoptosis (AUC_{RA_N}).

	$AUC_{massturnover}$ (% of ΔM)	$AUC_{numberturnover}$ (% of ΔN)	ΔAUC (%)
replication	622	653	-5
OSB	3004	2574	17
apoptosis	-3526	-3127	13

Table 6.2: Differences between beta cell mass and beta cell number turnovers in young humans over the period 2 weeks-39 years. $AUC_{massturnover}$ and $AUC_{numberturnover}$ represent respectively the overall contributions (from either replication or OSB or apoptosis) to ΔM (net change in beta cell mass) and ΔN (net change in beta cell number). ΔAUC is the percent relative difference between $AUC_{massturnover}$ and $AUC_{numberturnover}$. The first two columns report the total contributions from replication, other sources of beta cells, and apoptosis to beta cell mass (number) over the period 2 weeks-39 years. These quantities are expressed as percentage of the net change in beta cell mass (or number) over the same period in order to make possible the comparisons. The last column contains the values of this comparison, i.e. percent relative difference.

Mean Age of a Beta Cell and Mean Beta Cell Lifetime in Young Humans

As performed in the rat study, to estimate the mean age of a beta cell and the mean beta cell lifetime from the available data it was reasonable to assume that t corresponds to the start of gestation. In an individual, the mean period of gestation is circa 9 months (i.e. 0.8 year).

The smoothed profiles of total number of beta cells, $N(t)$ (Eq. (4.7)), the new beta cell formation, $B(t)$ (Eq. (4.23)), and the *per capita* beta cell death rate, $\mu(t)$ (Eq. (4.25)) interpolated from t=0 to t corresponding to the first available sample (t=0.8+0 year) are shown in Figure 6.21. Three different kinds of interpolations were tested: linear, cubic spline, and piecewise cubic Hermite. While the first and the third interpolations provided reliable curves for N, B, and μ from zero to t corresponding to the first available sample, the cubic spline interpolation presented negative values for N. For this reason it was no longer considered in the following.

The linear interpolations of the new beta cell formation and the *per capita* beta cell death rate were used to calculate the density $n(a,t)$ of beta cells of age a at time t according to Eq. (4.31). Figure 6.22 - top panel depicts the resulting $n(a,t)$ for all t in the range 0-39.8 years. Figure 6.22 - lower panel shows the probability density function $pdf_n(a,t)$ for t corresponding to 0 (i.e. 2 weeks), 10, 20, 30, and 39 years of age. At birth there was a high probability density of new born beta cells (8.2 $year^{-1}$); this quantity decreased to 0.2 $year^{-1}$ at 10 years of age, and increased thereafter up to 2.3 $year^{-1}$ at 39 years of age. The overall conclusions were essentially the same when the piecewise cubic Hermite rather than linear interpolation

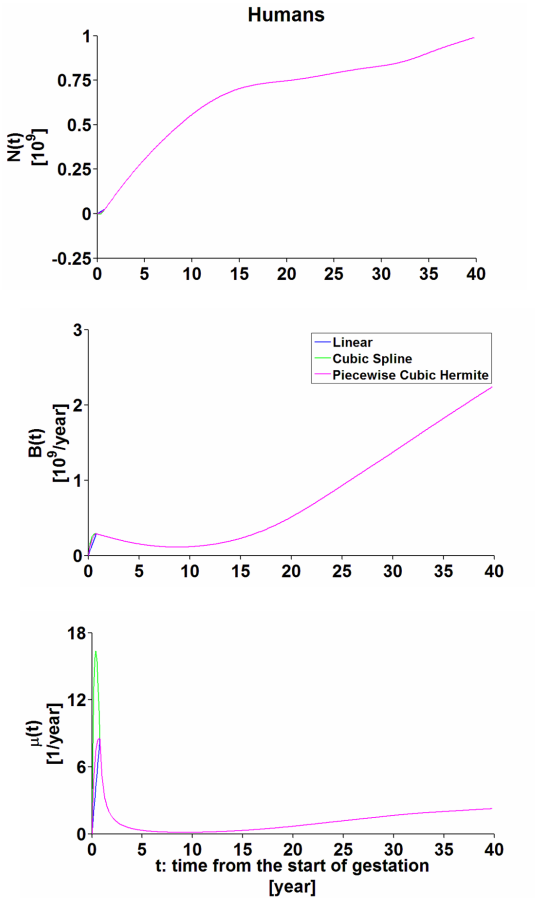

Figure 6.21: The total number of beta cells $N(t)$ (top panel), the new beta cell formation $B(t)$ (middle panel), and the *per capita* beta cell death rate $\mu(t)$ (lower panel) in young humans. These profiles were obtained by performing either a linear (in blue), cubic spline (in green) or a piecewise cubic Hermite (in pink) interpolation from zero (t=0 is the start of gestation that lasts circa 0.8 year in humans) to t corresponding to the first available datum (i.e. 2 weeks of age).

was considered.

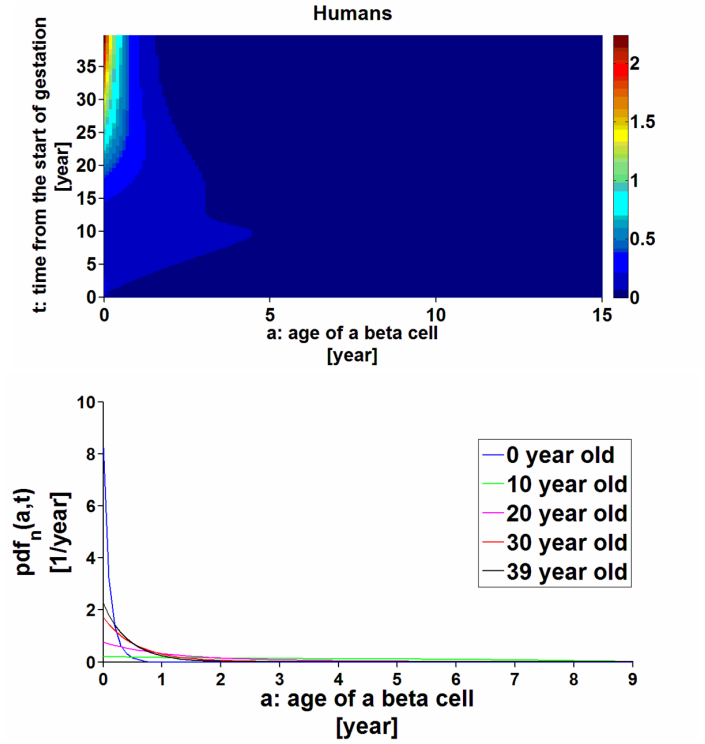

Figure 6.22: The density $n(a,t)$ (10^9/year) of beta cells of age a at time t in young humans (top panel). The density was obtained for all t in the range 0-39.8 years by substituting the linear interpolations of the new beta cell formation and the *per capita* beta cell death rate into Eq. (4.31). Light colors correspond to high values of $n(a,t)$, dark colors to low values. Lower panel shows the curves of the probability density function $pdf_n(a,t)$ for t corresponding to 0 (i.e. 2 weeks), 10, 20, 30, and 39 years of age. These curves describe how beta cells are distributed basing on their own age.

The obtained density $n(a,t)$ was used to calculate the mean age of a beta cell by Eq. (4.32). Figure 6.23 shows the resulting mean age of a beta cell as a function of the time t from the start of gestation (period 0-39.8 years). In young humans the mean age of a beta cell was in the range 0-3.9 years (average: 1.6 years). The profiles of the mean age of a beta cell obtained by either linear or piecewise cubic Hermite interpolations of the new beta cell formation and the *per capita* beta cell death rate were similar.

The *per capita* beta cell death rate was used to calculate the mean beta cell lifetime according to Eq. (4.40). Figure 6.24 shows the mean beta cell lifetime as a function of the time t from the start of gestation (period 0-39.8 years). In young humans the mean beta cell lifetime was in the range

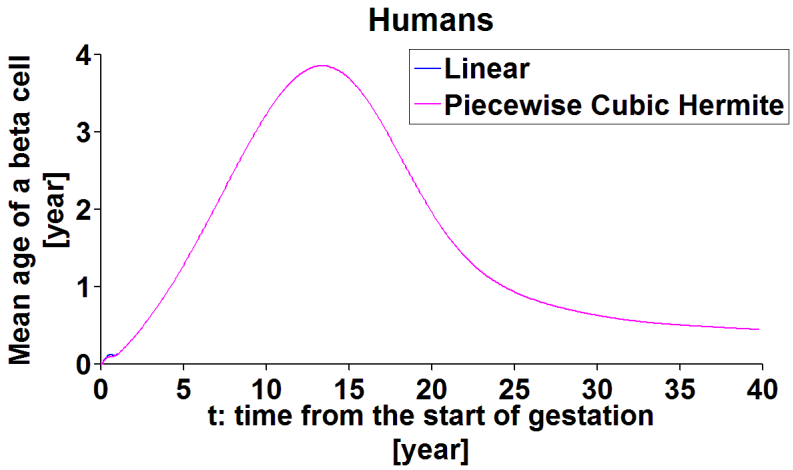

Figure 6.23: The mean age of a beta cell in young humans obtained by either linear (in blue) or piecewise cubic Hermite interpolation (in pink) of the new beta cell formation and the *per capita* beta cell death rate.

0-5.0 years (average: 1.9 years). The profiles of the mean beta cell lifetime obtained by either linear or piecewise cubic Hermite interpolation of *per capita* beta cell death rate were similar.

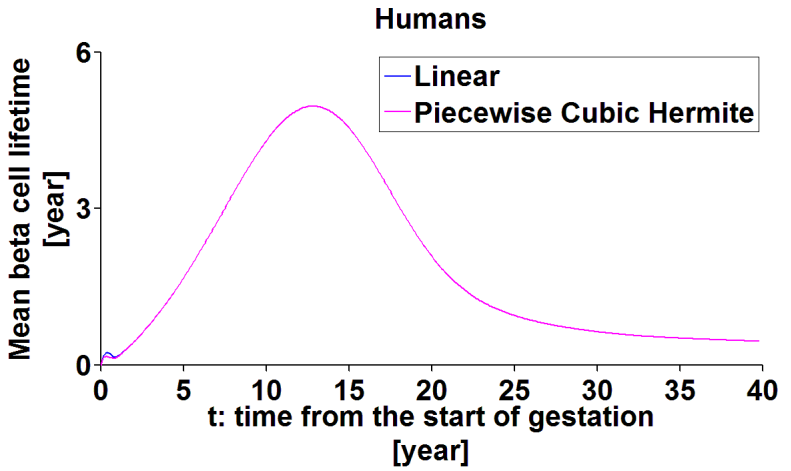

Figure 6.24: The mean beta cell lifetime in young humans obtained by either linear (in blue) or piecewise cubic Hermite interpolation (in pink) of *per capita* beta cell death rate.

To verify the impact of the assumptions of the model, the profile of the total number of beta cells ($N(t)$) was compared to the area under the curve of the density $n(a,t)$ according to Eq. (4.20). The profiles were similar (Figure 6.25) and the percent relative differences between the two quantities were less than 0.24%, assuring that the model assumptions did not introduce

a relevant bias into the results.

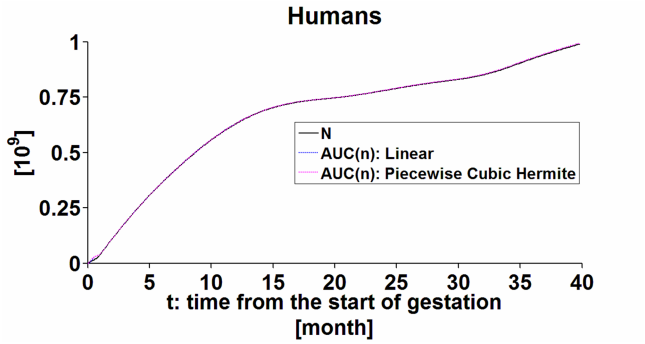

Figure 6.25: The total number of beta cells (black line) *versus* the area under the curve of the density $n(a,t)$ in young humans obtained either by linear (blue dashed line) of piecewise cubic Hermite interpolation (pink dashed line) of the new beta cell formation and the *per capita* beta cell death rate.

6.4 Adult Human Study

Significant Beta Cell Turnover

Assuming that beta cell mass, replication, and apoptosis were at steady state over the period of observation, we applied the model to compute beta cell mass turnover in steady state (Eq. (4.6)).

This analysis affirmed that there is significant ongoing beta cell turnover in adult humans (Figure 6.26). In young adult lean group the rate of beta cell apoptosis (1639±323 mg/year) far exceeded the rate of beta cell replication (107±52 mg/year), implying that for steady state beta cell mass to prevail, the majority of newly forming beta cells must be derived independently from beta cell replication, i.e. OSB (1532±312 mg/year). The pattern was comparable in elderly lean group: the rate of beta cell apoptosis was 2446±711 mg/year; the rate of beta cell replication 36±12 mg/year; OSB 2410±704 mg/year. In the young adult obese group there was an increase in the rate of apoptosis (6069±2117 mg/year, $P<0.05$) and in OSB (6020±2119 mg/year, $P<0.05$) with respect to the young adult lean group. In the young adult obese group the rate of beta cell replication was 49±9 mg/year.

Since the size of beta cells increased significantly in elderly lean *versus* young adult lean individuals (Figure 2.14 - top panel), we also assessed beta cell turnover by adapting the model to compute the turnover of beta cell numbers rather than mass (Eq. (4.12)). The pattern of beta cell turnover was comparable to that in the mass calculation, although as expected the

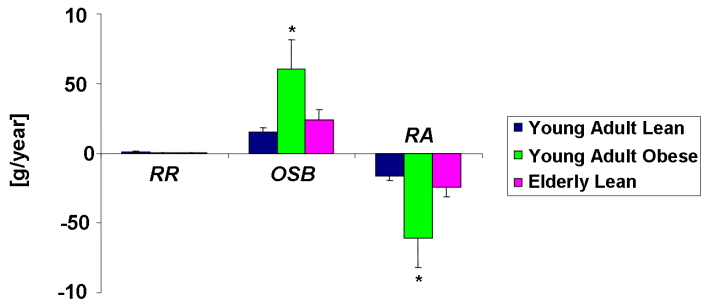

Figure 6.26: Beta cell mass turnover in young adult lean (in blue), young adult obese (in green), and elderly lean individuals (in pink). The first three bars show the contribution to beta cell mass formation from replication of existing beta cells (RR), the second three bars the contribution from OSB. The last three bars represent the loss due to beta cell apoptosis (RA). *: young adult lean *versus* young adult obese, P<0.05. Bars represent SEM.

gap between the two groups increased (Figure 6.27). In the young adult lean group using the cell number approach the rates of beta cell apoptosis and replication were $(1.69\pm0.34)\cdot10^9$ and $(0.10\pm0.05)\cdot10^9$ beta cells per year, with a computed OSB_N of $(1.59\pm0.33)\cdot10^9$ beta cells per year. In the elderly lean group using the cell number approach the rates of beta cell apoptosis and replication were $(2.79\pm1.23)\cdot10^9$ and $(0.05\pm0.02)\cdot10^9$ beta cells per year, with a calculated OSB_N of $(2.74\pm1.21)\cdot10^9$ beta cells per year. In the young adult obese group there was again an increase in the rate of apoptosis ($(6.86\pm2.58)\cdot10^9$ beta cells per year, P<0.05) and in OSB_N ($(6.80\pm2.59)\cdot10^9$ beta cells per year, P=0.0503) with respect to the young adult lean group. In the young adult obese group the rate of beta cell replication was $(0.06\pm0.01)\cdot10^9$ beta cells per year.

The Mean Age of a Beta Cell and The Mean Beta Cell Lifetime were Comparable in Young Adult Lean, Young Adult Obese, and Elderly Lean Individuals

Since the individuals are in their adulthood, it was reasonable to assume that beta cells present at birth are mostly dead at the time of the study.

The total number of beta cells (N), the new beta cell formation (B), and the *per capita* beta cell death rate (μ) were obtained in each individual from raw data. These quantities were used to calculate the density $n(a,t)$ in each individual according to Eq. (4.31) (Figure 6.28). Similarly, the curves of the probability density function were obtained in each individual by Eq. (4.21). Figure 6.29 depicts the resulting probability density function $pdf_n(a,t)$: for all the individuals there was a high probability density of

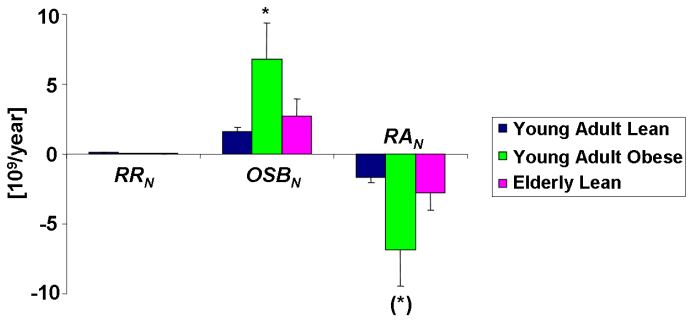

Figure 6.27: Beta cell number turnover in young adult lean (in blue), young adult obese (in green), and elderly lean individuals (in pink). The first three bars show the contribution to beta cell formation from replication of existing beta cells (RR_N), the second three bars the contribution from OSB_N. The last three bars represent the loss due to beta cell apoptosis (RA_N). *: young adult lean *versus* young adult obese, P<0.05; (*): young adult lean *versus* young adult obese, P=0.0503. Bars represent SEM.

new born beta cells (range in young adult lean group: 0.9-6.3 year^{-1}; range in young adult obese group: 0.5-12.3 year^{-1}; range in elderly lean group: 0.5-12.1 year^{-1}). For young adult lean individuals number five and twelve, for young adult obese individuals number one and six, and for elderly lean individuals number two, ten, and eleven it was not possible to determine the density $n(a,t)$ and the probability density function $pdf_n(a,t)$ since both the new beta cell formation and the *per capita* beta cell death rate were zero.

The mean age of a beta cell and the mean beta cell lifetime (Figure 6.30) were calculated as the reciprocal of the *per capita* beta cell death rate according to Eqs. (4.33) and (4.41). In young adult lean group these variables were 0.51±0.10 year (range: 0.15-1.11 year); in young adult obese individuals 0.48±0.19 year (range: 0.06-2.10 year); in elderly lean individuals 0.65±0.18 year (range: 0.07-1.90 year). For young adult lean individuals number five and twelve, for young adult obese individuals number one and six, and for elderly lean individuals number two, ten, and eleven it was not possible to determine these variables since *per capita* beta cell death rate was zero.

To verify the impact of the assumptions of the model, the total number of beta cells (N) was compared to the area under the curve of the density $n(a,t)$ according to Eq. (4.20). In all the three groups, the percent relative differences between the two quantities were less than 0.07%, assuring that the model assumptions did not introduce a relevant bias into the results.

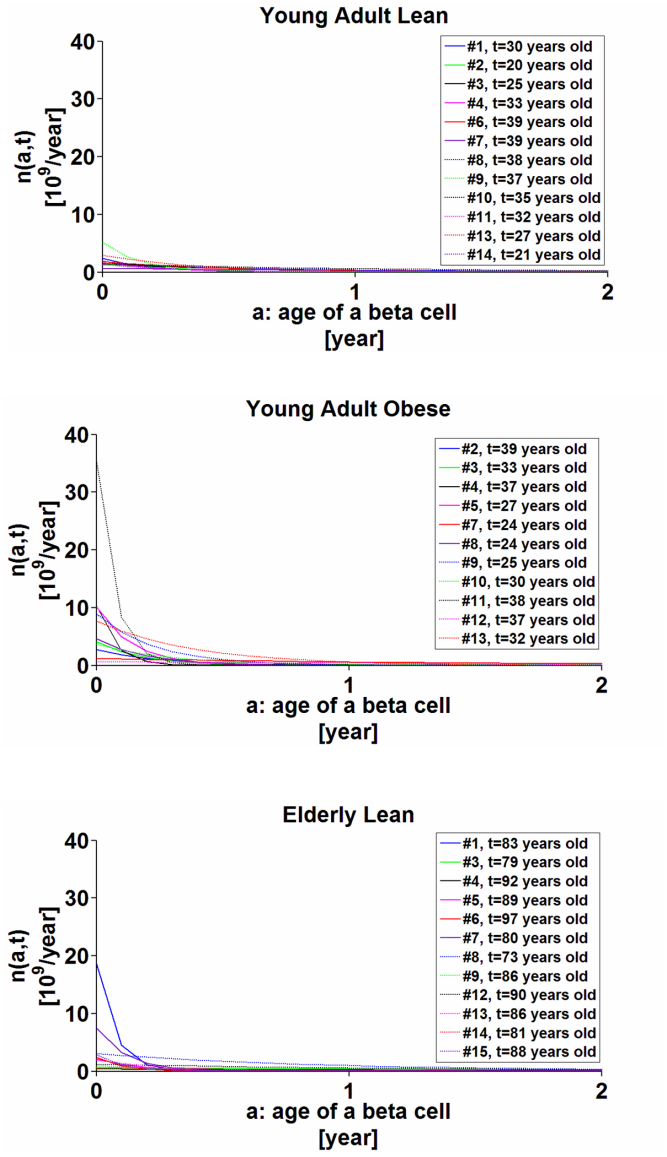

Figure 6.28: The density $n(a,t)$ of beta cells of age a in young adult lean (top panel), young adult obese (middle panel), and elderly lean individuals (lower panel) of age t. For young adult lean individuals number five and twelve, for young adult obese individuals number one and six, and for elderly lean individuals number two, ten, and eleven it was not possible to determine the density $n(a,t)$ since both the new beta cell formation and the *per capita* beta cell death rate were zero.

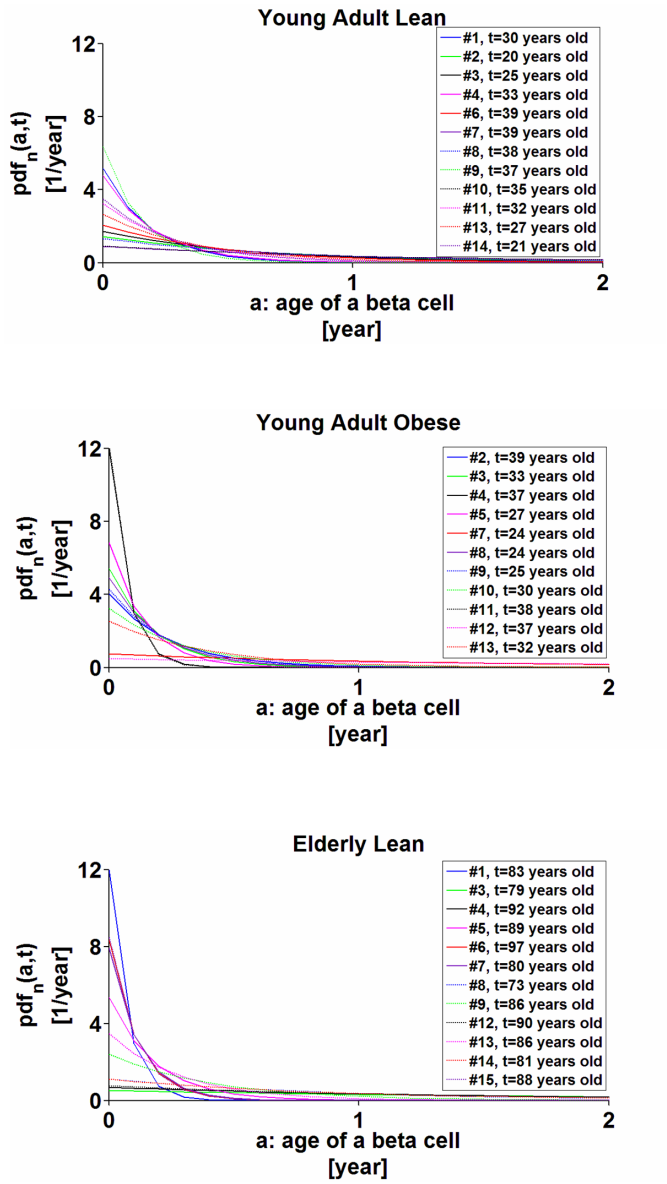

Figure 6.29: The probability density function $pdf_n(a,t)$ of beta cells of age a in young adult lean (top panel), young adult obese (middle panel), and elderly lean individuals (lower panel) of age t. For young adult lean individuals number five and twelve, for young adult obese individuals number one and six, and for elderly lean individuals number two, ten, and eleven it was not possible to determine the probability density function $pdf_n(a,t)$ since both the new beta cell formation and the *per capita* beta cell death rate were zero.

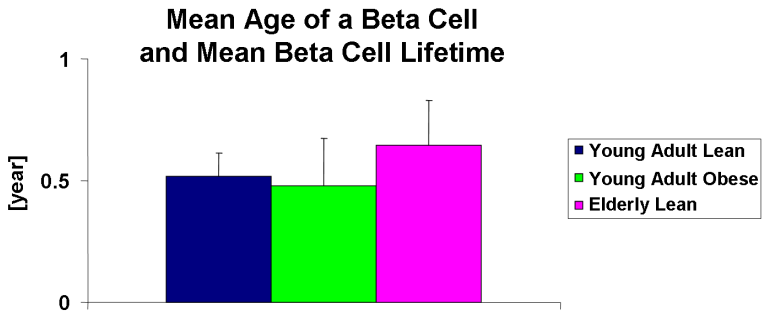

Figure 6.30: The mean age of a beta cell and the mean beta cell lifetime in young adult lean (blue), young adult obese (green), and elderly lean individuals (pink) of age t. Bars represent SEM.

Chapter 7

Discussion

The results of the rat, monkey, and human studies (*Chapter 6*) are separately discussed in the following.

7.1 Rat Study

The beta cell turnover model was applied to non diabetic rats from birth to adult life to gain insights into beta cell turnover during growth and maintenance of beta cell mass in health. Specifically, we tested the hypothesis that beta cell formation can be accounted for by duplication of existing beta cells. This hypothesis was rejected by the modeled data, and thus we conclude that formation and maintenance of beta cell mass depends on sources of beta cells independent of duplication of existing beta cells. Moreover, we conclude that the rate of formation of beta cells from this source (or sources) increases in the setting of increased beta cell apoptosis in the HIP rat model of T2DM. The effect of the increased formation of beta cells in the HIP rat was to slow the progression of beta cell loss, implying that there is attempted beta cell regeneration in this model of T2DM. Having established that changes in beta cell mass in vivo could be explained only by a source (or sources) of newly forming beta cells in addition to those arising from duplication of existing beta cells, we introduced the term other sources of beta cells, abbreviated to OSB. The term OSB was carefully chosen to not offer any prejudice as to the origins of these beta cells (*Chapter 1*), since the experimental approach here does not seek to identify their source.

Before accepting the principal conclusion of the present study, that there is indeed a quantitatively significant source of new beta cells that arise from a source distinct from duplication of existing beta cells, it is important to question the limitations of the approach used. In short, are the potential errors of sufficient magnitude that they could have permitted us to falsely

conclude that beta cells arise from sources other than beta cell replication? To address this, we used the approach of propagation of errors to establish the variance in the computed OSB and then taking this variance into account tested the hypothesis that OSB is different from zero. Even when taking into account the sum of the variance of individual measurements required to compute OSB, the hypothesis that OSB is different from zero was consistently proven (Figure 6.5), implying that OSB is not simply a result of sample variance. A second plausible source of error that might account for the conclusion that OSB exists could be errors in the factors used to convert the frequency of beta cell replication and apoptosis to rates of replication and apoptosis. To address this we examined the range of conversion factors that would be required to permit the observed changes in beta cell mass over time if OSB was equal to zero. The required conversion factors to conclude that OSB is zero (Figure 7.1) are implausible based on the published literature [1, 4, 47, 66, 75, 79]. Although these analyses suggest that OSB does indeed exist, as in most complex biological systems, it is impossible to exclude all possible sources of systematic bias. Some of the limitations in developing the model are listed in the description of model development (*Chapter 4*). In brief, these include the possible confounding effects of inhomogeneity in behavior of the beta cell pool with regard to turnover. It should also be emphasized that if beta cells defined here by detectable insulin by immunohistochemistry were to dedifferentiate to the extent that insulin was no longer detectable before undergoing replication, this would be assigned to OSB by the present approach.

The current study also examines the role of changes in individual beta cell size (volume) in involution and expansion of beta cell mass [21, 56]. For this purpose we examined beta cell turnover by two models, the first considering beta cell mass (Eq. (4.1)), where OSB includes changes in beta cell mass due to both the change in number of beta cells by other sources and changes in the mean beta cell size, and the second based on beta cell number (Eq. (4.7)). The small percent relative differences ($\leq$11%) between the two models shown in Table 6.1 reveal that the cell size does not much influence the estimation of beta cell turnover with beta cell mass data in the WT or HIP rats with aging.

The application of the model to evaluate beta cell turnover provided several interesting insights. First, the model implies that OSB provides an important contribution to the postnatal expansion of beta cell mass in the rat. This result differs with the conclusions of studies in mice that imply that the postnatal expansion of beta cell mass is derived exclusively by duplication of existing beta cells [8, 25, 36, 94]. One possible explanation is that rats differ from mice, although this seems unlikely. An alternative explanation is that the cells that give rise to pancreatic beta cells identified as $OSBs$ by this model are labeled by the same lineage markers as differ-

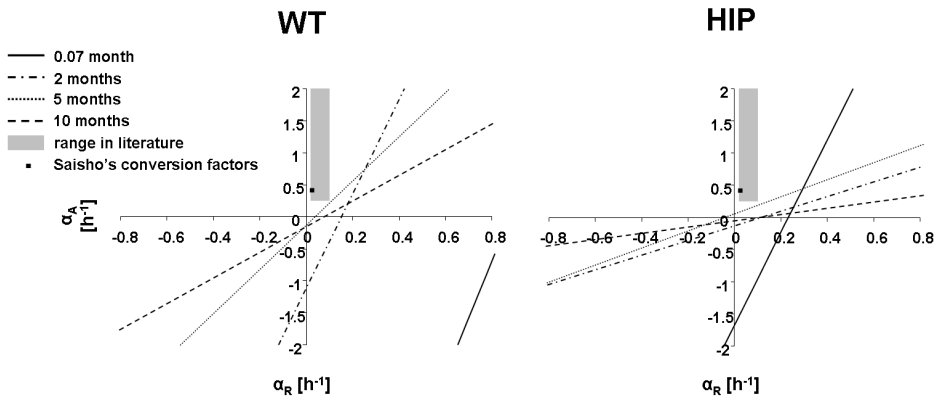

Figure 7.1: Conversion factors for beta cell replication and apoptosis required to conclude that there is no formation of beta cell from sources independent from beta cell replication - rat study. The pairs of values for the conversion factors for beta cell replication α_R and beta cell apoptosis α_A lying on each line represent possible values for α_R and α_A which allow to conclude that OSB is zero. In this figure are depicted those linear relations in WT (left panel) and HIP rats (right panel) for each analyzed age: 0.07 (continuous line), 2 (point-dashed line), 5 (dashed thin line), and 10 months (dashed line). In details, linear relations are obtained from Eq. (4.1) assuming OSB equal to zero for each time (age) point where the rate of change in beta cell mass, beta cell mass, and frequency of beta cell replication and apoptosis are known. The required conversion factors that would satisfy the mass balance described by Eq. (4.1) assuming OSB equal to zero are not in the plausible range (grey rectangle) based on the published literature [1, 4, 47, 66, 75, 79]: 0.02-0.1 h^{-1} for replication (corresponding to period of 10-50h for replication), 0.25-2 h^{-1} for apoptosis (corresponding to an execution period of apoptosis of 0.5-4h). Therefore, this analysis suggests that OSB does exist. The black square represents the conversion factors measured in beta cells and applied in the present turnover model [83].

entiated beta cells. Recent data support the concept that ductal progenitor cells have the capacity to form new beta cells both during postnatal growth and in response to injury [6, 43]. An insight that emerged by modeling beta cell turnover in the HIP rat is that the decline in beta cell mass in this model of type 2 diabetes is delayed by a compensatory increase in the rate of formation of beta cells from OSB. Indeed, it appears that OSB might be regulated and the principal mechanism for maintaining beta cell mass. In older wild type rats the rate of OSB increased as beta cell apoptosis increased with aging, and in the HIP rat the rate of increase in OSB was impressive albeit still insufficient to maintain beta cell mass in the face of a progressive increase in beta cell apoptosis.

The resulting components of beta cell turnover, i.e. new beta cell formation (duplication of existing beta cells plus other sources of beta cells rather

than beta cell replication) and beta cell death rate, were used to assess the mean age of a beta cell and the mean beta cell lifetime considering beta cells as a variegate population of cells that differ each other by their own age (Eqs. (4.32) and (4.40)).

In WT rats the mean age of a beta cell was 2.2 months (range 0-3.6 months), while in HIP rats it was almost halved (0.9 month; range 0-1.2 month), due to the higher probability density of young beta cells in HIP *versus* WT rats. These results are consistent with those reported in [31], where the resulting mean age of a beta cell in rats was in the range 0-3 months. As to the mean beta cell lifetime, in WT rats this variable was in the range 0-4.6 months (average: 3.2 months), while in HIP rats it was in the range 0-1.3 months (average: 1.0 month). These results reveal the difference between mean beta cell age and lifetime: while the first describes how old are on average beta cells in a individual and results in a function of both beta cell formation and loss (Eq. (4.32)), mean beta cell lifetime is only a function of beta cell loss (Eq. (4.40)) since it expresses the life expectancy of beta cells in an individual. Some of the limitations in developing the model to estimate the mean age of a beta cell and the mean beta cell lifetime are related to beta cell turnover model hypotheses that not include the possible confounding effects of inhomogeneity in behavior of beta cells with regard to turnover. Other limitations derive from the assumptions proper of the population model (Eq. (4.31)), that is: after an event of beta cell replication, one daughter cell retains the age of the parent cell and one is considered new; all beta cells have the same probability to die; t=0 corresponds to the start of gestation (*Chapter 4*). To verify the impact of the model assumptions, the profile of the total number of beta cells at time t (time from the start of gestation) was compared to the area under the curve of the density of beta cells of age a at time t according to Eq. (4.20). In both WT and HIP rats, the profiles were similar (Figure 6.10) and the percent relative differences between the two quantities were less than 9%, assuring that the model assumptions did not introduce a relevant bias into the results.

The application of the model to evaluate the mean age of a beta cell and the mean beta cell lifetime provides interesting insights into the possibility of using endogenous beta cell regeneration as a strategy to restore beta cell mass. According to our results, the time required for beta cell mass to be regenerated is around 4 months in adult WT and 1 month in adult HIP rats, reasonable numbers with respect to the life expectancy of a rat (circa 12 months). For this strategy to be implemented excessive apoptosis would need to be suppressed. Nevertheless, additional experiments and mathematical models are required to really quantify how long it would take to restore beta cell mass if apoptosis was decreased to normal.

7.2 Monkey Study

We report that beta cell turnover continues in adult non human primates, with newly formed beta cells derived primarily from sources of beta cells independent from duplication of existing beta cells. Moreover we report that beta cell formation continues in a STZ model of type 1 diabetes, although at a decreased rate (5.2±2.3 *versus* 31.7±7.1 mg/month) compared to non diabetic controls, but again primarily from OSB.

Measurement of beta cell turnover by a model based approach was used here in non human primates since lineage tracing is not readily accomplished in primates. The attributes and limitations of the model have been discussed in detail (*Chapter 4*). Conversion of the frequency of beta cell replication and apoptosis to the respective rates of replication and apoptosis was accomplished by conversion factors developed by a combination of in vivo time lapse imaging and subsequent immunohistochemistry [83]. These conversion factors were developed in rat islets and to the extent that they differ in non human primates, the present study may be in error. Given the low frequency of both beta cell apoptosis and replication, relatively large errors in quantification of beta cell turnover may arise unless a substantial number of cells are evaluated. To this end we quantified beta cell replication and apoptosis in circa 38000 and circa 87000 beta cells respectively.

We define OSB as beta cells arising from sources other than replication detected by Ki67 in insulin positive beta cells. One possible OSB using this definition would be duplication of degranulated beta cells that were not detected by insulin immunostaining. Also, if beta cells dedifferentiated and lost insulin immunoreactivity prior to duplication, by this definition these cells would be considered as arising from other sources of beta cells other than beta cell replication. In the absence of lineage tracing in non human primates we cannot fully exclude either of these possible sources of beta cells although (via infra) we did not detect insulin negative GLUT2 positive cells in either control or STZ pancreas (Figure 2.6 - panels C and F).

Ideally to model changes in beta cell turnover multiple measurements of beta cell mass and turnover would be acquired in the same individuals at different time points. Since it is currently not possible to quantify beta cell mass or beta cell turnover non-invasively, we elected to obtain two samples of pancreas from the same individual on two occasions, first by surgical open biopsy and second at euthanasia. The time between the first and second samples was varied between individuals as illustrated in Figure 2.5 in order to permit a range of measures of beta cell mass and turnover after acute induction of a deficit in beta cell mass by STZ. As expected, in the control group, there was no change in beta cell mass during the study period. Also the frequency of beta cell replication (by Ki67) and apoptosis (by TUNEL)

were comparable in control pancreas secured by surgical biopsy and at euthanasia, implying steady state beta cell turnover. When these data were further evaluated to compute beta cell turnover, the results imply that beta cell mass is renewed and sustained by ongoing beta cell turnover in non human primates. Consistent with rat study results, the majority of new beta cell formation in adult non human primates is derived independently from replication of existing beta cells. This is consistent with recent lineage tracing data in support of beta cell neogenesis from ductal precursors in mice [43].

Having documented and quantified beta cell turnover in adult non human primates, our secondary goal was to establish if beta cell turnover is sustained in an STZ model of type 1 diabetes. Moreover, we sought to establish if there was any evidence of an adaptive increase in beta cell formation in response to beta cell deficiency and diabetes in this model. The deficit in beta cell mass in the STZ monkeys was comparable to that in established type 1 diabetes in humans [11, 62]. To accomplish effective beta cell regeneration in the STZ non human primate model, beta cell formation would need to be adaptively increased to a rate that exceeds loss of beta cells through normal aging. However there was no increase in beta cell mass or amelioration of diabetes in the adult non human primates during the 6 months following induction of diabetes. OSB in STZ monkeys was sustained at a rate that maintained the fractional turnover rate of the remaining decreased number of beta cells at a comparable rate to that in control primates, but did not adaptively increase in response to hyperglycemia. These data are consistent with available data in humans with established type 1 diabetes where a low number of beta cells are often still detected, with minimal beta cell replication and a detectable but low frequency of beta cell apoptosis [62]. We previously proposed that the latter implies ongoing beta cell formation, but presumably at a rate that is insufficient to accomplish beta cell regeneration (a net increase in beta cell mass). In either type 1 diabetes or the STZ non human primates, effective beta cell regeneration would require formation of new beta cells at a rate that exceeds natural attrition. It is unclear to what extent OSB can adaptively increase, and if so how it is regulated. In the rat model of type 2 diabetes we observed a marked increase in beta cell formation from other sources other than beta cell replication that delayed loss of beta cell mass in response to a shortened beta cell life span through increased apoptosis. It is possible that the lack of an adaptive increased OSB in non human primates compared to rats was a species difference. Another possibility is that STZ induces toxicity in the precursor cells that give rise to OSB.

The absence of increased beta cell apoptosis in the STZ non human primate exposed to glucose values of 200 - 300 mg/dl for up to 6 months was unexpected given the reported glucose toxicity [74]. However most

studies that report actions of high glucose concentrations to induce beta cell apoptosis have either been undertaken in animal models with other mechanisms of beta cell toxicity present, or in isolated islets which have a high rate of beta cell apoptosis consequent upon anoxia. In the present study we noted that plasma membrane localization of GLUT2 transporter protein in beta cells of STZ non human primates was decreased, consistent with prior reports in rodents with diabetes [35, 44, 45]. Thus it is likely that beta cells adaptively protect themselves to long term glucose toxicity by decreasing access of glucose to the beta cell. Of course this in turn would likely compound impaired beta cell function [95].

The reciprocal of the *per capita* beta cell death rate (resulting from the components of the beta cell turnover, Eq. (4.25)) coincided with the mean age of a beta cell and the mean beta cell lifetime according to Eqs. (4.33) and (4.41). In control monkeys these variables were 4.8±1.6 months, while in STZ monkeys they were almost halved. For STZ monkeys number two and five it was not possible to determine these variables since *per capita* beta cell death rate was zero. Limitations in developing the model to estimate the mean age of a beta cell are listed in the description of model assumptions (*Chapter 4*). To verify the impact of these hypotheses, the profile of the total number of beta cells in a monkey of age t was compared to the area under the curve of the density of beta cells of age a at time t according to Eq. (4.20). In both control and STZ monkeys, the percent relative differences between the two quantities were less than 4%, assuring that the model assumptions did not introduce a relevant bias into the results.

As in the rat study, the application of the model to evaluate the mean age of a beta cell and the mean beta cell lifetime provides interesting insights into the possibility of using endogenous beta cell regeneration as a strategy to restore beta cell mass. According to our results, the time required for beta cell mass to be regenerated is around 5 months in adult non human primates and 2 month in adult STZ monkeys, reasonable numbers with respect to the life expectancy of a monkey (7-12 years). Nevertheless, additional experiments and mathematical models are required to really quantify how long it would take to restore beta cell mass in STZ monkeys, if beta cell turnover could be altered therapeutically.

7.3 Young Human Study

The beta cell turnover model was applied to young humans from 2 weeks to 39 years of age to gain insights into beta cell turnover during growth and maintenance of beta cell mass in health. Specifically, we tested the hypothesis that beta cell formation can be accounted for by replication of existing beta cells in childhood (0-15 years of age): this hypothesis was

confirmed by the modeled data. Furthermore the results show that around 20 years of age the contribution of other sources of beta cells other than beta cell replication became important in counterbalancing the considerable increase in the rate of beta cell apoptosis. Thus we conclude that formation of beta cell mass in childhood depends on duplication of existing beta cells, while its maintenance after 20 years of age is related to OSB.

The attributes and limitations of the model have been discussed in detail (*Chapter 4*). Conversion of the frequency of beta cell replication and apoptosis to the respective rates of replication and apoptosis was accomplished by conversion factors developed by a combination of in vivo time lapse imaging and subsequent immunohistochemistry [83]. These conversion factors were developed in rat islets and to the extent that they differ in humans, the present study may be in error. Although we performed some pilot studies with human islets, they were unsuitable for the purpose for several reasons. First of all, beta cell replication was almost never detected in human islets, even in culture on a cell matrix. Although beta cell replication is detectable in human infants, donor islets were available only from adults. Secondarily, in contrast to rodent islets, which are obtained immediately after death of a previously healthy animal, human islets for research are obtained from pancreases procured from terminally ill brain-dead donors after removal of multiple organs (heart, lungs, liver, and kidneys) for transplantation. Moreover, the isolated islets are then typically shipped overnight before use. Perhaps not surprisingly, these human donor islets typically have high rates of beta cell apoptosis and often a relatively small proportion of beta cells *versus* non beta cells. Therefore, we concluded from pilot studies that human islets were not suitable for the replication or apoptosis TLVM studies planned here. It is of interest that the frequency of replication by Ki67 and apoptosis by TUNEL staining in rat islets closely approximates that in human pancreas obtained during postnatal expansion [48, 63] as well as rodent pancreas procured at the same age [67, 69].

Other important limitations related to the scarcity of available data are widely described in [63]. In brief, these include the possibility that beta cell mass and especially beta cell turnover can be affected by postmortem change and by final illness leading to death. Furthermore, by definition, these studies are cross-sectional, since there is no opportunity to measure beta cell mass (or turnover) in vivo in humans on multiple occasions. The normal growth pattern (height and weight, [63]) in our group of cases suggest that the cases were for the most part representative of healthy children until death. Another limitation of these studies is the fact that autopsy pancreas was limited to pancreas tail. To compensate for the lack of a measured volume to compute beta cell mass, we previously generated a population curve by CT scan of pancreas volume growth during childhood and adulthood [82].

The application of the model to evaluate beta cell turnover provided several interesting insights. First, the model implies that beta cell replication is the primary mechanism subserving the postnatal expansion of beta cell mass in humans. This result differs with the conclusions of the rat study, but agrees with the studies in mice [8, 25, 36, 94]. Another insight that emerged by modeling beta cell turnover in adult humans (aged 20-39 years) is that OSB might be the principal mechanism for maintaining beta cell mass since in adulthood the rate of OSB increased as beta cell apoptosis increased with aging, as in older WT rats. The overall conclusions are essentially the same when beta cell number rather than beta cell mass is considered, thus confirming a modest role of individual beta cell size in involution and expansion of beta cell mass.

The resulting components of beta cell turnover, i.e. new beta cell formation (duplication of existing beta cells plus other sources of beta cells rather than beta cell replication) and rate of beta cell apoptosis, were used to assess the mean age of a beta cell and the mean beta cell lifetime considering beta cells as a variegate population of cells that differ each other by their own age (Eqs. (4.32) and (4.40)). In young the mean age of a beta cell was in the range 0-3.9 years (average: 1.6 years) and reached its maximum at circa 12 years of age of the individual. While the mean beta cell lifetime was in the range 0-5.0 years (average: 1.9 years). Again, as in the rat study, these results reveal the difference between mean beta cell age and lifetime: while the first describes how old are on average beta cells in a individual and results in a function of both beta cell formation and loss (Eq. (4.32)), mean beta cell lifetime is only a function of beta cell loss (Eq. (4.40)) since it expresses the life expectancy of beta cells in an individual. Some of the limitations in developing the model to estimate the mean age of a beta cell and the mean beta cell lifetime are listed in the description of model assumptions (*Chapter 4*). To verify the impact of these hypotheses, the profile of the total number of beta cells at time t (time from the start of gestation) was compared to the area under the curve of the density of beta cells of age a at time t according to Eq. (4.20). The profiles were similar (Figure 6.25) and the percent relative differences between the two quantities were less than 0.24%, assuring that the model assumptions did not introduce a relevant bias into the results.

As in the rat and monkey studies, the application of the model to evaluate the mean age of a beta cell and the mean beta cell lifetime provide interesting insights into time required for endogenous regeneration of beta cells to restore beta cell mass. According to our results, the time required for beta cell mass to be regenerated is around 2 years in young humans, reasonable numbers with respect to the life expectancy of an individual (circa 67 years). Nevertheless, additional experiments and mathematical models are required to really quantify how long it would take to regenerate beta cell

mass.

7.4 Adult Human Study

In this study we report that: 1) beta cell mass and beta cell turnover markedly increase in response to obesity; 2) there is active beta cell turnover and beta cell mass is maintained throughout adult life, 3) the newly formed beta cells in adult humans predominantly come from the other sources of beta cells (OSB) than beta cell replication.

The attributes and limitations of the model have been discussed in detail (*Chapter 4*). Conversion of the frequency of beta cell replication and apoptosis to the respective rates of replication and apoptosis was accomplished by conversion factors developed by a combination of in vivo time lapse imaging and subsequent immunohistochemistry [83]. These conversion factors were developed in rat islets and to the extent that they differ in humans, the present study may be in error (see *Young Human Study* for details). Other important limitations related to the scarcity of available data are widely described in [63] and briefly resumed in the young human study.

Despite in the young human study the resulting smoothed profiles for beta cell mass and turnover were not in steady state conditions in the range of age 20-39 years, in young lean, young obese, and elderly lean groups beta cell mass and turnover were considered in steady state because these quantities did not show a particular trend dependent on age. The resulting circa 50% increase in beta cell mass in response to obesity is consistent with previous autopsy studies with smaller sample size [13, 49, 71, 104]. Ogilvie reported that islets of Langerhans appeared to be enlarged in humans with obesity as early as 1933 [71]. Kloppel *et al.* reported that there is no increase in fractional beta cell area but two fold increase in pancreas parenchymal volume, resulting in circa 40% increase in beta cell mass in 4 obese humans compared to 7 lean humans [49]. Yoon et al. reported a positive linear correlation between fractional beta cell area and BMI in 9 non diabetic humans with a BMI of 22 to 27 in patients undergoing a partial pancreatectomy for pancreatic tumors [104]. We also previously reported circa 50% increase in fractional beta cell area in 31 obese non diabetic humans compared to 17 lean non diabetic humans [13]. But in this study the age of the groups were older and not matched between the groups (67±3 year in obese 78±3 year in lean) since the study was designed to compare non diabetics versus diabetics. Now we report circa 50% increase in beta cell mass in response to obesity in adult humans. This increase was accomplished by increased numbers of beta cells rather than increased cell size, affirming an increased capacity for new beta cell formation in obese humans.

When the young lean and the elderly lean groups were compared, we did

not find any increase in beta cell mass, but rather we observed an increase in individual beta cell size in the elder cases compared to the younger cases, suggesting an increasing beta cell workload with age. We also report that to maintain beta cell mass in life long, new beta cell formation from OSB may become more important with age. Tyrberg *et al.* previously reported that birth rate of human adult beta cells transplanted under the kidney capsule of normoglycemic mice was 0.4%/day by using 3H-thymidine incorporation, meaning the doubling time is circa 6 months [99]. We estimated the rate of beta cell replication of circa 0.02 to 0.04%/day by using Ki67 staining. This discrepancy between the two studies may be due to the use of different methodology. Since thymidine incorporation can not distinguish DNA synthesis from DNA repair [15], this method could overestimate the rate of beta cell replication. Beta cell turnover also can be different in transplanted human islets used in the former study from normal islets in vivo. However, it should be noted that there is a huge variation in beta cell replication (0 to 0.4%) as well as beta cell mass among individuals, one would assume that there is a huge variation in beta cell turnover in humans. Recent genome wide association studies also revealed several type 2 diabetes susceptible genes which are associated with beta cell replication or apoptosis [85, 88, 108], implying different beta cell turnover capacity among individuals may be associated with a risk of type 2 diabetes. However, while 0.4% beta cell replication translates 0.2%/day beta cell replication, meaning the beta cell doubling time of circa 1.5 years, even this high beta cell replication rate is still insufficient to compensate the mean beta cell apoptosis rate (circa 1%/day) to maintain beta cell mass in adult life, strongly suggesting the major role of OSB for new beta cell formation in adult humans, as shown in rodents and monkeys.

The reciprocal of the *per capita* beta cell death rate (resulting from the components of the beta cell turnover, Eq. (4.25)) coincided with the mean age of a beta cell and the mean beta cell lifetime according to Eqs. (4.33) and (4.41). In young lean, young obese, and elderly lean individuals these variables equalled circa 6 months. For young lean individuals number five and twelve, for young obese individuals number one and six, and for elderly lean individuals number two, ten, and eleven it was not possible to calculate these variables since *per capita* beta cell death rate was zero. Limitations in developing the model to estimate the mean age of a beta cell and the mean beta cell lifetime are listed in the description of model assumptions (*Chapter 4*). To verify the impact of these hypotheses, the profile of the total number of beta cells in an individual of age t was compared to the area under the curve of the density of beta cells of age a at time t according to Eq. (4.20). The percent relative differences between the two quantities were less than 0.07%, assuring that the model assumptions did not introduce a relevant bias into the results.

As in the rat, monkey, and young human studies, the application of the model to evaluate the mean age of a beta cell and the mean beta cell lifetime provide interesting insights into time required for endogenous regeneration of beta cells to restore beta cell mass. According to our results, the time required for beta cell mass to be regenerated is around 6 months in adult humans, reasonable numbers with respect to the life expectancy of an individual. Nevertheless, additional experiments and mathematical models are required to really quantify how long it would take to regenerate beta cell mass.

Chapter 8

Conclusions

In collaboration with the Larry Hillblom Islet Research Center at David Geffen School of Medicine, University of California Los Angeles, a dynamic model to estimate beta cell turnover from measurements of beta cell mass (related to beta cell number by beta cell volume) and frequencies of beta cell replication and apoptosis was developed and discussed. The model describes beta cell mass as the balance between beta cell formation and loss. Beta cells are added either by replication of existing beta cells or by other sources of beta cells (OSB), and they are mainly lost through beta cell apoptosis. Frequencies of beta cell replication and apoptosis were converted to rates in order to relate replication and apoptosis time-contributions to rate of change in beta cell mass. Factors to pass from frequencies to rates were obtained from calibration curves between frequencies measured by immunofluorescence technique and rates achieved by time-lapse video microscopy on the same pancreatic islets from 1 month old rats [83]. The model is based on a number of assumptions: the homogeneity of beta cell characteristics and dynamics, i.e. all beta cells share the volume, the probability to replicate [8] or die, and the conversion factors for beta cell replication and apoptosis. Moreover, since it was almost impossible to obtain data on beta cell turnover from an individual at multiple time points, a group of individuals examined at different time points was used to predict beta cell turnover over time in the population from which those individuals were sampled. The resulting components of beta cell turnover, i.e. new beta cell formation (replication of existing beta cells plus other sources of beta cells rather than beta cell replication) and beta cell death (apoptosis) rate, were used to develop a population model to assess the mean age of a beta cell and the mean beta cell lifetime. The resulting model is a variation of the classical McKendrick-von Foerster equation and describes beta cells as a variegate population of cells that differ each other by their own age.

The novel insights that emerge by applying the model to different species,

i.e. rats [58], monkeys, and humans are:

1. There is ongoing beta cell turnover in non diabetic rats, monkeys, and humans through adult life.

2. Formation and maintenance of adult beta cells largely depend on OSB in non diabetic rats, monkeys, and humans.

3. The rate of formation of new beta cells from other sources of beta cells increases substantially in the face of the increased rate of beta cell apoptosis in the HIP rat model of type 2 diabetes, delaying the decline in beta cell mass in this model. In contrast, beta cell turnover is low in the streptozotocin (STZ) monkey model of T1DM, compared to non diabetic controls. The extent that beta cells are formed in the STZ monkey is again primarily from OSB.

4. Beta cell replication is the primary mechanism subserving the postnatal expansion of beta cell mass in childhood, while in adulthood OSB might be the principal mechanism for maintaining beta cell mass in face of an increased rate of beta cell apoptosis.

5. Beta cell mass and beta cell turnover increase in response to obesity in humans.

6. The estimated mean age of a beta cell and mean beta cell let us postulate that it is possible to use endogenous beta cell regeneration as a strategy to restore beta cell mass. Nevertheless, the combination of additional experiments and mathematical models is required to assess how long it would take if apoptosis was decreased to normal, to restore beta cell mass in diabetes.

The presented models provide for the first time information about the existence of sources of beta cells other than beta cell replication and estimates of the mean age of a beta cell and the mean beta cell lifetime in rats, monkeys, and humans. The results will have a great impact from a clinical point of view considering that: a) the origin of beta cells is actively debated, i.e. some propose duplication of existing beta cells, and others suggest formation of new beta cells from a variety of sources [15]; b) restoration of glycemic control in type 1 and type 2 diabetes through endogenous regeneration could be a potential alternative strategy to pancreas transplantation given the insufficient number of pancreases available for transplantation and the risks of prolonged immunosuppression; c) the unique experimental approach to identify other sources of beta cells is the cell-lineage tracing that is not available in humans [94, 69, 25, 8]. Furthermore, the results encourage: a) future studies on beta cell turnover in patients with diabetes; b) the development of *ad hoc* experiments that identify the possible other sources

of beta cells rather than beta cell replication; c) to plan both experiments and mathematical models to establish the forms and the time required for endogenous regeneration of beta cell mass.

Contents

Bibliography

[1] Al-Rubeai M. and Fussenegger M. In *Cell Engineering - Apoptosis* ed. (Dordrecht: Kluwer Academic Publishers), 2004.

[2] Atkinson M.A. ADA Outstanding Scientific Achievement Lecture 2004. Thirty years of investigating the autoimmune basis for type 1 diabetes: why can't we prevent or reverse this disease? *Diabetes* 54: 1253-1263, 2005.

[3] Barker D.J., Hales C.N., Fall C.H., Osmond C., Phipps K., and Clark P.M. Type 2 (non-insulin-dependent) diabetes mellitus, hypertension and hyperlipidaemia (syndrome X): relation to reduced fetal growth. *Diabetologia* 36(1): 62-7, 1993.

[4] Baker A.J., Mooney A., Hughes J., Lombardi D., Johnson R.J., and Savill J. Mesangial cell apoptosis: the major mechanism for resolution of glomerular hypercellularity in experimental mesangial proliferative nephritis. *J Clin Invest* 94: 21052116, 1994.

[5] Bernard C., Berthault M.F., Saulnier C., and Ktorza A. Neogenesis vs. apoptosis As main components of pancreatic beta cell ass changes in glucose-infused normal and mildly diabetic adult rats. *Faseb J* 13: 1195-1205, 1999.

[6] Bonner-Weir S., Inada A., Yatoh S., Li W.C., Aye T., Toschi E., and Sharma A. Transdifferentiation of pancreatic ductal cells to endocrine cells. *Biochem Soc Trans* 36: 353-356, 2008.

[7] Bonner-Weir S., Taneja M., Weir G.C., Tatarkiewicz K., Song K.H., Sharma A., and O'Neil J.J. In vitro cultivation of human islets from expanded ductal tissue. *Proc Natl Acad Sci U.S.A.* 97: 7999-8004, 2000.

[8] Brennand K., Huangfu D., and Melton D. All beta cells contribute equally to islet growth and maintenance. *PLoS biology* 5: e163, 2007.

[9] Brissova M., Fowler M.J., Nicholson W.E., Chu A., Hirshberg B., Harlan D.M., and Powers A.C. Assessment of human pancreatic islet architecture and composition by laser scanning confocal microscopy. *J Histochem Cytochem* 53(9): 1087-97, 2005.

[10] Brissova M. and Powers A.C. Architecture of Pancreatic Islets. In *Pancreatic beta cell in health and disease*, Seino S. and Bell G.I., ed. (Japan: Springer), pp. 3-11, 2008.

[11] Butler A.E., Galasso R., Meier J.J., Basu R., Rizza R.A., and Butler P.C. Modestly increased beta cell apoptosis but no increased beta cell replication in recent-onset type 1 diabetic patients who died of diabetic ketoacidosis. *Diabetologia* 50:2323-2331, 2007.

[12] Butler A.E., Jang J., Gurlo T., Carty M.D., Soeller W.C., and Butler P.C. Diabetes due to a progressive defect in beta cell mass in rats transgenic for human islet amyloid polypeptide (HIP Rat): a new model for type 2 diabetes. *Diabetes* 53(6): 1509-16, 2004.

[13] Butler A.E., Janson J., Bonner-Weir S., Ritzel R., Rizza R.A., and Butler P.C. Beta cell deficit and increased beta cell apoptosis in humans with type 2 diabetes. *Diabetes* 52: 102-110, 2003.

[14] Butler A.E., Janson J., Soeller W.C., Butler P.C. Increased beta cell apoptosis prevents adaptive increase in beta cell mass in mouse model of type 2 diabetes: evidence for role of islet amyloid formation rather than direct action of amyloid. *Diabetes* 52:2304 2314, 2003.

[15] Butler P.C., Meier J.J., Butler A.E., and Bhushan A. The replication of beta cells in normal physiology, in disease, and for therapy. *Nat Clin Pract Endocrinol Metab* 3: 758-768, 2007.

[16] Cabrera O., Berman D.M., Kenyon N.S., Ricordi C., Berggren P.O., and Caicedo A. The unique cytoarchitecture of human pancreatic islets has implications for islet cell function. *Proc Natl Acad Sci U.S.A.* 103(7): 2334-9, 2006.

[17] Caswell H. In *Matrix population models* ed. (Sinauer Associates, Inc. Publishers. Sunderland, Massachusetts), 1989.

[18] Chen B., Wang L., Hu S., Zhou L., Wang R., Wachtel M.S., Frezza E.D. Would pancreas duct-epithelium-derived stem/progenitor cells enhance islet allograft survival by means of islets recruitment and tolerance induction in Edmonton protocol era? *Med Hypotheses* 70: 661664, 2008.

[19] Coles H.S., Burne J.F., and Raff M.C. Large-scale normal cell death in the developing rat kidney and its reduction by epidermal growth factor. *Development* 118: 777-784, 1993.

[20] Collins R.J., Harmon B.V., Gob G.C., and Kerr J.F. Internucleosomal DNA cleavage should not be the sole criterion for identifying apoptosis. *Int J Radiat Biol* 61(4): 451-3, 1992.

[21] Del Prato S., Wishner W.J., Gromada J., and Schluchter B.J. Beta cell mass plasticity in type 2 diabetes. *Diabetes Obes Metab* 6: 319-331, 2004.

[22] Deming W.E. In *Data Reduction and Error Analysis for the Physical Sciences* ed. (New York: Wiley), 1943.

[23] De Nicolao G., Sparacino G., and Cobelli C. Nonparametric input estimation in physiological systems: problems, methods, and case studies. *Automatica* 33: 851-870, 1997.

[24] de Rooij S.R., Painter R.C., Roseboom T.J., Phillips D.I., Osmond C., Barker D.J., Tanck M.W., Michels R.P., Bossuyt P.M., and Bleker O.P. Glucose tolerance at age 58 and the decline of glucose tolerance in comparison with age 50 in people prenatally exposed to the Dutch famine. *Diabetologia* 49(4): 637-43, 2006.

[25] Dor Y., Brown J., Martinez O.I., and Melton D.A. Adult pancreatic beta cells are formed by self-duplication rather than stem-cell differentiation. *Nature* 429(6987): 41-6, 2004.

[26] Ebato C., Uchida T., Arakawa M., Komatsu M., Ueno T., Komiya K., Azuma K., Hirose T., Tanaka K., Kominami E., Kawamori R., Fujitani Y., and Watada H. Autophagy is important in islet homeostasis and compensatory increase of beta cell mass in response to high-fat diet. *Cell Metab* 8(4): 275-6, 2008.

[27] Edinger A.L. and Thompson C.B. Death by design: apoptosis, necrosis, and autophagy. *Curr Opin Cell Biol* 16(6): 663-9, 2004.

[28] Eizirik D.L. and Mandrup-Poulsen T. A choice of deaththe signal-transduction of immune-mediated beta-cell apoptosis. *Diabetologia* 44: 2115-2133, 2001.

[29] Ellis R.E., Yuan J.Y., and Horvitz H.R. Mechanisms and functions of cell death. *Annu Rev Cell Biol* 7: 663-698, 1991.

[30] Finegood D.T., McArthur M.D., Kojwang D., Thomas M.J., Topp B.G., Leonard T., and Buckingham R.E. Beta cell mass dynamics in Zucker diabetic fatty rats. Rosiglitazone prevents the rise in net cell death. *Diabetes* 50: 10211029, 2001.

[31] Finegood D.T., Scaglia L., and Bonner-Weir S. Dynamics of beta cell mass in the growing rat pancreas. Estimation with a simple mathematical model. *Diabetes* 44: 249-256, 1995.

[32] Foa P., Maiolo A.T., Lombardi L., Toivonen H., Rytomaa T., and Polli E.E. Growth pattern of the human promyelocytic leukaemia cell line HL60. *Cell Tissue Kinetics* 15: 399404, 1982.

[33] Forrester H.B., Albright N., Ling C.C., and Dewey W.C. Computerized video time-lapse analysis of apoptosis of REC:Myc cells X-irradiated in different phases of the cell cycle. *Radiat Res* 154: 625-639, 2000.

[34] Foulis A.K. and Stewart J.A. The pancreas in recent-onset type 1 (insulin-dependent) diabetes mellitus: insulin content of islets, insulitis and associated changes in the exocrine acinar tissue. *Diabetologia* 26(6): 456-61, 1984.

[35] Frese T., Bazwinsky I., Muhlbauer E., and Peschke E. Circadian and age-dependent expression patterns of GLUT2 and glucokinase in the pancreatic beta-cell of diabetic and nondiabetic rats. *Horm Metab Res* 39:567-574, 2007.

[36] Georgia S. and Bhushan A. Beta cell replication is the primary mechanism for maintaining postnatal beta cell mass. *J Clin Invest* 114(7): 963-8, 2004.

[37] Gold R., Schmied M., Giegerich G., Breitschopf H., Hartung H.P., Toyka K.V., and Lassmann H. Differentiation between cellular apoptosis and necrosis by the combined use of in situ tailing and nick translation techniques. *Lab Invest* 71(2):219-25, 1994.

[38] Hanley S. and Rosenberg L. Islet-derived progenitors as a source of in vitro islet regeneration. *Methods Mol Biol* 482: 371-385, 2009.

[39] Hovorka R., Chappell M.J., Godfrey K.R., Madden F.N., Rouse M.K., and Soons P.A.. CODE: A deconvolution program implementing a regularisation method of deconvolution constrained to non-negative values: Description and pilot evaluation. *Biopharm Drug Dispos* 19:39-53, 1998.

[40] Huang C.J., Lin C.Y., Haataja L., Gurlo T., Butler A.E., Rizza R.A., and Butler P.C. High expression rates of human islet amyloid polypeptide induce endoplasmic reticulum stress mediated beta cell apoptosis, a characteristic of humans with type 2 but not type 1 diabetes. *Diabetes* 56: 2016-2027, 2007.

[41] Hunt B.R. Biased estimation for nonparametric identification of linear systems. *Math Biosci* 10: 215-237, 1971.

[42] Ichii H., Inverardi L., Pileggi A., Molano R.D., Cabrera O., Caicedo A., Messinger S., Kuroda Y., Berggren P.O., and Ricordi C. A novel method for the assessment of cellular composition and beta cell viability in human islet preparations. *Am J Transplant* 5(7): 1635-45, 2005.

[43] Inada A., Nienaber C., Katsuta H., Fujitani Y., Levine J., Morita R., Sharma A., and Bonner-Weir S. Carbonic anhydrase II-positive pancreatic cells are progenitors for both endocrine and exocrine pancreas after birth. *Proc Natl Acad Sci U.S.A.* 105: 19915-19919, 2008.

[44] Jorns A., Klempnauer J., Tiedge M., and Lenzen S. Recovery of pancreatic beta cells in response to long-term normoglycemia after pancreas or islet transplantation in severely streptozotocin diabetic adult rats. *Pancreas* 23:186-196, 2001.

[45] Jorns A., Tiedge M., Ziv E., Shafrir E., and Lenzen S. Gradual loss of pancreatic beta-cell insulin, glucokinase and GLUT2 glucose transporter immunoreactivities during the time course of nutritionally induced type-2 diabetes in Psammomys obesus (sand rat). *Virchows* Arch 440:63-69, 2002.

[46] Jung H.S., Chung K.W., Won Kim J., Kim J., Komatsu M., Tanaka K., Nguyen Y.H., Kang T.M., Yoon K.H., Kim J.W., Jeong Y.T., Han M.S., Lee M.K., Kim K.W., Shin J., and Lee M.S. Loss of autophagy diminishes pancreatic beta cell mass and function with resultant hyperglycemia. *Cell Metab* 8(4): 318-24, 2008.

[47] Kalashnik L., Bridgeman C.J., King A.R., Francis S.E., Mikhalovsky S., Wallis C., Denyer S.P., Crossman D., and Faragher R.G. A cell kinetic analysis of human umbilical vein endothelial cells. *Mech Ageing Dev* 120: 2332, 2000.

[48] Kassem S.A., Ariel I., Thornton P.S., Scheimberg I., and Glaser B. Beta cell proliferation and apoptosis in the developing normal human pancreas and in hyperinsulinism of infancy. *Diabetes* 49(8): 1325-33, 2000.

[49] Kloppel G., Lohr M., Habich K., Oberholzer M., and Heitz P.U. Islet pathology and the pathogenesis of type 1 and type 2 diabetes mellitus revisited. *Surv Synth Pathol Res* 4: 110125, 1985.

[50] Krystek M. and Anton M. A weighted total least squares algorithm for fitting a straight line. *Meas Sci Technol* 18: 34383442, 2007.

[51] Kushner J.A., Ciemerych M.A., Sicinska E., Wartschow L.M., Teta M., Long S.Y., Sicinski P., and White M.F. Cyclins D2 and D1 are essential for postnatal pancreatic beta cell growth. *Mol Cell Biol* 25(9): 3752-62, 2005.

[52] Lawless J.F. In *Statistical models and methods for lifetime data* ed. (Wiley Series in Probability and Mathematical Statistics, John Wiley and Sons Inc., Canada), 1982.

[53] Lingohr M.K., Buettner R., and Rhodes C.J. Pancreatic beta cell growth and survival: a role in obesity-linked type 2 diabetes? *Trends Mol Med* 8(8): 375-84, 2002.

[54] Lipsett M. and Finegood D.T. Beta cell neogenesis during prolonged hyperglycemia in rats. *Diabetes* 51: 1834-1841, 2002.

[55] Ludvik B., Nolan J.J., Baloga J., Sacks D., and Olefsky J. Effect of obesity on insulin resistance in normal subjects and patients with NIDDM. *Diabetes* 44: 11211125, 1995.

[56] Lupi R. and Del Prato S. Beta cell apoptosis in type 2 diabetes: quantitative and functional consequences. *Diabetes Metab* 34 Suppl 2: S56-64, 2008.

[57] Magni P., Bellazzi R., and De Nicolao G. Bayesian function learning using MCMC methods. *IEEE Trans Pattern Analysis and Machine Intelligence* 20, 1319-1331, 1998.

[58] Manesso E., Toffolo G.M., Saisho Y., Butler A.E., Matveyenko A.V., Cobelli C., and Butler P.C. Dynamics of beta cell turnover: evidence for beta cell turnover and regeneration from sources of beta cells other than beta cell replication in the HIP rat. *Am J Physiol Endocrinol Metab* 297(2): E323-30, 2009.

[59] Maree A.F., Komba M., Finegood D.T., and Edelstein-Keshet L. A quantitative comparison of rates of phagocytosis and digestion of apoptotic cells by macrophages from normal (BALB/c) and diabetes-prone (NOD) mice. *J Appl Physiol* 104: 157-169, 2008.

[60] Matveyenko A.V. and Butler P.C. Beta cell deficit due to increased apoptosis in the human islet amyloid polypeptide transgenic (HIP) rat recapitulates the metabolic defects present in type 2 diabetes. *Diabetes* 55(7): 2106-14, 2006.

[61] Matveyenko A.V., Gurlo T., Daval M., Butler A.E., and Butler P.C. Successful versus failed adaptation to high-fat diet-induced insulin resistance: the role of IAPP-induced beta-cell endoplasmic reticulum stress. *Diabetes* 58(4): 906-16, 2009.

[62] Meier J.J., Bhushan A., Butler A.E., Rizza R.A., and Butler P.C. Sustained beta cell apoptosis in patients with long-standing type 1 diabetes: indirect evidence for islet regeneration? *Diabetologia* 48(11): 2221-8, 2005.

[63] Meier J.J., Butler A.E., Saisho Y., Monchamp T., Galasso R., Bhushan A., Rizza R.A., and Butler P.C. Beta cell replication is the primary mechanism subserving the postnatal expansion of beta cell mass in humans. *Diabetes* 57(6): 1584-94, 2008.

[64] Meier J.J. and Butler P.C. Insulin secretion. In *Endocrinology* DeGroot L.J. and Jameson J.L., ed. (Philadelphia: Elsevier Saunders), pp. 961-973, 2005.

[65] Meier J.J., Lin J.C., Butler A.E., Galasso R., Martinez D.S., and Butler P.C. Direct evidence of attempted beta cell regeneration in an 89-year-old patient with recent-onset type 1 diabetes. *Diabetologia* 49(8): 1838-44, 2006.

[66] Meier J.J., Ritzel R.A., Maedler K., Gurlo T., and Butler P.C. Increased vulnerability of newly forming beta cells to cytokine-induced cell death. *Diabetologia* 49: 83-89, 2006.

[67] Montanya E., Nacher V., Biarnes M., and Soler J. Linear correlation between beta-cell mass and body weight throughout the lifespan in Lewis rats: role of beta-cell hyperplasia and hypertrophy. *Diabetes* 49: 1341-1346, 2000.

[68] Moore A. Advances in beta cell imaging. *Eur J Radiol* 70: 254257, 2009.

[69] Nir T., Melton D.A., Dor Y. Recovery from diabetes in mice by beta cell regeneration. *J Clin Invest* 117: 2553-2561, 2007.

[70] Noguchi H., Xu G., Matsumoto S., Kaneto H., Kobayashi N., Bonner-Weir S., and Hayashi S. Induction of pancreatic stem/progenitor cells into insulin-producing cells by adenoviral-mediated gene transfer technology. *Cell Transplantation* 15: 929-938, 2006.

[71] Ogilvie R.F. The islands of langerhans in 19 cases of obesity. *J Pathol Bacteriol* 37: 473481, 1933.

[72] Perry V.H., Henderson Z., and Linden R. Postnatal changes in retinal ganglion cell and optic axon populations in the pigmented rat. *J Comp Neurol* 219: 356-368, 1983.

[73] Phillips D.L. A technique for the numerical solution of certain integral equations of the first kind. *J Ass Comput Mach* 9: 97-101, 1962.

[74] Poitout V. and Robertson R.P. Glucolipotoxicity: fuel excess and beta-cell dysfunction. *Endocr Rev* 29:351-366, 2008.

[75] Potten C and Wilson J. In *Apoptosis: The Life and Death of Cells.* ed. (New York: Cambridge University Press), 2004.

[76] Rane S.G., Dubus P., Mettus R.V., Galbreath E.J., Boden G., Reddy E.P., and Barbacid M. Loss of Cdk4 expression causes insulin-deficient diabetes and Cdk4 activation results in beta-islet cell hyperplasia. *Nat Genet* 22(1): 44-52, 1999.

[77] Rankin M.M., Kushner J.A. Adaptive beta cell proliferation is severely restricted with advanced age. *Diabetes* 58: 13651372, 2009.

[78] Ritzel R.A., Butler A.E., Rizza R.A., Veldhuis J.D., and Butler P.C. Relationship between beta cell mass and fasting blood glucose concentration in humans. *Diabetes Care* 29(3): 717-8, 2006.

[79] Ritzel R.A. and Butler P.C. Replication increases beta cell vulnerability to human islet amyloid polypeptide-induced apoptosis. *Diabetes* 52(7): 1701-8, 2003.

[80] Ronot X., Hecquet C., Jaffray P., Guiguet M., Adolphe M., Fontagne J., and Lechat P. Proliferation kinetics of rabbit articular chondrocytes in primary culture and at the first passage. *Cell Tissue Kinetics* 16: 531-537, 1983.

[81] Russ H.A., Bar Y., Ravassard P., and Efrat S. In vitro proliferation of cells derived from adult human beta cells revealed by cell-lineage tracing. *Diabetes* 57: 1575-1583, 2008.

[82] Saisho Y., Butler A.E., Meier J.J., Monchamp T., Allen-Auerbach M., Rizza R.A., and Butler P.C. Pancreas volumes in humans from birth to age one hundred taking into account sex, obesity and presence of type 2 diabetes. *Clin Anat* 20: 933-942, 2007.

[83] Saisho Y., Manesso E., Gurlo T., Huang C.J., Toffolo G.M., Cobelli C., and Butler P.C. Development of factors to convert frequency to rate for beta cell replication and apoptosis quantified by time-lapse video microscopy and immunohistochemistry. *Am J Physiol Endocrinol Metab* 296: E89-E96, 2009.

[84] Sapir T., Shternhall K., Meivar-Levy I., Blumenfeld T., Cohen H., Skutelsky E., Eventov-Friedman S., Barshack I., Goldberg I., Pri-Chen S., Ben-Dor L., Polak-Charcon S., Karasik A., Shimon I., Mor E., and Ferber S. Cell-replacement therapy for diabetes: Generating functional insulin-producing tissue from adult human liver cells. *Proc Natl Acad Sci U.S.A.* 102: 7964-7969, 2005.

[85] Scott L.J., Mohlke K.L., Bonnycastle L.L., Willer C.J., Li Y., Duren W.L., Erdos M.R., Stringham H.M., Chines P.S., Jackson A.U., Prokunina-Olsson L., Ding C.J., Swift A.J., Narisu N., Hu T., Pruim R., Xiao R., Li X.Y., Conneely K.N., Riebow N.L., Sprau A.G., Tong M., White P.P., Hetrick K.N., Barnhart M.W., Bark C.W., Goldstein J.L., Watkins L., Xiang F., Saramies J., Buchanan T.A., Watanabe R.M., Valle T.T., Kinnunen L., Abecasis G.R., Pugh E.W., Doheny K.F., Bergman R.N., Tuomilehto J., Collins F.S., and Boehnke M. A genome-wide association study of type 2 diabetes in Finns detects multiple susceptibility variants. *Science* 316(5829):1341-5, 2007.

[86] Shintani T. and Klionsky D.J. Autophagy in health and disease: a double-edged sword. *Science* 306(5698): 990-5, 2004.

[87] Sit K.H. and Chen D.L. Transient G2M arrest and subsequent release of apoptotic and mitotic cells in vanadyl(4)-prepulsed human Chang liver cells. *Cell Death Differ* 4(3): 216-23, 1997.

[88] Sladek R., Rocheleau G., Rung J., Dina C., Shen L., Serre D., Boutin P., Vincent D., Belisle A., Hadjadj S., Balkau B., Heude B., Charpentier G., Hudson T.J., Montpetit A., Pshezhetsky A.V., Prentki M., Posner B.I., Balding D.J., Meyre D., Polychronakos C., and Froguel P. A genome-wide association study identifies novel risk loci for type 2 diabetes. *Nature* 445(7130): 881-5, 2007.

[89] Sparacino G., De Nicolao G., and Cobelli C. Deconvolution. In *Modeling Methodology for Physiology and Medicine (Biomedical Engineering Series)*, Carson E. and Cobelli C., ed. (Academic Press, San Diego, California, USA), pp. 45-76, 2001.

[90] Stefan Y., Orci L., Malaisse-Lagae F., Perrelet A., Patel Y., and Unger R.H. Quantitation of endocrine cell content in the pancreas of nondiabetic and diabetic humans. *Diabetes* 31(8 Pt 1): 694-700, 1982.

[91] Sutherland R.L., Hall R.E., and Taylor I.W. Cell proliferation kinetics of MCF-7 human mammary carcinoma cells in culture and effects of tamoxifen on exponentially growing and plateau-phase cells. *Cancer Res* 43: 3998-4006, 1983.

[92] Swenne I. The role of glucose in the in vitro regulation of cell cycle kinetics and proliferation of fetal pancreatic beta cells. *Diabetes* 31: 754-760, 1982.

[93] Swenne I. Effects of aging on the regenerative capacity of the pancreatic beta cell of the rat. *Diabetes* 32: 14-19, 1983.

[94] Teta M., Rankin M.M., Long S.Y., Stein G.M., and Kushner J.A. Growth and regeneration of adult beta cells does not involve specialized progenitors. *Dev Cell* 12(5): 817-26, 2007.

[95] Thorens B., Guillam M.T., Beermann F., Burcelin R., and Jaquet M. Transgenic reexpression of GLUT1 or GLUT2 in pancreatic beta cells rescues GLUT2-null mice from early death and restores normal glucose-stimulated insulin secretion. *J Biol Chem* 275:23751-23758, 2000.

[96] Tikhonov A.N. Solution of incorrectly formulated problems and the regularization method. *Soviet Math Dokl* 4: 1624, 1963.

[97] Topp B.G., Atkinson L.L., and Finegood D.T. Beta cell function, and beta cell mass during the development of diabetes in fa/fa rats. *Am J Physiol Endocrinol Metab* 293: E1730-1735, 2007.

[98] Tschen S.I., Dhawan S., Gurlo T., and Bhushan A. Age-dependent decline in beta cell proliferation restricts the capacity of beta cell regeneration in mice. *Diabetes* 58(6): 1312-20, 2009.

[99] Tyrberg B., Ustinov J., Otonkoski T., and Andersson A. Stimulated endocrine cell proliferation and differentiation in transplanted human pancreatic islets: effects of the ob gene and compensatory growth of the implantation organ. *Diabetes* 50(2): 301-7, 2001.

[100] van Furth R., Elzenga-Claasen I., van Schadewijk-Nieuwstad M., Diesselhoff- den Dulk M.M., Toivonen H., and Rytomaa T. Cell kinetic analysis of a murine macrophage cell line. *Eur J Cell Biol* 44: 93-96, 1987.

[101] Veng-Pedersen P. An algorithm and computer program for deconvolution in linear pharmacokinetics. *J Pharmacokin Biopharm* 8: 463-481, 1980.

[102] Verotta D. Estimation and model selection in constrained deconvolution. *Annals of Biomedical Engineering* 21: 605-620, 1993.

[103] Xu X., D'Hoker J., Stange G., Bonne S., De Leu N., Xiao X., Van de Casteele M., Mellitzer G., Ling Z., Pipeleers D., Bouwens L., Scharfmann R., Gradwohl G., and Heimberg H. Beta cells can be generated from endogenous progenitors in injured adult mouse pancreas. *Cell* 132: 197-207, 2008.

[104] Yoon K.H., Lee J.H., Kim J.W., Cho J.H., Choi Y.H., Ko S.H., Zimmet P., and Son H.Y. Epidemic obesity and type 2 diabetes in Asia. *Lancet* 368(9548): 1681-8, 2006.

[105] Webb S.J., Harrison D.J., and Wyllie A.H. Apoptosis: an overview of the process and its relevance in disease. *Adv Pharmacol* 41: 1-34, 1997.

[106] Weibel E.R. Stereological principles for morphometry in electron microscopy. *Int Rev Cytol* 26:235-302, 1969.

[107] Woo K.B., Funkhouser W.K., Sullivan C., and Alabaster O. Analysis of the proliferation kinetics of Burkitts lymphoma cells. *Cell Tissue Kinetics* 13: 591-604, 1980.

[108] Zeggini E., Weedon M.N., Lindgren C.M., Frayling T.M., Elliott K.S., Lango H., Timpson N.J., Perry J.R., Rayner N.W., Freathy R.M., Barrett J.C., Shields B., Morris A.P., Ellard S., Groves C.J., Harries L.W., Marchini J.L., Owen K.R., Knight B., Cardon L.R., Walker M., Hitman G.A., Morris A.D., Doney A.S.; Wellcome Trust Case Control Consortium (WTCCC), McCarthy M.I., and Hattersley A.T. Replication of genome-wide association signals in UK samples reveals risk loci for type 2 diabetes. *Science* 316(5829): 1336-41, 2007.

[109] Zulewski H., Abraham E.J., Gerlach M.J., Daniel P.B., Moritz W., Muller B., Vallejo M., Thomas M.K., and Habener J.F. Multipotential nestin-positive stem cells isolated from adult pancreatic islets differentiate ex vivo into pancreatic endocrine, exocrine, and hepatic phenotypes. *Diabetes* 50: 521-533, 2001.

List of Figures

List of Tables